AD_____

Award Number: DAMD17-02-1-0215

TITLE: Molecular Characterization of Squamous Cell Carcinomas from Recessive Dystrophic Epidermolysis Bullosa

PRINCIPAL INVESTIGATOR: My G. Mahoney, Ph.D.
Ulrich Rodeck, Ph.D.
Jouni Uitto, M.D., Ph.D.

CONTRACTING ORGANIZATION: Thomas Jefferson University
Philadelphia, Pennsylvania 19107

REPORT DATE: September 2006

TYPE OF REPORT: Final

PREPARED FOR: U.S. Army Medical Research and Materiel Command
Fort Detrick, Maryland 21702-5012

REPORT DOCUMENTATION PAGE

Form Approved
OMB No. 0704-0188

1. REPORT DATE *(DD-MM-YYYY)*	2. REPORT TYPE	3. DATES COVERED *(From - To)*
01-09-2006	Final	29 May 2002 – 31 Aug 2006

4. TITLE AND SUBTITLE

Molecular Characterization of Squamous Cell Carcinomas from Recessive Dystrophic Epidermolysis Bullosa

5a. CONTRACT NUMBER

5b. GRANT NUMBER
DAMD17-02-1-0215

5c. PROGRAM ELEMENT NUMBER

6. AUTHOR(S)

My G. Mahoney, Ph.D.; Ulrich Rodeck, Ph.D. and Jouni Uitto, M.D., Ph.D.

E-Mail: my.mahoney@jefferson.edu

5d. PROJECT NUMBER

5e. TASK NUMBER

5f. WORK UNIT NUMBER

7. PERFORMING ORGANIZATION NAME(S) AND ADDRESS(ES)

Thomas Jefferson University
Philadelphia, Pennsylvania 19107

8. PERFORMING ORGANIZATION REPORT NUMBER

9. SPONSORING / MONITORING AGENCY NAME(S) AND ADDRESS(ES)
U.S. Army Medical Research and Materiel Command
Fort Detrick, Maryland 21702-5012

10. SPONSOR/MONITOR'S ACRONYM(S)

11. SPONSOR/MONITOR'S REPORT NUMBER(S)

12. DISTRIBUTION / AVAILABILITY STATEMENT
Approved for Public Release; Distribution Unlimited

13. SUPPLEMENTARY NOTES

14. ABSTRACT

Patients with recessive dystrophic epidermolysis bullosa (RDEB) frequently present with squamous cell carcinomas (SCCs) probably as a result of chronic blistering and extensive scarring. These tumors are clinically aggressive as they metastasize readily. The metastasis-associated protein (MTA)-1, a transcription suppressor, is overexpressed in several epithelial neoplasms including SCCs. Our preliminary results demonstrate that MTA1 expression is induced by activation of the epidermal growth factor receptor (EGFR). As deregulation of EGFR signaling is frequently observed in aggressive epithelial neoplasms we propose to study the role of EGFR signaling and MTA1 expression in SCCs derived in RDEB patients. Our Specific Aims are to establish cell lines derived from SCCs in non-RDEB and RDEB patients, characterize the malignant phenotype of these cells as it relates to EGFR expression and signaling and to expression of MTA1, examine the contribution of EGFR/MTA1 to proliferation, invasiveness, and cell survival and identify EGFRdependent signaling pathways contributing to MTA1 expression in these cells. The results from this research will provide invaluable tools for future analysis of the pathobiology of carcinoma cells and will ascertain whether EGFR/MTA1 signaling pathways contributes significantly to the metastasis and invasiveness of SCC derived from RDEB patients.

15. SUBJECT TERMS
Epidermolysis bullosa, epidermal growth factor, metastasis-associated protein, proliferation, differentiation, survival

16. SECURITY CLASSIFICATION OF:			17. LIMITATION OF ABSTRACT	18. NUMBER OF PAGES	19a. NAME OF RESPONSIBLE PERSON
a. REPORT	b. ABSTRACT	c. THIS PAGE			USAMRMC
U	U	U	UU	93	19b. TELEPHONE NUMBER *(include area code)*

Table of Contents

Cover	**1**
SF298	**2**
Table of Contents	**3**
Introduction	**4**
Body	**4**
Key Research Accomplishments	**7**
Reportable Outcomes	**7**
Conclusions	**7**
References	**8**
Appendices	**8**

INTRODUCTION

A malignant cancer is characterized by its metastatic and invasive properties. Thus, identifying and characterizing the genes that are involved in metastasis will provide the means to predict and select patients for aggressive therapy or will lead to the development of novel treatments to inhibit this mechanism of cancer spreading. Tremendous progress has been made in identifying genes that are involved in tumor development, progression, and metastasis. One such gene is the metastasis tumor antigen 1 (MTA1), member of the large family of metastasis-associated genes (MTAs) (1). MTA1 is overexpressed in and correlates well with many highly metastatic cancers including human epithelial-derived breast and esophageal carcinomas (2). Epidermolysis bullosa (EB) is a group of heritable genetic skin blistering diseases caused by the disruption of the normal function of the basement membrane zone (3, 4). As a result of chronic blistering, re-epithelialization, and extensive scarring, RDEB patients frequently develop highly invasive squamous cell carcinomas (SCC). The overall goal of our research through DAMD17-02-1-0215 is to study RDEB-derived SCCs and ascertain whether the epidermal growth factor receptor- (EGFR) and/or MTA1 mediated signaling pathways contribute significantly to the highly aggressive malignant phenotype these cells. We originally proposed four Specific Aims. Specific Aims 1 and 2 were to establish epithelial keratinocyte SCC cell lines from RDEB and non-RDEB skin biopsies and characterize characterize the malignant phenotype (growth, invasiveness, and survival potential) of these cells. Specific Aims 3 and 4 were to examine the contribution of MTA1 to epithelial cell proliferation, invasiveness, and survival and to identify the signaling pathways that are relevant to MTA1 expression.

BODY

This final report will summarize our accomplishments, pitfalls, and future research plans.

Specific Aims 1 and 2

In order to study the biology of tumor cells from RDEB, we had proposed to establish these cells in culture. This is a critical part of this proposal because these cells would serve as excellent tools for any future studies involving keratinocyte tumor biology. We collected many skin samples from RDEB-SCCs but were unsuccessful at establishing or maintaining these keratinocytes in culture. Due to this technical difficulty and set back, we obtained through American Tissue-Type Culture epithelial cell lines representing different stages of keratinocyte tumor progression. In addition, we also characterized SCCs and RDEB-SCCs (*in situ*). We successfully generated antibodies specific against MTA1 and MTA3 used these antibodies to demonstrate their subcellular localization in epidermal keratinocytes (*in situ*) as well as cultured keratinocytes during different stages of the cell cycle. We established a correlation between the invasive potential of SCCs and the expression level of MTA1/MTA3. Furthermore, we demonstrated that the EGF-R regulates MTA1 expression, which in turn can bind to and activate the MTA3 promoter (5). This finding is significant since the activation of EGF-R has been strongly implicated in the malignant transformation of epithelial keratinocytes.

Specific Aims 3 and 4

The major goal of these Aims is to determine the role of MTA1 in modulating proliferation, differentiation, invasiveness, and survival of keratinocytes. We successfully established variants of human immortalized keratinocytes (HaCaT cells) by expressing MTA1 cDNA in both the sense and antisense orientations (6). Epithelial cells lacking MTA1 showed decreased cellular metabolism, a reduction in cell cycle progression, and appeared morphologically similar to quiescent non-proliferating cells. On the other hand, forced MTA1 expression enhanced cell progression through mitosis, thereby increasing cell proliferation. In addition, forced MTA1 expression also enhanced keratinocyte migration and invasiveness and increased cell survival in an anchorage independent state possibly through the anti-apoptotic Bcl-2 family member Bcl-X_L. Thus, our results demonstrate that MTA1 expression contributes to several aspects of the metastatic phenotype including enhanced cellular proliferation and survival. It has been proposed that hypoacetylation of histones favors transcriptional silencing, a potential underlying cause of cell proliferation and cancer. MTA1 has been shown to interact directly with and enhance the histone deacetylase activity of the nucleosome-remodeling complex. Our current work will demonstrate a novel role of MTA1 in DNA repair and spindle assembly checkpoint during mitosis, cellular processes that when go awry, would favor carcinogenesis.

Role of MTA1 During Tumor Development

Traditionally, strong cell-cell adhesion has been viewed as a mechanical impediment to invasion and metastasis of malignant cells. Thus, the frequent loss of E-cadherin expression as observed in multiple epithelial tumors has been linked to weakened cell-cell adhesion enabling egress of tumor cells from the primary tumor bed and metastatic dissemination (7, 8). Although desmosomal cell-cell adhesion has been considered in a similar vein as E-cadherin, the relationship between loss of desmosomal adhesion and clinical outcomes of epithelial neoplasia is less clear. The desmosomal protein desmoglein 2 is frequently overexpressed or abnormally expressed in select epithelial malignancies including squamous cell carcinomas (9-11). Similarly, genetic profiling of prostate cancer cell lines showed increased expression of desmoglein 2 in a metastatic cell line as compared to it's non-metastatic syngeneic precursor cell (12). Thus to further study the role of MTA1 during tumor development and progression and to combine our research interests in the role of cell adhesion during tumorigenesis, we recently developed transgenic mice with aberrant expression of desmoglein 2 (13). Transgenic mice developed a hyperproliferative skin phenotype and cultured keratinocytes from transgenic mouse skin showed an apoptosis-resistant phenotype similar to the MTA1-overexpressing cells (see above). We also observed enhanced activation of multiple growth and survival pathways including PI-3-kinase/AKT, MEK/MAPK, STAT3, and NF-κB in the transgenic skin *in situ*. In addition, transgenic mice developed intraepidermal skin lesions resembling precancerous papillomas and were more susceptible to chemical carcinogen-induced skin tumorigenesis (see below).

We sought to identify genes associated the hyperproliferative phenotype by comparing the expression profile of transgenic with cDNA from wild-type skin as control, using a cDNA chip

providing 23,000 genes. We observed more than 150 genes were downregulated and 1110 genes were upregulated by more than twofold in transgenic over the control skin. A number of genes important during epithelial malignant transformation including (distal-less 4-homeobox, estradiol 17-beta-dehydrogenase, mitotic checkpoint protein kinase (Bub1), cyclin B2, cancer susceptibility protein (Brca1) and dipeptidylpeptidase 4) were upregulated. The most surprising finding was the threefold upregulation of MTA1 and MTA3. The role of MTA1 in the development of intraepidermal skin lesions and the susceptibility of these transgenic mice to chemical carcinogen-induced skin tumorigenesis will be pursued.

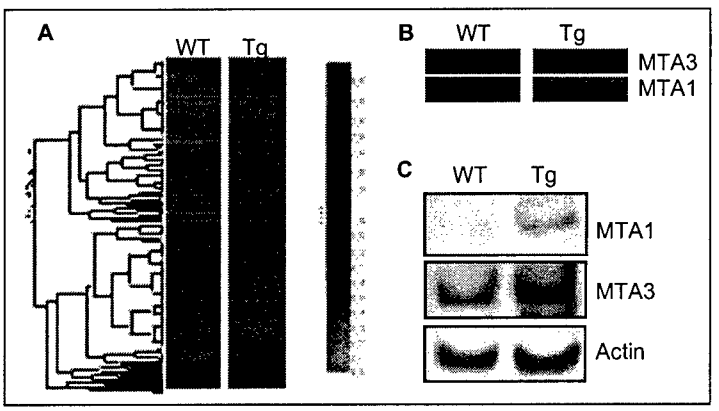

Clustering of genes showing > twofold change (2878 genes) between transgenic and wild-type. (A) Microarray results were analyzed using Genespring 7.2 software. Normalization was done by the following method. Values below 0.01 were set to 0.01. Each measurement was divided by the 50th percentile of all measurements in that sample. Fold change in the expression values between the groups was then calculated Clustering: Gene tree clustering was done on genes showing more than 2 fold change between groups Inv-Dsg2 transgenic (Tg) and wild-type (WT) using standard correlation. (B) Upregulation of MTA1 and MTA3 RNA by threefold in transgenic compared to WT skin by microarray. (C) Immunoblotting analysis of total skin lysate showing upregulation of both MTA1 and MTA3 proteins in transgenic over wild-type skin. Actin for loading control.

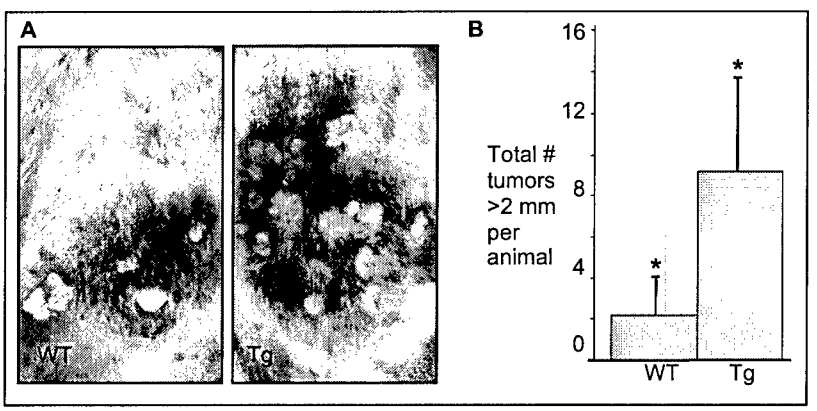

Increased tumorigencity in transgenic mice. (A) After 25 weeks of DMBA/TPA treatment, the transgenic mice developed more tumors than wild-type littermates. (B) The frequency and average number of papillomas or papillomas over 2 mm in wild-type and transgenic mice after 25 weeks of tumor promotion.

Thus, we have established a transgenic mouse model showing a previously unrecognized cross talk between cell-cell adhesion proteins and MTA1 expression. This work has allowed us to submit a joint grant application to the NIH focusing the role of adhesion protein-mediated MTA1 expression during tumor development and malignant transformation.

Manuscript in preparation:

Brennan D and MG Mahoney. Microarray profiles of chemical-induced skin carcinomas: Insights into epithelial cell-cell adhesion and tumor predisposition and progression. *J Cancer Res.*

KEY RESEARCH ACCOMPLISHMENTS

- We showed that MTA1 expression contributes to several aspects of the malignant phenotype of epithelial keratinocytes. MTA1 expression is upregulated in SCCs. We characterized the role of MTA1 in DNA repair and mitotic spindle assembly checkpoint as a potential mechanism regulating epithelial cell transformation.

- We established a transgenic mouse model that developed epidermal hyperproliferation and benign papillomas and were more susceptible to chemical-induced carcinogenesis. Transgenic keratinocytes showed deregulated signaling pathways associated with increased growth rate and anchorage-independent cell survival and enhanced MTA1 expression (*in vitro* and *in vivo*). This mouse model allows us to further study the role of MTA1 in tumor development and progression. It will have wide implications not only for cell biology and transformation of complex epithelia, but also for simple epithelia including breast tissue in which MTA1 has been implicated in the hyperproliferative/malignant phenotype.

REPORTABLE OUTCOMES

The PDFs of these manuscripts are appended to this report:

Brennan D, Y Hu, S Joubeh, YW Choi, D Whitaker-Menezes, T O'Brien, J Uitto, U Rodeck, and MG Mahoney. (In press) Suprabasal Dsg2 expression in transgenic mouse skin confers a hyperproliferative and apoptosis-resistant phenotype to keratinocytes. *J Cell Science.*

Mishra SK, AH Talukder, AE Gururaj, Z Yang, RR Singh, MG Mahoney, C Franci, RK Vadlamudi, and R Kumar. (2004) Upstream determinants of estrogen receptor-alpha regulation of metastatic tumor antigen 3 pathway. *J Biol Chem* 279:32709-32715.

Mahoney MG, A Simpson, M Jost, M Noé, C Kari, D Pepe, YW Choi, J Uitto, and U Rodeck (2002) Metastasis-associated protein (MTA)1 enhances migration, invasion, and anchorage-independent survival of immortalized human keratinocytes. *Oncogene* 21:2161-2170.

Simpson A, J Uitto, U Rodeck, and MG Mahoney (2001) Differential expression and subcellular distribution of mouse metastasis-associated proteins Mta1 and Mta3. *Gene* 273:29-39.

CONCLUSIONS

This funding has allowed us to accomplish many of the objectives described in our original proposal. We plan to continue characterizing the signaling pathways commonly implicated in epidermal hyperplasia and carcinogenesis, i.e. the PI-3-kinase/AKT, NF-κB, and

the Raf/MEK/MAPK pathways. Most importantly, we will focus on the role of MTA1 in skin tumor development and progression.

REFERENCES

1. Manavathi B, Kumar R. The metastasis tumor antigens – an emerging family of multifaceted master coregulators. *J Biol Chem* In Press.
2. Hofer MD, Tapia C, Browne TJ, Mirlacher M, Sauter G, Rubin MA. A comprehensive analysis of the expression of the metastasis-associated gene 1 in human neoplastic tissue. *Arch Pathol Lab Med* 2006;130:989-96.
3. Pulkkinen L, Uitto J. Mutation analysis and molecular genetics of epidermolysis bullosa. Matrix Biol 1999;18:29-42.
4. Uitto J, Richard G. progress in epidermolysis bullosa: from epohums to molecular genetic classification. Clin Dermatol 2005;23:33-40.
5. Mishra SK, Talukder AH, Gururaj AE, et al. Upstream determinants of estrogen receptor-alpha regulation of metastatic tumor antigen 3 pathway. J Biol Chem 2004;279(31):32709-15.
6. Mahoney MG, Simpson A, Jost M, et al. Metastasis-associated protein (MTA)1 enhances migration, invasion, and anchorage-independent survival of immortalized human keratinocytes. Oncogene 2002;21(14):2161-70.
7. Behrens J, Frixen U, Schipper J, Weidner M, Birchmeier W. Cell adhesion in invasion and metastasis. Semin Cell Biol 1992;3(3):169-78.
8. Takeichi M. Cadherins in cancer: implications for invasion and metastasis. Curr Opin Cell Biol 1993;5(5):806-11.
9. Biedermann K, Vogelsang H, Becker I, et al. Desmoglein 2 is expressed abnormally rather than mutated in familial and sporadic gastric cancer. J Pathol 2005;207(2):199-206.
10. Kurzen H, Munzing I, Hartschuh W. Expression of desmosomal proteins in squamous cell carcinomas of the skin. J Cutan Pathol 2003;30(10):621-30.
11. Harada H, Iwatsuki K, Ohtsuka M, Han G, Kaneko F. Abnormal desmoglein expression by squamous cell carinoma cells. Acta Derm Venereol 1996;76:417-20.
12. Trojan L, Schaaf A, Steidler A, et al. Identification of metastasis-associated genes in prostate cancer by genetic profiling of human prostate cancer cell lines. Anticancer Res 2005;25:183-91.
13. Brennan D, Hu Y, Joubeh S, et al. Suprabasal Dsg2 expression in transgenic mouse skin confers a hyperproliferative and apoptosis-resistant phenotype to keratinocytes. J Cell Science In Press.

APPENDIX

Brennan D, Y Hu, S Joubeh, YW Choi, D Whitaker-Menezes, T O'Brien, J Uitto, U Rodeck, and MG Mahoney. (In press) Suprabasal Dsg2 expression in transgenic mouse skin confers a hyperproliferative and apoptosis-resistant phenotype to keratinocytes. *J Cell Science.*

Mishra SK, AH Talukder, AE Gururaj, Z Yang, RR Singh, MG Mahoney, C Franci, RK Vadlamudi, Kumar R. (2004) Upstream determinants of estrogen receptor-alpha regulation of metastatic tumor antigen 3 pathway. *J Biol Chem* 279:32709-15.

Mahoney, M.G.
Mahoney MG, A Simpson, M Jost, M Noé, C Kari, D Pepe, YW Choi, J Uitto, and U Rodeck (2002) Metastasis-associated protein (MTA)1 enhances migration, invasion, and anchorage-independent survival of immortalized human keratinocytes. *Oncogene* 21:2161-70.

Simpson A, J Uitto, U Rodeck, and MG Mahoney (2001) Differential expression and subcellular distribution of mouse metastasis-associated proteins Mta1 and Mta3. *Gene* 273:29-39.

In Press: Journal of Cell Science

Suprabasal Dsg2 expression in transgenic mouse skin confers a hyperproliferative and apoptosis-resistant phenotype to keratinocytes

Donna Brennan[1], Ying Hu[1], Sohaila Joubeh[1], Yoo Won Choi[1], Diana Whitaker-Menezes[2], Thomas O'Brien[1,3], Jouni Uitto[1], Ulrich Rodeck[1], and Mỹ G. Mahoney[1]*

Department of Dermatology and Cutaneous Biology[1] and Department of Pathology, Anatomy and Cell Biology[2], Thomas Jefferson University, and Lankenau Institute for Medical Research[3], Philadelphia, PA, U.S.A.

Running Title: Desmoglein 2 alters epidermal proliferation

Total number of words: 8183

Keywords: Carcinogenesis, Desmoglein, Differentiation, Hyperplasia, Keratinocyte

Abbreviations: BrdU, bromodeoxyuridine; CE, cornified envelope; Dsg, desmoglein; DMBA, 7,12-dimethylbenz[*a*]anthracene; Inv, involucrin; TPA, 12-*O*-tetradecanoylphorbol 13-acetate

*Address for Correspondence:

Mỹ G. Mahoney, Ph.D.
Department of Dermatology and Cutaneous Biology
Jefferson Medical College
233 S. 10th Street
Suite 419 BLSB
Philadelphia, PA 19107
Tel: 215-503-3240
Fax: 215-503-5788
Email: my.mahoney@jefferson.edu

Summary

Desmoglein 2 (Dsg2), a component of the desmosomal cell-cell adhesion structure, has been linked to invasion and metastasis in squamous cell carcinomas. However, it is unknown whether and how Dsg2 contributes to the malignant phenotype of keratinocytes. In this study, we addressed the consequences of Dsg2 overexpression under control of the involucrin promoter (Inv-Dsg2) in the epidermis of transgenic mice. These mice exhibited epidermal hyperkeratosis with slightly disrupted early and late differentiation markers, but intact epidermal barrier function. However, Inv-Dsg2 transgene expression was associated with extensive epidermal hyperplasia and increased keratinocyte proliferation in basal and suprabasal epidermal strata. Cultured Inv-Dsg2 keratinocytes showed enhanced cell survival in the anchorage-independent state that was critically dependent on EGF receptor activation and NF-κB activity. Consistent with the hyperproliferative/apoptosis-resistant phenotype of Inv-Dsg2 transgenic keratinocytes, we observed enhanced activation of multiple growth and survival pathways including PI-3-kinase/AKT, MEK/MAPK, STAT3, and NF-κB in the transgenic skin in situ. Finally, Inv-Dsg2 transgenic mice developed intraepidermal skin lesions resembling precancerous papillomas and were more susceptible to chemically induced carcinogenesis. In summary, overexpression of Dsg2 in epidermal keratinocytes deregulates multiple signaling pathways associated with increased growth rate, anchorage-independent cell survival, and the development of skin tumors in vivo.

Introduction

Desmosomes are intercellular junctions found primarily in epithelial tissues but also in certain non-epithelial tissues including the meninges, dendritic reticular cells of lymph node follicles, and myocardium (Cheng and Koch, 2004; Franke et al., 2006; McDonald et al., 2004). These adhesion structures are essential to maintaining tissue architecture during embryonic development and in the adult organism (Garrod et al., 2002). Desmosomes establish cell-cell contact through three families of proteins including the desmosomal cadherins, armadillo, and plakin proteins (Yin and Green, 2004; Kottke et al., 2006). Desmosomal cadherins include desmogleins (Dsg) and desmocollins (Dsc), which associate by both heterophilic and homophilic interactions (Chitaev and Troyanovsky, 1997; He et al., 2003). On the cytoplasmic side, desmosomal cadherins bind to plakoglobin, plakophilins 1-4, and the intermediate filament binding protein desmoplakin. The hallmark feature of the desmosomes is the linkage of this transmembrane protein complex to keratin intermediate filaments forming a highly organized structure that allows cells and tissues to withstand mechanical stress and disruption (Cowin, 1994; Cowin and Burke, 1996; Green and Jones, 1996).

Four distinct desmogleins (Dsg1-4) have been reported with differential expression profiles dependent on the tissue type and differentiation state (Cheng and Koch, 2004; Garrod et al., 2002; Mahoney et al., 2006). Unlike Dsg1 and Dsg3 whose expression is restricted to complex stratified epithelia, Dsg2 and Dsg4 are expressed in a wide range of other cell types. For example, Dsg2 has been detected in simple epithelia including the stomach mucosa and intestines as well as in select non-epithelial tissues such as the myocardium (Koch et al., 1992; Schäfer et al., 1994; Schäfer et al., 1996). Despite rapid recent progress in understanding the role of desmogleins in epidermal cell adhesion and morphogenesis, the contribution of Dsg2 to

these phenomena is poorly understood. Although elegant work has recently been done using reconstitution studies in cultured cells (Getsios et al., 2004), the adhesive properties of Dsg2 in the context of other co-expressed desmoglein family members in the in vivo context remain largely undefined. Interestingly, in humans, mutations in *DSG2* gene are associated with Arrhythmogenic Right Ventricular Cardiomyopathy (Pilichou et al., 2006). The development and characterization of *Dsg2* null mice has reinforced the notion that Dsg2 has important biological roles beyond epidermal cell-cell adhesion as these mice die at, or shortly after implantation (Eshkind et al., 2002). While this circumstance precluded an investigation of Dsg2 as it relates to epidermal functions, Dsg2 null mice revealed that Dsg2 contributes to embryonic stem cell proliferation particularly in the inner cell mass of the developing blastocyst. In addition to being a structural component of desmosomes, Dsg2 is overexpressed or abnormally expressed in select epithelial malignancies including squamous cell carcinomas (Biedermann et al., 2005; Denning et al., 1998; Harada et al., 1996; Kurzen et al., 2003; Schäfer et al., 1996). Similarly, genetic profiling of prostate cancer cell lines showed increased expression of Dsg2 in a metastatic cell line as compared to it's non-metastatic syngeneic precursor cell (Trojan et al., 2005).

To investigate Dsg2 functions in epidermal biology, we established transgenic mice expressing Dsg2 in the differentiating layers of the epidermis under control of the involucrin promoter (Inv-Dsg2). Here we describe that Inv-Dsg2 transgenic mice exhibited epidermal hyperplasia associated with an increase in cell proliferation and enhanced activation of the PI-3-kinase/AKT, MEK/MAPK, STAT3 and NF-κB signaling pathways. In addition, transgenic keratinocytes acquired resistance to apoptosis incurred in the anchorage-independent state (anoikis). Finally, Inv-Dsg2 transgenic mice were prone to papilloma development both

spontaneously and upon application of chemical carcinogens. Collectively, these results highlight previously unrecognized aspects of Dsg2 in support of malignant transformation of epithelial cells. The Inv-Dsg2 mice provide a facile model system for in-depth studies of this phenomenon in the in vivo context.

Results

Characterization of transgene expression in Inv-Dsg2 transgenic mice

To express Dsg2 in the suprabasal epidermis, we subcloned mouse Dsg2-Flag cDNA into the pH3700-pL2 parental vector epitope at the *Not*I restriction site down-stream of the involucrin promoter (Fig. 1A). We obtained seven male and one female founder mice, bred the male founders back to C57Bl/6 females and screened the F1 generation by PCR. Two independent transgenic lines were maintained showing similar phenotype among all progeny. Inv-Dsg2 transgenic mice developed normally (healthy, fertile, and normal lifespan) with no gross abnormalities in skin or hair appearance compared to wild-type littermates.

We assessed the expression of the Dsg2-Flag transgene in adult (3 months old) transgenic skin by immunostaining with an anti-Flag (Fig. 1B, left panels) and Dsg2-specific MP6 antibodies (Fig. 1B, middle panels). As expected, Dsg2 and Flag antibodies strongly reacted with suprabasal cell layers of the transgenic epidermis revealing similar staining patterns (Fig. 1B, right panels). Immunoblotting analysis of total skin lysates from adult control and transgenic mice confirmed the immunofluorescence data (Fig. 1C) as the MP6 and the anti-Flag antibodies detected a similar size band in adult transgenic skin lysates. As expected, little if any endogenous Dsg2 was detected in the wild-type skin lysate by the MP6 antibody (Fig. 1C,B). These results demonstrate expression of the transgene Dsg2-Flag in the differentiated cell layers of the epidermis. Note that MP6 and Flag antibodies can not be used on paraffin embedded tissues thus limiting the present analysis to frozen sections which are not ideal for obtaining punctate cell-cell border staining in the differentiated layers of the mouse epidermis.

Histological changes associated with Inv-Dsg2 transgene expression in mouse epidermis

To examine transgene-induced alterations in the epidermis (Fig. 2), we collected back skin (A-D, I,J), ears (E,F), and tongues (G,H) from transgenic (B,D,F,H,J) and wild-type (A,C,E,G,I) littermates at birth and at 3 months of age. Tissue sections were stained with hematoxylin and eosin. All transgenic skin samples exhibited hyperplasia and slight hyperkeratosis. This phenotype was most evident in the skin of adult animals (compare Fig. 2D to Fig. 2C and Fig. 2I to Fig. 2J). In addition, keratinocytes in the stratum spinosum of transgenic skin were larger with bigger nuclei. A thicker granular layer with some nuclei retention was also apparent (Fig. 2B,D). We also observed pink translucent flattened eosinophilic keratinocytes in the transgenic ear (open arrow in Fig. 2F) similar to the stratum lucidum of thick skin (Montagna et al., 1989). Transgenic mice also contained a "sticky" stratum corneum (* in Fig. 2B,D) similar to that of the Inv-mDsg3 transgenic mice previously described (Elias et al., 2001). The irregular and fragmented stratum corneum of Inv-Dsg2 transgenic epidermis was similar in appearance to that observed in dry scaly skin where stratum corneum production occurs at a faster rate than normal (Harding, 2004). In addition, we observed slightly hyperplastic epidermis in the tongue of adult transgenic compared to wild-type mice (Fig. 2G,H). Note that transgenic lines carrying a lower transgene expression developed a less extensive epidermal hyperproliferative phenotype. In addition, compared to heterozygous transgenics, homozygous littermates showed increased transgene expression and as well as a more dramatic hyperproliferation (data not shown). In summary, suprabasal expression of Dsg2 was associated with increased epidermal thickening, a phenotype becoming more prominent in adult animals.

To further examine the transition between the stratum granulosum and stratum corneum, electron microscopy was performed on back skin from wild-type and transgenic mice (Fig. 3).

Consistent with the light microscopic observations we observed subtle morphological abnormalities particularly at the stratum granulosum–stratum corneum interface. Furthermore, the corneocytes of the Inv-Dsg2 skin were much thicker in the axial direction (Fig. 3, brackets). The Inv-Dsg2 skin further demonstrated increased thickness of the granular cell layer, as evidenced by the presence of more keratohyalin granules. We did not observe any abnormalities in desmosome size and appearance in the granular cell layers of wild-type and transgenic skin. In control epidermis, an abrupt transition was observed from the granular layer to the stratum corneum (Fig. 3A). The desmosomes in the last granular cell layer of wild-type epidermis retained the dense plaque with electron dense cytokeratin filament bundles, while a less distinct plaque sans cytokeratins was observed on the opposing face (Fig. 3A, arrows). This was less prominent in the Inv-Dsg2 transgenic skin. Similar to the Inv-mDsg3 transgenic mice (Elias et al., 2001), we observed a high number of electron dense intercellular structures (Fig. 3B, arrow heads) that became detached (Fig. 3B, *) in the cleft of separated corneocytes. Note, other than slightly larger cells as observed by histology, no significant morphological differences were observed between the keratinocytes of the basal and spinous layers of Inv-Dsg2 transgenic and control wild-type animals (not shown).

Effects of suprabasal Dsg2 expression on expression of epidermal adhesion, structural, and differentiation proteins

Next we examined the effect of suprabasal expression of Dsg2 on the molecular composition of desmosomal junctions by immunohistochemical analysis of desmogleins (Dsg1-α, -β, and -γ, and Dsg3) and desmosomal plaque proteins (desmoplakin and plakoglobin). Overexpression of Dsg2 did not markedly alter the expression pattern of any of these proteins (Fig. S1A). The distribution of adhesion proteins, especially those concentrated in the upper layers such as the

three Dsg1 isoforms, appears to be broader in the transgenic mice, probably due to the increase in the total number of cell layers. Interestingly, the expression of desmoplakin (Fig. S1Ai,j) and plakoglobin (Fig. S1Ak,l) slightly were increased in the transgenic skin. Insets in Figure S1Ai,k show wild-type images taken at the same exposure time as Figure S1Aj,l. Note that Dsg4 was expressed at low levels in the mouse epidermis and that suprabasal expression of Inv-Dsg2 transgenic mice did not affect Dsg4 expression (not shown). Finally, the expression of proteins within the adherens junctions, such as E-cadherin and β-catenin, were not affected in the Inv-Dsg2 transgenic epidermis (Fig. S1B).

Next we asked whether overexpression of Dsg2 in the superficial epidermis had an effect on the expression and organization of cytoskeletal and differentiation proteins. By immunofluorescence we observed that suprabasal Dsg2 expression was associated with altered expression patterns of several biochemical markers for keratinocyte differentiation, including cytokeratins (CK), involucrin, loricrin, and filaggrin (Fig. 4). CK14 was detected only in the basal layer of the control wild-type skin, but its expression extended into the suprabasal cell layers of the transgenic epidermis (Fig. 4A). Similarly, immunoblot analysis of epidermal protein extracts revealed enhanced expression of CK14 in transgenic as compared to wild-type skin (Fig. 4B). CK10 expression was similarly increased in transgenic skin extracts (Fig. 4B) and was localized to the superficial epidermis of transgenic skin (Fig. 4A). Under homeostatic conditions, CK6 expression is restricted to the hair follicles, whereas it extends into the interfollicular epidermis under hyperproliferative conditions, for example psoriatic lesions (Heyden et al., 1994; Mils et al., 1992; Stoler et al., 1988) or during wound healing (Coulombe, 1997; McGowan and Coulombe, 1998). Interestingly, we observed intermittent expression of CK6 in the interfollicular epidermis of the Inv-Dsg2 transgenic, whereas CK6 was completely

absent from interfollicular epidermis of control wild-type littermate (Fig. 4A). Because CK6 expression in the interfollicular epidermis was sparse while high in the hair follicles, immunoblotting detected similar levels of CK6 in both wild-type and transgenic skin lysates (Fig. 4B). Induction of CK6 and CK14 expression in the suprabasal epidermis is further indicative of altered epidermal differentiation in the Inv-Dsg2 transgenic mice.

Consistent with the thickening of the granular cell layers, we observed an increase in expression of cornified envelope proteins including the differentiation marker involucrin (Fig. 4A,B). Filaggrin, an intermediate filament-associated protein expressed during the late stages of differentiation in the granular cells of the epidermis (Yaffe et al., 1993), was also over-expressed in the transgenic epidermis (Fig. 4A,B). Upon longer exposure, the wild-type filaggrin immunoblot showed a similar protein banding pattern to that of the transgenic blot (not shown). Similar to findings in transgenic mice expressing human Dsg3 under the keratin 1 promoter control (K1-hDsg3), the Inv-Dsg2 transgenic epidermis revealed an increase in granular cell layers as shown by the increased number of cells stained positive for loricrin, a cornified envelope precursor protein (Fig. 4A). These results were confirmed by immunoblotting (Fig. 4B).

We next sought to determine the effect of Dsg2 overexpression on the subcellular location of desmosomal components in the Inv-Dsg2 transgenic skin. First, we extracted adult wild-type and transgenic skin in Triton-soluble and -insoluble fractions. Immunoblotting analysis showed Dsg2-Flag in both Triton-soluble and -insoluble fractions while other desmosomal proteins (Dsg1, 3, and 4 and desmoplakin) were found exclusively in the Triton-insoluble fraction (Fig. S2A). It is unclear whether the presence of Dsg2-Flag in the Triton-soluble fraction of transgenic mice is due to high protein expression or a novel functional role of Dsg2 independent

of desmosomes. As expected, plakoglobin, and β-catenin were detected in both Triton-soluble and -insoluble fractions. Thus, suprabasal expression of Dsg2 did not alter the Triton solubility of desmosomal proteins.

To elucidate the potential mechanism underlining epidermal hyperproliferation in the Inv-Dsg2 transgenic skin, we performed additional subcellular fractionation of wild-type and transgenic skin. Total skin proteins were purified for crude (soluble) cytoplasmic, enriched (wash) cytoplasmic, crude nuclear (high salt), and enriched nuclear/cytoskeletal (insoluble) proteins. Interestingly, the expressed Dsg2-Flag transgene was detected not only in the cytoplasmic but also the nuclear fractions (Fig. S2B). This finding is significant since Dsg2 is overexpressed in squamous cell carcinomas of the skin. It is unknown whether Dsg2 is present in the nuclei of these carcinomas or whether Dsg2 serves any functions in the nucleus. The other desmosomal proteins were localized mainly in the insoluble pool along with cytokeratins (Fig. S2B).

The armadillo family of adhesion/signaling proteins found in desmosomal and adherens junctions include β-catenin, plakoglobin, and plakophilin 1. Plakoglobin was recently shown to play an important role in negatively-regulating the expression of the proto-oncogene c-Myc (Williamson et al., 2006). Thus, we performed subcellular fractionation to determine whether epidermal hyperproliferation in Dsg2 transgenic mice is due to down-regulation of the nuclear pool of plakoglobin (Fig. S2B). Immunoblotting analysis showed the subcellular pools including the nuclear fraction of plakoglobin were relatively unchanged in transgenic compared to wild-type skin. Unexpectedly, while the cytoskeletal pool of β-catenin was unchanged between the wild-type and transgenic animals, both the cytoplasmic and nuclear pools of β-

catenin were significantly reduced in Inv-Dsg2 transgenic compared to control wild-type skin (Fig. S2B). Thus, suprabasal expression of Dsg2 did not alter plakoglobin expression or subcellular localization but did reduce the cytoplasmic and nuclear levels of β-catenin. It remains to be determined in future studies how this observation relates to the upregulation of c-Myc expression in transgenic mice.

To further investigate the thickening of the granular layers, we isolated cornified envelopes (CEs) from wild-type and Inv-Dsg2 transgenic newborn (1-2 days) and adult (3 months) skin and ear (Table 1). This analysis revealed only a marginal increase in CE production in transgenic newborn dorsal and in adult mouse ear skin as compared to wild-type skin. These results are consistent with the histology data showing only minor hyperplasia in newborn skin and adult ear epithelia (Fig. 2A,B). By contrast and consistent with the age-dependent increase in hyperplasia (Fig. 2C,D), a dramatic increase in CE production was seen in adult back skin of Inv-Dsg2 transgenic relative to wild-type animals (Table 1). Although the number of CEs increased in the transgenic skin, we observed no significant difference in their susceptibility to stress by ultrasound treatment under the conditions chosen (data not shown).

Suprabasal expression of Dsg2 altered the adhesive strength of the stratum corneum

In newborn Inv-Dsg2 transgenic mice, we observed abnormal organization and fragmentation of the corneal layers (Fig. S3A, arrows and bracket). To assess functional consequences of the morphological changes in the stratum corneum, we tape-stripped transgenic and control wild-type littermates. The stratum corneum of control mice detached in organized sheets while the transgenic mice showed scattered fragmented sheets of corneocytes (Fig. S3B). After ten tape strips, the stratum corneum in transgenic mice and normal littermates appeared more similar

although there were still more corneocytes removed from the control compared to the transgenic skin. These results demonstrate moderate changes in morphology and mechanical properties of the stratum corneum in Inv-Dsg2 transgenic mice.

Epidermal hyperproliferation in Inv-Dsg2 transgenic mice

To assess the proliferative state of the Inv-Dsg2 epidermis, skin sections of wild-type and transgenic mice were stained with an antibody to the proliferating cell nuclear antigen (PCNA); an increase in PCNA staining generally correlates with mitotic activity and cell proliferation. In wild-type skin, we observed intermittent staining of nuclei in the basal cell layer (arrow in Fig. 5A). In contrast, virtually all nuclei in the basal layer of the transgenic epidermis were stained with the PCNA (Fig. 5B). Additionally, some transgenic suprabasal cells were also positive for PCNA (Fig. 5B, arrows). These results are consistent with epidermal hyperproliferation. To further investigate the proliferative state of the transgenic epidermis, we injected wild-type and transgenic mice with BrdU, a halogenated thymidine analog that integrates into the DNA of actively dividing cells progressing through S-phase of the cell cycle. We identified actively dividing cells within an hour of BrdU treatment and observed markedly enhanced BrdU-labeled cells in the transgenic (13 ± 6 per 100 basal cells) over wild-type epidermis (2 ± 2 per 100 basal cells) (Fig. 5C,D). In further support of epidermal hyperproliferation in transgenic epidermis we observed enhanced expression of the c-Myc relative to wild-type epidermis (Fig. 6). Thus, overexpression of Dsg2 in the superficial epidermis results in epidermal hyperplasia associated with enhanced proliferation of keratinocytes.

Deregulated signal transduction pathways in the epidermis of Inv-Dsg2 transgenic mice

Next, we investigated activation states of signaling pathways commonly implicated in epidermal

hyperplasia, i.e. the mitogen-activated Raf/MEK/MAPK and the PI-3-kinase/AKT pathways. This analysis revealed slight increase in total AKT, markedly higher levels of AKT phosphorylation on both Ser473 and Thr308, and of the AKT target GSK-3β on Ser9 in transgenic epidermis as compared to epidermis from wild-type mice (Fig. 6). AKT-Thr308 is phosphorylated by the phosphoinositide-dependent protein kinase(PDK)1 (Mora et al., 2004) which also showed higher phosphorylation levels in Inv-Dsg2 trasngenic epidermis. Additionally, we examined phosphorylation level of PTEN, a negative regulatory phosphatase of the PI-3-kinase/AKT pathway. Phosphorylation of PTEN has been described to sequester PTEN in the cytoplasm, thus preventing recruitment of this negative regulator of PI-3-kinase to the cell membrane (Das et al., 2003). Consistent with increased PI-3-kinase/AKT activity in transgenic epidermis we observed increased in both total PTEN and PTEN Ser308 phosphorylation (Fig. 6). The Raf/MEK/MAPK signaling axis was similarly deregulated in transgenic epidermis with increased steady-state phosphorylation of Raf, MEK1/2, and p42/44 MAPK as well as the MAPK target p90RSK (Fig. 6).

We next examined the expression and phosphorylation levels of STAT3, a cytokine-activated transcription factor that upregulates oncogenes such as c-Myc and Bcl-X_L. STAT3 has been proposed to be a key player in regulating cell cycle and tumor progression in squamous cell carcinomas. Increased STAT3 phosphorylation was detected in transgenic relative to wild-type skin (Fig. 6). No change in total STAT3 was detected in wild-type and transgenic skin. Collectively, these results demonstrate that increased epidermal proliferation in Inv-Dsg2 transgenic mice was associated with enhanced activation of at least three major signaling pathways including PI-3-kinase/AKT, MEK/MAPK, and STAT3.

Dsg2 overexpression enhances anchorage-independent keratinocyte survival

In order to determine functional aspects of Dsg2 overexpression for keratinocyte biology in vitro, we established keratinocyte cultures from Inv-Dsg2 transgenic and wild-type newborn mouse back skin. This was accomplished by initiating cell lines in culture medium containing low Ca^{2+} (0.08 mM). Under these conditions, the Dsg2-Flag transgene was not expressed because the involucrin promoter was not induced (Fig. 7A,B). However, addition of Ca^{2+} (1 mM) induced both differentiation and transgene expression as determined by immunoblot and immunofluorescence analysis of the Flag tag (Fig. 7A,B). Note that Dsg1 isoforms were not expressed until 2-3 days after calcium treatment (data not shown). Similar to the in vivo model, overexpression of Dsg2 also enhanced STAT3 phosphorylation in cultured keratinocytes (Fig. 7A). Cellular differentiation upon calcium treatment was confirmed by upregulation of involucrin expression (Fig. 7A). An alternative method to induce keratinocyte differentiation is to place these cells into forced suspension culture, which prevents anchorage to the extracellular matrix. Loss of cell matrix adhesion leads to robust induction of involucrin expression in human keratinocytes (Rodeck, unpublished observation). Thus we expected that the Dsg2 transgene under control of the involucrin promoter would be similarly induced. Indeed, we observed robust involucrin and Dsg2 transgene expression in forced suspension culture in transgenic but not wild-type keratinocytes (Fig. 7C).

This circumstance allowed us to monitor effects of Dsg2 overexpression to keratinocyte biology in the anchorage-independent state. In the absence of extracellular matrix attachment, epithelial cells including keratinocytes undergo a specialized programmed cell death referred to as "anoikis" (Frisch and Francis, 1994). To ascertain potential effects of Dsg2 overexpression on cell survival in the anchorage-independent state, transgenic and wild-type cells were seeded

on top of an agarose layer which prevents cell attachment to substrate (forced suspension culture) followed by transfer of cells to cell culture-treated plastic; upon reseeding only viable cells will reattach and commence proliferation (Mahoney et al., 2002b; Rodeck et al., 1997b). Survival and proliferation of rescued cells was scored by observing colony formation of reseeded cells visualized by crystal violet staining. These experiments revealed a clear survival advantage of the Inv-Dsg2 transgenic over wild-type keratinocytes (Fig. 8A). Not only did more transgenic keratinocytes reattach after prolonged (3 days) forced-suspension culture, but they also formed larger colonies than wild-type keratinocytes upon further incubation (Fig. 8A). Collectively these results suggest that Dsg2 overexpression increases resistance of keratinocytes to anoikis. They are consistent with high level of expression of the pro-survival protein Bcl-X_L in transgenic epidermis (Fig. 6) and raise the question which signaling pathways supports anchorage-independent cell survival.

This question was addressed by performing forced suspension/rescue experiments in the presence of pharmacological inhibitors of signaling pathways targeting activation of the EGFR, PI-3-kinase, MEK1/2, and NF-κB. Activation of the NF-κB pathway has previously been implicated in epithelial cell survival in three-dimensional mammary cell tissue reconstructs (Rodeck et al., 1997a; Weaver et al., 2002; Zahir et al., 2003) and in human keratinocyte suspension cultures (Ren et al., 2006). To assess the importance of NF-κB signaling in growth and survival of Inv-Dsg2 transgenic keratinocytes, we used the pharmacologic inhibitor, Bay11-7082, which inhibits NF-κB activity by inhibiting IκB-alpha phosphorylation thus preventing nuclear translocation of NF-κB dimers. Bay11-7082 abolished proliferation and survival of Inv-Dsg2 transgenic as well as wild-type keratinocytes in the anoikis setting (Fig. 8B). The epidermal growth factor receptor (EGF-R) activation has been shown to provide a measure of

protection against death of keratinocytes cells in suspension (Jost et al., 2001b). Here we show that activation of EGF-R with exogenous EGF enhanced growth and survival of transgenic keratinocytes, but was unable to reverse the effect of Bay11-7082 (Fig. 8B). Similar results were obtained with MG132, a proteasome inhibitor that prevents IκB degradation (not shown). Interestingly, inhibitors of MEK1/2 (U0126) and PI-3-kinase had only marginal effects on mouse keratinocyte survival regardless of transgene expression (not shown). To assess the activation state of NF-κB in Inv-Dsg2 transgenic epidermis, we examined the expression and subcellular localization of NF-κB p65 protein in situ. We observed a dramatic increase in p65 expression in transgenic compared to wild-type skin by immunblotting (Fig. 8C) and immunofluorescent staining (Fig. 8D). In addition, NF-κB p65 protein was detected in cell nuclei indicative of activation in transgenic but not wild-type skin (Fig. 8D). Collectively, these results demonstrate that Dsg2-mediated cell survival is controlled, in part, by EGFR- and NF-κB-dependent signaling events.

Tumor formation in Inv-Dsg2 transgenic epidermis

Previously, overexpression of Dsg2 has been described in squamous cell carcinomas of the skin (Denning et al., 1998; Harada et al., 1996; Schäfer et al., 1996). Interestingly, histological analysis revealed sporadic and spontaneous appearance of benign papillomas in over half of our Inv-Dsg2 transgenic animals at 6 weeks (Fig. 9A) and 3 months of age (Fig. 9B) in the absence of carcinogen treatment. By contrast, none of the wild-type mice examined developed epidermal hyperplasia or papillomas (Fig. 9A,B, upper panels). In the Inv-Dsg2 transgenic animals, we observed extensive hyperkeratosis (box), marked hyperproliferation (arrows) with epidermal outgrowths extending over the existing epidermis forming two complete skin layers. When

these outgrowths came in contact with each other, they appeared to merge, often encapsulating (*) the stratum corneum.

The hyperpoliferative/apoptosis resistant phenotype of Inv-Dsg2 transgenic keratinocytes raised the question whether the transgenic mice would be prone to carcinogen-induced tumor development. To determine whether the transgenic mice were more susceptible to chemical-induced carcinogenesis, we treated transgenic and wild-type control littermates once with DMBA followed by twice weekly TPA treatments to promote tumor formation. The transgenic mice showed significantly increased susceptibility to skin tumor formation compared to wild-type littermates (Fig. 9C). The transgenic mice developed higher total number of tumors 12.4 ± 6.1 (mean and standard deviation at week 25) compared wild-type mice at the same time point with only 4.8 ± 4.1 tumors (Student's *t* test, P=0.0152) (Fig. 9D). This difference was even more pronounced when we counted only papillomas with diameters greater than 2 mm with transgenic mice averaging 8.9 ± 4.5 tumors per animal compared to wild-type with only 2.1 ± 2.1 tumors (Student's *t* test, P=0.0063) (Fig. 9E). These results are consistent with a functional role of Dsg2 overexpression by keratinocytes in tumor development. Despite enhanced tumor development in the transgenic mice, histological analysis showed no significant differences in the architecture of the transgenic and wild-type papillomas (Fig. 9F). At 25 weeks, the papillomas in both groups were well differentiated with minor hyperkeratosis. No gross signs of invasiveness or secondary tumors were observed in the livers or lungs, known target organs of invasive carcinomas.

Discussion

This report describes the establishment and characterization of Inv-Dsg2 transgenic mice, in which Dsg2 expression was directed by the involucrin promoter to the differentiating cell layers of the epidermis. Ectopic Dsg2 expression resulted in subtle perturbation of epidermal differentiation and alterations in expression of some desmosomal and terminal differentiation proteins. Furthermore, mild structural abnormalities in the stratum corneum were evident morphologically as determined by tape stripping.

The rather moderate changes in differentiation and hyperkeratosis of Inv-Dsg2 transgenic epidermis were contrasted by epidermal hyperplasia, which was most pronounced in adult animals. Epidermal hyperplasia manifested as enhanced thickness due to an increase in cellularity up to 10 cell layers. The hyperplasia in the transgenic adult mouse skin was associated with increased PCNA staining and BrDU labeling indicative of accelerated cell cycle progression and proliferation. The hyperproliferative phenotype in situ was accompanied by multiple molecular alterations consistent with accelerated cell cycle progression. We observed a marked increase in c-Myc expression in the transgenic relative to wild-type skin. Activation of c-Myc in basal keratinocytes has been previously linked to hyperproliferation (Arnold and Watt, 2001; Frye et al., 2003; Waikel et al., 2001) while suprabasal c-Myc activation is linked to proliferation and disruption of terminal differentiation (Pelengaris et al., 1999; Waikel et al., 1999). Interestingly, epidermal hyperplasia and hyperkeratosis observed in Inv-Dsg2 transgenic mice is reminiscent of the ML-*myc2* transgenic mice overexpressing c-Myc in the differentiated epidermis under control of the loricrin promoter (Waikel et al., 1999).

Consistent with the hyperproliferative phenotype, we observed high activation states of the PI-3kinase/AKT, Raf/MEK/MAPK, STAT3, and NF-κB signaling pathways in transgenic skin. Previous work has implicated these signaling events not only in keratinocyte proliferation but also in enhanced keratinocyte survival in experimental conditions that induce apoptosis of normal keratinocytes, notably deprivation of extracellular matrix interaction (Jost et al., 2001b; Ren et al., 2006). Indeed, we observed markedly higher rates of anchorage-independent survival of Inv-Dsg2 transgenic when compared to wild-type keratinocytes. This effect was, at least in part, due to activation of EGF-R and NF-κB signaling as demonstrated by use of EGF and pharmacological inhibitors of NF-κB pathways. Previous work has implicated both signaling pathways in aberrant anchorage-independent survival of human keratinocytes (Jost et al., 2001a; Jost et al., 2001b; Ren et al., 2006). Furthermore, deregulated EGF-R (Chan et al., 2004; Hansen et al., 2000; Merlino et al., 1985; Ozawa et al., 1989; Sibilia et al., 2000; Woodworth et al., 2000) and NF-κB (Chung et al., 2004; Dong et al., 2001; Duffey et al., 1999; Loercher et al., 2004) signaling have been described in human squamous cell carcinomas, and both pathways have been linked to upregulation of the anti-apoptotic Bcl-2 family member Bcl-X_L in epithelial cells. Consistent with these earlier results, we observed high expression level of Bcl-X_L in transgenic but not wild-type epidermis. Most importantly, we also observed high rates of spontaneous and carcinogen-induced papilloma formation in the epidermis of Inv-Dsg2 transgenic mice. To our knowledge, we are first to report that misexpression of a desmosomal cadherin in the epidermis affects susceptibility to skin tumor development. This result, however, is consistent with previous reports of Dsg2 overexpression in human squamous cell carcinomas. We propose that the inappropriate Dsg2 expression contributes to epidermal tumorigenicity by deregulating signal transduction pathways altering the hyperproliferative and apoptosis-

resistance phenotype of keratinocytes. We submit that the Inv-Dsg2 mice described here provide an excellent in vivo model system to further investigate signaling events downstream of Dsg2 overexpression as they relate to roles of desmosomal cadherins beyond maintenance of cell adhesion and tissue integrity.

These results contrast with previous observations of decreased Dsg2 expression during tumor development (Rieger-Christ et al., 2005;Yashiro et al., 2006). Specifically, restoring PG expression in bladder carcinoma cells resulted in elevated level of Dsg2 expression and suppression of migration and tumorigenic potential (Reiger-Christ et al., 2005). Of note this study primarily focused on functional roles of PG in heterogeneous bladder carcinoma cell lines whereas the present study is concerned with deregulated Dsg-2 expression in keratinocytes. It is possible that these discrepant findings reflect the transformed state of the particular cell lines studied. Alternatively, Dsg2 expression may play different roles in different tissues.

Previous work has implicated desmosomal cadherins in epidermal proliferation, differentiation, and morphogenesis (Chidgey et al., 2001; Elias et al., 2001; Eshkind et al., 2002; Hardman et al., 2005; Merritt et al., 2002). For example, expressing Dsc1 in the proliferative basal layer, where it is not normally expressed, using the K14 promoter did not affect epidermal morphogenesis and development (Henkler et al., 2001) whereas ectopic expression of Dsc3, which normally is restricted to the basal cell layer, in the spinous layers using the K1 promoter altered epidermal differentiation (Hardman et al., 2005). Targeting Dsg3 expression to the spinous layers using the K1 promoter also affected epidermal proliferation and differentiation (Merritt et al., 2002). Furthermore, expressing Dsg3 in the upper spinous and granular layers using the involucrin promoter disrupted epidermal barrier function (Elias et al., 2001). The histological and ultrastructural changes observed in the Inv-Dsg2 mice described here were

significantly different from those of the Inv-mDsg3 transgenic mice (Elias et al., 2001). Shortly after birth the Inv-mDsg3 mice die of dehydration due to transepidermal water loss while the Inv-Dsg2 mice described in this report survived to adulthood without any obvious loss of epidermal barrier function. The outer stratum corneum of the newborn Inv-mDsg3 transgenic skin resembled that of the oral mucosa, whereas the Inv-Dsg2 transgenic stratum corneum displayed only minor "stickiness" behavior in the early transition between the granular to corneal layers. The remaining upper layers of the stratum corneum had the appearance of the normal "basket weave" pattern although it was fragmented and unorganized upon further inspection. Thus, overexpression of either Dsg3 or Dsg2 in the differentiating epidermal strata has dramatically different consequences for epidermal barrier function. A possible compensatory mechanism to prevent this severe skin barrier phenotype may be the upregulation of CE components such as SPRRP2D and SPRRP2H, members of the small proline rich family of proteins (Jarnik et al., 1996), which were observed overexpressed in Inv-Dsg2 transgenic compared to wild-type skin (Mahoney, unpublished RT-PCR results). In addition, both early and late differentiation proteins, such as CK10 and filaggrin respectively, were perturbed in adult Inv-Dsg2 transgenic mice. In particular, we observed significant induction of CK14 into suprabasal layers of Inv-Dsg2 possibly indicating a more proliferative basal-like phenotype of those cells. Thus, the aberrant and fragile phenotype of the stratum corneum in our Inv-Dsg2 transgenic mice may be due to the high suprabasal expression of CK6 and CK14 mimicking that of the oral mucosal epithelium (Lindberg and Rheinwald, 1990).

Materials and Methods

Antibodies

Antibodies used were: Flag M2 (1:2000, Sigma); pan-cytokeratin (1:1000, Biomeda, Foster City, CA); β-actin (1:5000) and cytokeratin 14 (1:1000) (Calbiochem, San Diego, CA); MP6 (1:5000); BrdU-FITC (neat), E-cadherin (1:2500), γ-catenin (1:2000), and β-catenin (1:500, BD Biosciences, San Jose, CA); PCNA (1:1000, Oncogene Science, Cambridge MA); AP61 Dsg1-α (1:50); AP498 Dsg1-β (1:2); Ab15 Dsg1-γ (1:10,000); 4B3 Dsg3 (1:64,000) and AP904 Dsg3 (1:200); involucrin (1:1000, BabCo, Berkeley, CA); loricrin (1:1000) and filaggrin (1:2000, Covance research labs, Cumberland, VA); cytokeratin 6 (1:20, Novocastra, Newcastle upon Tyne, UK); cytokeratin 10 (1:500, NeoMakers, Fremont, CA); 27B2 Dsg1, 6F9 β-catenin, 23F4 desmoplakin, and 11E4 plakoglobin (1:100) (Wahl et al., 1996); all cell signaling antibodies (1:1000, Cell Signaling Technology, Danvers, MA): P-Raf (9421), P-MEK1/2 (9121), P-MAPK (9101), P-p90RSK (9341), PTEN (9552), P-PTEN (9551) P-PDK1 (3061), STAT3 (9132), P-STAT3 (9131), AKT (9272), P-AKT (ser 473) (9271), P-AKT (thr 308) (9275), P-GSK-3β (9336), and c-Myc (9492); Bcl-X_L (1:1000, Signal Transduction Lab); NF-κB p65 (1:1000, Santa Cruz Biotech, Santa Cruz, CA); FITC- and TxR-conjugated secondary antibodies (1:200, Molecular probes, Eugene, OR); HRP-conjugated secondary antibodies (1:5000, Jackson labs, Bar Harbor, Maine).

Generation of transgenic mice

Mouse Dsg2 (mDsg2) cDNA was cloned using methods previously described (Mahoney et al., 2002a). The nucleotide primer (5'-GGC GGC CGC CTA CTT GTC ATC GTC GTC CTT GTA GTC GGA GTA AGA ATG CTG TAC AG-3') was used by polymerase chain reaction (PCR) to

add the Flag epitope (underlined) to the 3' end of mDsg2 cDNA. Sequence was confirmed by automated nucleotide sequencing (ABI, Foster City, CA). The mDsg2-Flag cDNA was inserted in place of the β-galactosidase gene (excised with *Not*I) in the involucrin promoter vector pH3700-pL2 (Fig. 1A). The involucrin promoter-mDsg2-FLAG transgene was excised with *Sal*I and microinjected into the male pronuclei of B6C3F1 mice zygotes, which were then implanted into CD-1 foster mothers.

Genotyping of progeny was established by PCR using DNA extracted from tail clippings according to the manufacturer's protocol (PureGene kit, Gentra system, Minneapolis, MN). Primers 5'-CAC TAG CAT TCT TGA CCG G-3' (exon 4) and 5'-GCA-TTC-AGA-GTC-TCC-GGG-T-3' (exon 6) were used to generate a 1406 bp PCR product from genomic DNA or a 243 bp product from the Inv-Dsg2 transgenic cDNA. PCR reactions were performed in 50 µl reaction volume containing 10 ng of mouse genomic DNA, 200 µM of each nucleotide, 0.25 µM primers, 20% (vol/vol) buffer Q, 2.5 U of Taq polymerase, and standard reaction buffer (Qiagen Inc., Valencia, CA). The PCR conditions were 95°C for 3 min, followed by 35 cycles of 95°C for 30 sec, 58°C for 1 min, and 72°C for 1 min.

Newborn, 6 weeks, and adult (3 months) wild-type and transgenic littermates were used for these studies. All animals were back-crossed to C57Bl/6J 5 times. Some immunohistochemistry experiments were performed on animals between crosses 3-5. Similar results were observed.

Histology and transmission electron microscopy

Unless otherwise indicated, all chemicals were from either Sigma (St. Louis, MO) or Fisher (Waltham, MA). For histology, skin tissues were fixed at room temperature overnight in a 10% formalin solution. Tissues were then processed for paraffin embedding, sectioned (4 μm),

mounted on glass slides, and stained with hematoxylin and eosin. For electron microscopy, skin samples were collected in 4% paraformaldehyde, 2.5% gluteraldehyde in 0.1 M sodium cacodylate pH 7.4, with 8.0 mM $CaCl_2$. After several washes in 0.1 M sodium cacodylate, pH 7.4, the tissue was post-fixed in 1% osmium tetroxide in 0.1 M sodium cacodylate, pH 7.4 for 1 hour, dehydrated through a graded ethanol series, followed by propylene oxide, infiltrated and embedded in a mixture of EMbed 812, nadic methyl anhydride, dodecenyl succinic anhydride and DMP-30 (Electron Microscopy Sciences, Hatfield, PA). Thin sections were cut using a Reichert UCT ultramicrotome and post-stained with uranyl acetate and bismuth subnitrate. Tissue sections were examined using a Tecnai 12 transmission electron microscope equipped with a Gatan Ultrascan US1000 2 K digital camera (FEI Company, Hillsboro, Oregon).

Tissue extraction

Mouse back skin was pulverized in liquid nitrogen in RIPA buffer (50 mM Tris-HCl (pH 7.5), 150 mM NaCl, 1% Nonidet P-40, 0.5% deoxycholate, 0.1% SDS and protease inhibitor (PI) cocktail (Roche Diagnostics, Indianapolis, IN) or Urea lysis buffer for high molecular weight proteins such as desmoplakin (9 M Urea, 1% SDS, 10% glycerol, 63 mM Tris (pH 6.8), 0.01% pyronin, and 0. 5% β-mercaptoethanol).

To extract Triton X-100 soluble and insoluble proteins, adult wild-type and transgenic dorsal skin was snap-frozen in liquid nitrogen and processed as previously described (Vasioukhin et al., 2001). Tissues were homogenized in Triton solubilization buffer (10 mM Tris-Hcl, pH 7.5, 150 mM NaCl, 5 mM EDTA, 1% Triton X-100, 1 mM DTT, 1 mM phenylmethylsulfonyl fluoride, and PI. The Triton-insoluble pellet was solubilized in the same buffer + 9M Urea.

Extraction of cytoplasmic and nuclear proteins was prepared as previously described (Corsini

et al., 1996). Buffers used were hypotonic lysis buffer (10 mM HEPES, pH 7.9, 10 mM KCl, 10 mM EDTA, 1 mM DTT, 0.4% IGEPAL, 1 mM PMSF, and 1X protease inhibitor mix), high salt buffer (10 mM HEPES, pH 7.9, 0.2 M NaCl, 0.5 mM EDTA, 5% glycerol, 1 mM DTT, 1 mM PMSF, and PI) and Urea buffer (9 M Urea containing high salt buffer).

Immunoblotting and immunohistochemistry

Protein concentration was determined (Pierce BCA kit, Pierce Biotech, Rockford, IL) and immunoblotting was performed as described previously (Brennan et al., 2004) with 5-20 μg of protein in each lane resolved over 5-10% SDS-PAGE (Bio-Rad Laboratories, Hercules, CA). Signals were detected with chemiluminescence (ECL; Amersham Biosciences, Piscataway, NJ).

For immunofluorescence, OCT-fixed tissue sections (5 μm) were prepared as previously described (Mahoney et al., 2006) with DAPI (100 ng/ml) for DNA counterstaining. OCT-fixed tissues were used with the following antibodies: Flag, MP6, CK6, CK10, 23F4, 11E4, and β-catenin. For some antibodies, tissue sections (4 μm) from formalin-fixed and paraffin-embedded tissues were used as previously described (Mahoney et al., 2006). Antibodies used with this method were: AP61, AP498, Ab15, AP904, involucrin, filaggrin, K14, and BrdU.

Keratinocyte proliferation in vivo

Newborn and adult wild-type and transgenic mice were injected subcutaneously in the back with BrdU at 50 mg/kg and sacrificed 1 hour later. Back skin was fixed in 10% formalin, paraffin embedded, and sections (4 μm) were subsequently co-stained with BrdU and CK14 antibodies. BrdU-labeled nuclei in the interfollicular regions were counted in each field and the total number of nuclei was determined.

Anchorage-independent survival assay

We established cultured keratinocytes from newborn mouse skin and maintained in CnT medium (CELLnTEC, Bern, Switzerland) as previously described (Caldelari et al., 2000). Forced suspension cultures were performed as described previously (Jost et al., 2001b; Mahoney et al., 2002b). Growth factors and inhibitors of signal transduction events were used at the following concentrations: EGF, 10 ng/ml; Bay11-7082 (Biomol, Plymouth Meeting, PA), 0.5-5 μM; and MG132 (Assay Designs, Ann Arbor, MI), 10-100 μM.

Two-step chemical-induced carcinogenesis

Adult wild-type and transgenic mice (6-8 weeks old) from 3 different litters were treated once with DMBA (7,12-dimethylbenz[a]anthracene) followed by TPA (12-*O*-tetradecanoylphorbol 13-acetate) treatment twice weekly according to established protocols (Guo et al., 2005). Briefly, experimental mice were shaved once on the dorsal skin with an electric razor and DMBA (400 nmol in 200 μl acetone) was painted onto the exposed skin 24 hours later. One week after initiation with DMBA, TPA (17 nmol in 200 μl acetone) was applied twice weekly for up to 25 weeks. The statistical significance of differences in papilloma formation between transgenic and wild-type mice was determined with a Student's *t*-test.

Tape stripping and cornified envelope extraction

For tape stripping analysis, newborn mice were tape stripped 10 times using D-Squame disks (CuDerm Corp., Dallas, TX) as previously described (Dreher et al., 1998). Tapes were adhered onto glass slides and photographed under phase-contrast. For purification of cornified envelopes (CE), skin biopsies (6 mm) were boiled for 20 minutes in isolation buffer (20 mM Tris-HCl, pH

7.5, 5 mM EDTA, 10 mM DTT, and 2% SDS) essentially as previously described (Jarnik et al., 1996). After centrifugation (5,000 *g*, 10 minutes), CEs were washed twice at room temperature with a wash buffer (20 mM Tris-HCl, pH 7.5, 5 mM EDTA, 10 mM DTT, and 0.2% SDS). CEs were photographed and concentration determined by hemacytometer.

Acknowledgements

We thank Drs. Lorne Taichman (State U. New York, Stony Brook, NY) for the pH3700-pL2 targeting vector, John Stanley (U. Pennsylvania, Philadelphia, PA) for the Dsg3 antibodies, Lutz Langbein (German Cancer Research Center, Heidelberg, Germany) for the MP6 antibodies, and James Wahl (U. Nebraska Medical Center, Omaha, NE) for the desmosomal antibodies. We thank Dr. Csaba Kari (Thomas Jefferson U.) for critically reading this manuscript. This work was supported by grants from the Dermatology Foundation (Mahoney) and the National Institutes of Health (Rodeck, CA81008; Mahoney, AR47938).

References

Arnold, I. and Watt, F. M. (2001). c-Myc activation in transgenic mouse epidermis results in mobilization of stem cells and differentiation of their progeny. *Curr. Biol.* **11**, 558-568.

Biedermann, K., Vogelsang, H., Becker, I., et al. (2005). Desmoglein 2 is expressed abnormally rather than mutated in familial and sporadic gastric cancer. *J. Pathol.* **207**,199-206.

Brennan, D., Hu, Y., Kljuic, A., Choi, Y., Joubeh, S., Bashkin, M., Wahl, J., Fertala, A., Pulkkinen, L., Uitto, J. et al. (2004). Differential structural properties and expression patterns suggest functional significance for multiple mouse desmoglein 1 isoforms. *Differentiation* **72**, 434-449.

Caldelari, R., Suter, M. M., Baumann, D., de Bruin A., Müller, E. (2000). Long-term culture of murine epidermal keratinocytes. *J. Invest. Dermatol.* **114**, 1064-1065.

Chan, K. S., Carbajal, S., Kiguchi, K., Clifford, J., Sano, S. and DiGiovanni, J. (2004). Epidermal growth factor receptor-mediated activation of Stat3 during multistage skin carcinogenesis. *Cancer Res.* **64**, 2382-2399.

Cheng, X. and Koch, P. J. (2004). In vivo function of desmosomes. *J. Dermatol.* **31**, 171-187.

Chidgey, M., Brakebusch, C., Gustafsson, E., Cruchley, A., Hail, C., Kirk, S., Merritt, A., North, A., Tselepis, C., Hewitt, J. et al. (2001). Mice lacking desmocollin 1 show epidermal fragility accompanied by barrier defects and abnormal differentiation. *J. Cell Biol.* **155**, 821-832.

Chitaev, N. A. and Troyanovsky, S. M. (1997). Direct Ca^{2+} dependent heterophilic interaction between desmosomal cadherins, desmoglein and desmocollin, contributes to cell adhesion. *J. Cell Biol.* **138**, 193-201.

Chung, C. H., Parker, J. S., Karaca, G., Wu, J., Funkhouser, W. K., Moore, D., Butterfoss, D., Xiang, D., Zanation, A., Yin, X. et al. (2004). Molecular classification of head and neck squamous cell carcinomas using patterns of gene expression. *Cancer Cell.* **5**, 489-500.

Corsini, E., Schubert, C., Marinovich, M. and Galli, C. L. (1996). Role of mitochondria in tributyltin-induced interleukin-1alpha production in murine keratinocytes. *J. Invest. Dermatol.* **107**, 720–725.

Coulombe, P. A. (1997). Towards a molecular definition of keratinocyte activation after acute injury to stratified epithelia. *Biochem. Biophys. Res. Commun.* ***236***, 231-238.

Cowin, P. (1994). Unraveling the cytoplasmic interactions of the cadherin superfamily. *Proc. Natl. Acad. Sci. USA* **91**, 10759-10761.

Cowin, P. and Burke, B. (1996). Cytoskeleton-membrane interactions. *Curr. Opin. Cell Biol.* **8**, 56-65.

Das, S., Dixon, J. E. and Cho, W. (2003). Membrane-binding and activation mechanism of PTEN. *Proc. Natl. Acad. Sci. USA* **100**, 7491-7496.

Denning, M. F., Guy, S. G., Ellerbroek, S. M., Norvell, S. M., Kowalczyk, A. P. and Green, K. J. (1998). The expression of desmoglein isoforms in cultured human keratinocytes is regulated by calcium, serum, and protein kinase C. *Exp. Cell Res.* **239**, 50-59.

Dong, G., Loukinova, E., Chen, Z., Gangi, L., Chanturita, T. I., Liu, E. T. and Van Waes, C. (2001). Molecular profiling of transformed and metastatic murine squamous carcinoma cells by differential display and cDNA microarray reveals altered expression of multiple genes related to growth, apoptosis, angiogenesis, and the NF-kappaB signal pathway. *Cancer Res.* **61**, 4797-4808.

Dreher, F., Arens, A., Hostynek, J. J., Mudumba, S., Ademola, J. and Maibach, H. I. (1998). Colorimetric method for quantifying human stratum corneum removed by adhesive-tape stripping. *Acta. Derm. Venereol.* **78**, 186-189.

Duffey, D. C., Chen, Z., Dong, G., Ondrey, F. G., Wolf, J. S., Brown, K., Siebenlist, U. and Van Waes, C. (1999). Expression of a dominant-negative mutant inhibitor-B of nuclear factor-B in human head and neck squamous cell carcinoma inhibits survival, proinflammatory cytokine expression, and tumor growth in vivo. *Cancer Res.* **59**, 3468–3474.

Elias, P. M., Matsuyoshi, N., Wu, H., Lin, C., Wang, Z. H., Brown, B. E. and Stanley, J. R. (2001). Desmoglein isoform distribution affects stratum corneum structure and function. *J. Cell Biol.* **153**, 243-249.

Eshkind, L., Tian, Q., Schmidt, A., Franke, W. W., Windoffer, R. and Leube, R. E. (2002). Loss of desmoglein 2 suggests essential functions for early embryonic development and proliferation of embryonal stem cells. *Eur. J. Cell Biol.* **81**, 592-598.

Franke, W. W., Borrmann, C. M., Grund, C. and Pieperhoff, S. (2006). The area composita of adhering junctions connecting heart muscle cells of vertebrates. I. Molecular definition in intercalated disks of cardiomyocytes by immunoelectron microscopy of desmosomal proteins. *Eur. J. Cell Biol.* **85**, 69-82.

Frisch, S. M. and Francis, H. (1994). Disruption of epithelial cell-matrix interactions induces apoptosis. *J. Cell Biol.* **124**, 619-626.

Frye, M., Gardner, C., Li, E. R., Arnold, I. and Watt, F. M. (2003). Evidence that Myc activation depletes the epidermal stem cell compartment by modulating adhesive interactions with the local microenvironment. *Development* **130**, 2793-2808.

Garrod, D. R., Merritt, A. J. and Nie, Z. (2002). Desmosomal cadherins. *Curr. Opin. Cell Biol.* **14**, 537-545.

Green, K. J. and Jones, J. C. (1996). Desmosomes and hemidesmosomes: structure and function of molecular components. *FASEB J.* **10**, 871-881.

Getsios, S., Amergo, E. V., Dusek, R. L., Ishii, K., Sheu, L., Godsel, L. M. and Green, K. J. (2004). Coordinated expression of desmoglein 1 and desmocollin 1 regulates intercellular adhesion. *Differentiation* **72**, 419-433.

Guo, Y., Cleveland, J. L. and O'Brien, T. G. (2005). Haploinsufficiency for odc modifies mouse skin tumor susceptibility. *Cancer Res.* **65**, 1146-1149.

Hansen, L. A., Woodson, R. L., 2nd, Holbus, S., Strain, K., Lo, Y. C. and Yuspa, S. H. (2000). The epidermal growth factor receptor is required to maintain the proliferative population in the basal compartment of epidermal tumors. *Cancer Res.* **60**, 3328-3332.

Harada, H., Iwatsuki, K., Ohtsuka, M., Han, G. and Kaneko, F. (1996). Abnormal desmoglein expression by squamous cell carinoma cells. *Acta. Derm. Venereol.* **76**, 417-420.

Harding, C. R. (2004). The stratum corneum: structure and function in health and disease. *Dermatol. Ther.* **17**, 6-15.

Hardman, M. J., Liu, K., Avilion, A. A., Merritt, A., Brennan, K., Garrod, D. R. and Byrne, C. (2005). Desmosomal cadherin misexpression alters beta-catenin stability and epidermal differentiation. *Mol. Cell Biol.* **25**, 969-978.

He, W., Cowin, P. and Stokes, D. L. (2003). Untangling desmosomal knots with electron tomography. *Science* **302**, 109-113.

Henkler, F., Strom, M., Mathers, K., Cordingley, H., Sullivan, K. and King, I. (2001). Transgenic misexpression of the differentiation-specific desmocollin isoform 1 in basal keratinocytes. *J. Invest. Dermatol.* **116**, 144-149.

Heyden, A., Lutzow-Holm, C., Clausen, O. P., Brandtzaeg, P. and Huitfeldt, H. S. (1994). Expression of keratins K6 and K16 in regenerating mouse epidermis is less restricted by cell replication than the expression of K1 and K10. *Epithelial Cell Biol.* **3**, 96-101.

Jarnik, M., Kartasova, T., Steinert, P. M., Lichti, U. and Steven, A. C. (1996). Differential expression and cell envelope incorporation of small proline-rich protein 1 in different cornified epithelia. *J. Cell Sci.* **109**, 1381-1391.

Jost, M., Gasparro, F. P., Jensen, P. J. and Rodeck, U. (2001a). Keratinocyte apoptosis induced by ultraviolet B radiation and CD95 ligation -- differential protection through epidermal growth factor receptor activation and Bcl-x(L) expression. *J. Invest. Dermatol.* **116**, 860-866.

Jost, M., Huggett, T. M., Kari, C. and Rodeck, U. (2001b). Matrix-independent survival of human keratinocytes through an EGF receptor/MAPK-kinase-dependent pathway. *Mol. Biol. Cell.* **12**, 1519-1527.

Koch, P. J., Goldschmidt, M. D., Zimbelmann, R., Troyanovsky, R. and Franke, W. W. (1992). Complexity and expression patterns of the desmosomal cadherins. *Proc. Natl. Acad. Sci. USA* **89**, 353-357.

Kottke, M. D., Delva, E. and Kowalczyk, A. P. (2006). The desmosome: cell science lessons from human diseases. *J. Cell Sci.* **119**, 797-806.

Kurzen, H., Munzing, I. and Hartschuh, W. (2003). Expression of desmosomal proteins in squamous cell carcinomas of the skin. *J. Cutan. Pathol.* **30,** 621-630.

Lindberg, K. and Rheinwald, J. G. (1990). Three distinct keratinocyte subtypes identified in human oral epithelium by their patterns of keratin expression in culture and in xenografts. *Differentiation* **45**, 230-241.

Loercher, A., Lee, T. L., Ricker, J. L., Howard, A., Geoghegen, J., Chen, Z., Sunwoo, J. B., Sitcheran, R., Chuang, E. Y., Mitchell, J. B. et al. (2004). Nuclear factor-kappaB is an important modulator of the altered gene expression profile and malignant phenotype in squamous cell. *Cancer Res.* **64**, 6511-6523.

Mahoney, M. G., Hu, Y., Brennan, D., Bazzi, H., Christiano, A. M. and Wahl, J. K. Jr. (2006). Delineation of diversified desmoglein distribution in stratified squamous epithelia: implications in diseases. *Exp. Dermatol.* **15**, 101-109.

Mahoney, M. G., Simpson, A., Aho, S., Uitto, J. and Pulkkinen, L. (2002a). Interspecies conservation and differential expression of mouse desmoglein gene family. *Exp. Derm.* **11**, 115-125.

Mahoney, M. G., Simpson, A., Jost, M., Noe, M., Kari, C., Pepe, D., Choi, Y. W., Uitto, J. and Rodeck, U. (2002b). Metastasis-associated protein (MTA)1 enhances migration, invasion, and anchorage-independent survival of immortalized human keratinocytes. *Oncogene* **21**, 2161-2170.

McDonald, S. L., Edington, H. D., Kirkwood, J. M. and Becker, D. (2004). Expression analysis of genes identified by molecular profiling of VGP melanomas and MGP melanoma-positive lymph nodes. *Cancer Biol. Ther.* **3**, 110-120.

McGowan, K. and Coulombe, P. (1998). The wound repair-associated keratins 6, 16, and 17. Insights into the role of intermediate filaments in specifying keratinocyte cytoarchitecture. New York: Plenum Press.

Merlino, G. T., Xu, Y. H., Richert, N., Clark, A. J., Ishii, S., Banks-Schlegel, S. and Pastan, I. (1985). Elevated epidermal growth factor receptor gene copy number and expression in a squamous carcinoma cell line. *J. Clin. Invest.* **75**, 1077-1079.

Merritt, A. J., Berika, M. Y., Zhai, W., Kirk, S. E., Ji, B., Hardman, M. J. and Garrod, D. R. (2002). Suprabasal desmoglein 3 expression in the epidermis of transgenic mice results in hyperproliferation and abnormal differentiation. *Mol. Cell Biol.* **22**, 5846-5858.

Mils, V., Vincent, C., Croute, F. and Serre, G. (1992). The expression of desmosomal and corneodesmosomal antigens shows specific variations during the terminal differentiation of epidermis and hair follicle epithelia. *J. Histochem. Cytochem.* **40**, 1329-1337.

Montagna, W., Kirchner, S. and Carlisle, K. (1989). Histology of sun-damaged human skin. *J Am. Acad. Dermatol.* **5**, 907-918.

Mora, A., Komander, D., van Aalten, D. M. and Alessi, D. R. (2004). PDK1, the master regulator of AGC kinase signal transduction. *Semin. Cell Dev. Biol.* **15**, 161-170.

Ozawa, S., Ueda, M., Ando, N., Shimizu, N. and Abe, O. (1989). Prognostic significance of epidermal growth factor receptor in esophageal squamous cell carcinomas. *Cancer* **63**, 2169-2173.

Pelengaris, S., Littlewood, T., Khan, M., Elia, G. and Evan, G. (1999). Reversible activation of c-Myc in skin: induction of a complex neoplastic phenotype by a single oncogenic lesion. *Mol. Cell.* **3**, 565-577.

Pilichou, K., Nava, A., Basso, C., Beffagna, G., Bauce, B., Lorenzon, A., Frigo, G.,Vettori, A., Valente M, Towbin, J., Thiene, G., Danieli, G.A., Rampazzo, A. (2006) Mutations in desmoglein-2 gene are associated with arrhythmogenic right ventricular cardiomyopathy. *Circulation* **113**, 1171-1179.

Ren, Q., Kari, C., Quadros, M. R., Burd, R., McCue, P., Dicker, A. P. and Rodeck, U. (2006). Malignant transformation of immortalized HaCaT keratinocytes through deregulated nuclear factor kappaB signaling. *Cancer Res.* **66**, 5209-5215.

Rieger-Christ, K. M. , Ng, L., Hanley, R. S. , Durrani, O., Ma, H., Yee, A. S., Libertino, J. A. and Summerhayes, I. C. (2005). Restoration of plakoglobin expression in bladder carcinoma cell lines suppresses cell migration and tumorigenic potential. *Br. J. Cancer* **92**, 2153-2159.

Rodeck, U., Jost, M., DuHadaway, J., Kari, C., Jensen, P. J., Risse, B. and Ewert, D. L. (1997a). Regulation of Bcl-xL expression in human keratinocytes by cell-substratum adhesion and the epidermal growth factor receptor. *Proc. Natl. Acad. Sci. USA* **94**, 5067-5072.

Rodeck, U., Jost, M., Kari, C., Shih, D.-T., Lavker, R. M., Ewert, D. L. and Jensen, P. J. (1997b). EGF-R dependent regulation of keratinocyte survival. *J. Cell Sci.* **110**, 113-121.

Schäfer, S., Koch, P. J. and Franke, W. W. (1994). Identification of the ubiquitous human desmoglein, Dsg2, and the expression catalogue of the desmoglein subfamily of desmosomal cadherins. *Exp. Cell Res.* **211**, 391-399.

Schäfer, S., Stumpp, S. and Franke, W. W. (1996). Immunological identification and characterization of the desmosomal cadherin Dsg2 in coupled and uncoupled epithelial cells and in human tissues. *Differentiation* **60**, 99-108.

Sibilia, M., Fleischmann, A., Behrens, A., Stingl, L., Carroll, J., Watt, F. M., Schlessinger, J. and Wagner, E. F. (2000). The EGF receptor provides an essential survival signal for SOS-dependent skin tumor development. *Cell* **102**, 211-220.

Stoler, A., Kopan, R., Duvic, M. and Fuchs, E. (1988). Use of monospecific antisera and cRNA probes to localize the major changes in keratin expression during normal and abnormal epidermal differentiation. *J. Cell Biol.* **107**, 427-446.

Trojan, L., Schaaf, A., Steidler, A., et al. (2005). Identification of metastasis-associated genes in prostate cancer by genetic profiling of human prostate cancer cell lines. *Anticancer Res.* **25**, 183-191.

Vasioukhin, V., Bowers, E., Bauer, C., Degenstein, L. and Fuchs, E. (2001). Desmoplakin is essential in epidermal sheet formation. *Nat. Cell Biol.* **3**, 1076–1085.

Wahl, J. K., Sacco, P. A., MaGranahan-Sadler, T. M., Sauppe, L. M., Wheelock, M. J. and Johnson, K. R. (1996). Plakoglobin domains that define its association with the desmosomal cadherins and the classical cadherins: identification of unique and shared domains. *J. Cell Sci.* **109**, 1143-1154.

Waikel, R. L., Kawachi, Y., Waikel, P. A., Wang, X. J. and Roop, D. R. (2001). Deregulated expression of c-Myc depletes epidermal stem cells. *Nat. Genet.* **28**, 165-168.

Waikel, R. L., Wang, X. J. and Roop, D. R. (1999). Targeted expression of c-Myc in the epidermis alters normal proliferation, differentiation and UV-B induced apoptosis. *Oncogene* **18**, 4870-4878.

Weaver, V. M., Lelievre, S., Lakins, J. N., Chrenek, M. A., Jones, J. C., Giancotti, F., Werb, Z. and Bissell, M. J. (2002). Beta4 integrin-dependent formation of polarized three-dimensional architecture confers resistance to apoptosis in normal and malignant mammary epithelium. *Cancer Cell.* **2**, 205-216.

Williamson, L., Raess, N. A., Caldelari, R., Zakher, A., de Bruin A, Posthaus, H., Bolli, R., Hunziker, T., Suter, M. M. and Muller, E. J. (2006). Pemphigus vulgaris identifies plakoglobin as key suppressor of c-Myc in the skin. *EMBO J.* **25(14)**, 3298-3309.

Woodworth, C. D., Gaiotti, D., Michael, E., Hansen, L. and Nees, M. (2000). Targeted disruption of the epidermal growth factor receptor inhibits development of papillomas and carcinomas from human papillomavirus-immortalized keratinocytes. *Cancer Res.* **60**, 4397-4402.

Yaffe, M. B., Murthy, S. and Eckert, R. L. (1993). Evidence that involucrin is a covalently linked constituent of highly purified cultured keratinocyte cornified envelopes. *J. Invest. Dermatol.* **100**, 3-9.

Yashiro, M., Nishioka, N. and Hirakawa, K. (2006). Decreased expression of the adhesion molecule desmoglein-2 is associated with diffuse-type gastric carcinoma. *Eur. J. Cancer* **14**, 2397-2403.

Yin, T. and Green, K. J. (2004). Regulation of desmosome assembly and adhesion. *Semin. Cell Dev. Biol.* **15**, 665-677.

Zahir, N., Lakins, J. N., Russell, A., Ming, W., Chatterjee, C. R., G.I., Marinkovich, M. P. and Weaver, V. M. (2003). Autocrine laminin-5 ligates alpha6beta4 integrin and activates RAC and NFkappaB to mediate anchorage-independent survival of mammary tumors. *J. Cell Biol.* **163**, 1397-1407.

Figure Legends

Fig. 1. Targeting construct and Dsg2-Flag expression in transgenic mice. (A) Schematic diagram of the mDsg2-Flag transgenic construct inserted at *Not*I restriction sites downstream of the involucrin promoter in the pH2700-pL2 vector (mDsg2, mouse desmoglein 2 cDNA; Flag, nucleotide sequence encoding for the Flag octapeptide; polyA, polyadenylation signal). (B) Immunofluorescence of wild-type (upper panels) and Inv-Dsg2 transgenic (lower panels) adult mouse skin stained with Flag (green, left panels) and Dsg2 MP6 (red, middle panels) antibodies showing expression of Dsg2-Flag in the transgenic, but not control epidermis. Co-staining (merge, right panels) for Dsg2 and Flag in the Inv-Dsg2 transgenic but not control wild-type skin. Nuclear staining with DAPI (blue). (C) Immunoblot analysis of adult control and transgenic mouse skin extracts with Flag and MP6 antibodies showing Dsg2 and Flag expression in the transgenic but not wild-type skin. Blots were reprobed with actin antibody as a loading control. In all figures: Tg, transgenic; WT, wild-type.

Fig. 2. Inv-Dsg2 mice develop epidermal hyperplasia. (A-J) Hematoxylin/eosin staining of back skin of newborn (A,B) and adult back skin (C,D,I,J), ear (E,F), and tongue (G,H) of wild-type control (A,C,E,G,I) and Inv-Dsg2 transgenic (B,D,F,H,J) littermate mice. Newborn and adult mice were 2 days and 3 months old, respectively. Histological analysis shows varying degrees of epidermal thickening in all Inv-Dsg2 transgenic tissues examined. Minor compaction (B,D; asterisk) and the presence of nuclei (B,D; arrows) was observed in the outermost granular/horny layer interface. A more dramatic difference in epidermal thickness was observed in the adult transgenic mice compared that of control littermates (C,D; brackets) and to newborn transgenic skin. Pink translucent flattened eosinophilic keratinocytes were apparent in the

stratum corneum (F; open arrow). Cells and nuclei in the spinous layers of transgenic epithelia appear slightly enlarged relative to those in wild-type epithelia. Scale bar = 25 μm.

Fig. 3. Transmission electron microscopy of control adult wild-type (A) and Inv-Dsg2 transgenic (B) epidermis. The granular cells appeared more compact and interconnected and corneocytes were thicker in the axial direction of the Inv-Dsg2 transgenic epidermis (brackets). Detached desmosomes with intercellular gaps were detected in the stratum corneum (*). Arrows, desmosomes at the granular/stratum corneum interface; arrow heads, desmosome-like electron dense intercellular structures; d, desmosome; k, keratohyalin granules. Scale bar = 1 μm.

Fig. 4. Changes in expression patterns of cornified envelope and keratin proteins in Inv-Dsg2 mice. (A) Immunofluorescent staining of 3-month old adult wild-type and Inv-Dsg2 transgenic mouse skin for cytokeratin (CK14, CK10, and CK6), involucrin (Inv), filaggrin (Fil), and loricrin (Lor). CK14 was observed only in the basal layer of control but extended into the suprabasal epidermal layers of Inv-Dsg2 mice. Increased expression of CK10 was observed in the Inv-Dsg2 epidermis. CK6 expression was observed in the interfollicular epidermis in the Inv-Dsg2 mice. Suprabasal Dsg2 expression was associated with expression of involucrin, filaggrin, and loricrin. Insets represent higher resolution and increased expose images. Nuclear staining with DAPI in blue. (B) Immunoblotting analysis of adult control wild-type and Inv-Dsg2 transgenic mouse skin with antibodies against Flag, Dsg1 (antibody 27B2; recognizes mouse Dsg1-α, Dsg1-β, and Dsg1-γ), Dsg3 (AP904), PG, CK6, CK10, CK14, Lor, Fil, and actin (loading control).

Fig. 5. Inv-Dsg2 transgenic mice show hyperproliferative epidermis and increase in mitotic

activity. Paraffin embedded sections of adult wild-type (A,C) and Inv-Dsg2 transgenic skin (B,D) were stained with antibodies to detect either PCNA expression (A,B) or BrdU incorporation (C,D; green). Insets show higher resolution images. Also shown in red (C,D) is immunostaining for CK14.

Fig. 6. Characterization of the signaling events in Inv-Dsg2 epidermis. Total protein lysates of wild-type and Inv-Dsg2 transgenic adult skin were analyzed by Western blotting analysis to assess activation (phosphorylation) states of signaling intermediates. Immunoblotting for actin, pan cytokeratin (CK), and β-tubulin expression showed equal loading of lanes.

Fig. 7. Establishment of cultured primary keratinocytes from Inv-Dsg2 transgenic and wild-type newborn mouse skin. (A) Immunoblotting analysis for the Flag tag of wild-type and transgenic cell lines grown in low (80 nM; –) or high (1 mM; +) calcium for 5 days. Dsg2-Flag (160 kDa) expression was detected in the calcium-treated transgenic but not the untreated transgenic or the wild-type control keratinocytes. Differentation was confirmed by increased involucrin expression (*) in response to calcium. Upregulation of Dsg2 enhanced P-STAT3 level but not total STAT3 in transgenic compared to wild-type. Epidermal loading control is actin. (B) Wild-type and transgenic keratinocytes were grown to confluency in low calcium containing CnT medium and then 1 mM calcium was added for 24 hrs. Cells were fixed and stained with Flag and DG3.10 antibodies. Wild-type but not transgenic keratinocytes expressed the Dsg2-Flag protein. DG3.10 recognized the endogenous Dsg2 in the wild-type and as well as the Dsg2-Flag in the transgenic cells. (C) Wild-type and Inv-Dsg2 transgenic cells were trypsinized and put in suspension culture for up to 72 hrs. Cells were collected at the time points indicated. Dsg2-Flag was detected by immunoblot analysis in Inv-Dsg2 cells within 24-72 hrs in suspension culture. Immunoblotting analysis for actin expression showed equal loading. Similar results were

observed with three independent wild-type and transgenic cell lines.

Fig. 8. Enhanced survival of Inv-Dsg2 keratinocytes in forced suspension culture is dependent on NF-κB activation. (A) Clonal growth of control and Inv-Dsg2 cell lines after 0, 24, 48, and 72 hrs in forced suspension culture was assessed by replating cells on tissue culture-treated plastic and allowing cell proliferation for 7-9 days after replating. Inv-Dsg2 transgenic, compared to wild-type cells, showed dramatically increased survival and re-growth in this setting. (B) Inv-Dsg2 transgenic cells were subjected to cell suspension culture for 48 hrs with EGF and/or Bay11-7082, an IκB-alpha phosphorylation inhibitor. Cell survival was assessed by replating cells on tissue cultured-treated plastic for 7 days. Activation of the EGF receptor with exogenous EGF further enhanced survival of Inv-Dsg2 transgenic cells in forced suspension cultures. Bay11-7082 inhibition of NK-κB completely abolished cell survival in suspension culture. EGF-R activation was unable to counteract the effect of Bay11-7082. (C) Immunoblot analysis of NF-κB p65 expression in wild-type and transgenic skin. Actin for loading control. (D) Immunoblot results were confirmed by immunofluorescent staining showing the presence of NF-κB p65 staining in nuclei of transgenic, as compared to wild-type skin. Dashed lines demarcate dermal/epidermal junction. Scale bar = 50 μm.

Fig. 9. Increased tumor formation in Inv-Dsg2 transgenic mice. (A,B) Histological analysis of epidermal hyperplasia and early forms of papillomas in Inv-Dsg2 transgenic but not control wild-type mice at 6 weeks (A) and 3 months (B) (10X). Arrows, hyperproliferation; box, hyperkeratosis; asterisk, encapsulated stratum corneum. (C) After 25 weeks of DMBA /TPA treatment, the Inv-Dsg2 transgenic mice developed more tumors than control wild-type mice. (D,E) The frequency and average number of papillomas in wild-type and transgenic mice after

25 weeks of tumor promotion. (F) Histopathological appearance of carcinogen-induced tumors from wild-type and transgenic mice showing differentiated and hyperkeratotic papillomas.

Supplementary Fig. S1. Alterations in the expression of adhesion proteins in Inv-Dsg2 mice. Indirect immunofluorescent staining of adult wild-type and transgenic skin using antibodies to desmosomal proteins (Dsg1-α, Dsg1-β, Dsg1-γ, Dsg3, desmoplakin, and plakoglobin) and adherens junction proteins (E-cadherin and β-catenin). Suprabasal expression of Dsg2 slightly enhanced the expression of desmosomal proteins but did not alter their expression pattern (A). Overexpression of Dsg2 did not dramatically alter the expression levels of E-cadherin or β-catenin (B). Insets for wild-type desmoplakin (i) and plakoglobin (k) stainings shows images obtained under the same exposure conditions used for transgenic (i to j and k to l) to further demonstrate the increase their expression level in the Inv-Dsg2 transgenic skin. Nuclear staining with DAPI in blue. DP, desmoplakin; PG, plakoglobin.

Supplementary Fig. S2. Effect of suprabasal Dsg2 on Triton-solubility and subcellular distribution of desmosomal proteins. Protein extraction was performed using adult wild-type and Inv-Dsg2 transgenic dorsal skin for Triton-soluble and -insoluble (A) and subcellular (soluble, high salt, and insoluble) (B) proteins. Immunoblot analysis showed the presence of Dsg2-Flag in the Triton-soluble pool while other desmosomal proteins were found exclusively in the Triton-insoluble pool (A). Cytokeratin (CK) and α-Tubulin levels were used as loading controls for the Triton X-100-insoluble and –soluble fractions, respectively. Subcellular fractionation followed by immunoblotting showed Dsg2-Flag in all samples including the cytoplasmic (soluble) and nuclear (high salts) fractions (B). The asterisk (*) demarcates a non-specific nuclear protein recognized by the Flag antibody. The nuclear pool of β-catenin was

reduced in the Inv-Dsg2 transgenic compared to wild-type skin. α-Tubulin, γ-tubulin, and cytokeratin served as loading controls for the cytoplasmic, nuclear, and insoluble pools, respectively. S, Triton-soluble; I, Triton-insoluble.

Supplementary Fig. S3. Suprabasal expression of Dsg2 perturbs formation of the stratum corneum. (A) Hematoxylin and eosin staining of dorsal skin of newborn wild-type and transgenic littermates revealed disconnected and fragmented layers (arrows) in the stratum corneum (bracket) of Inv-Dsg2 mice. (B) Newborn wild-type and Inv-Dsg2 transgenic mice were taped stripped 10 times on the dorsal skin using CuDerm adhesive tapes. Tapes were adhered to microscope slides and photographed under phase contrast. TS-1, tape strip #1; TS-10, tape strip #10.

Table 1. Increase in cornified envelopes in Inv-Dsg2 transgenic skin.

Tissue	**Percent Tg/WT**	**Number of animals**
Newborn Dorsal Skin	117.0 ± 16.7	WT=5;Tg=8
Adult Ear	127.9 ± 40.7	WT=7;Tg=18
Adult Dorsal Skin	386.4 ± 156.0	WT=5;Tg=9

Transgenic, Tg; wild-type, WT.

A

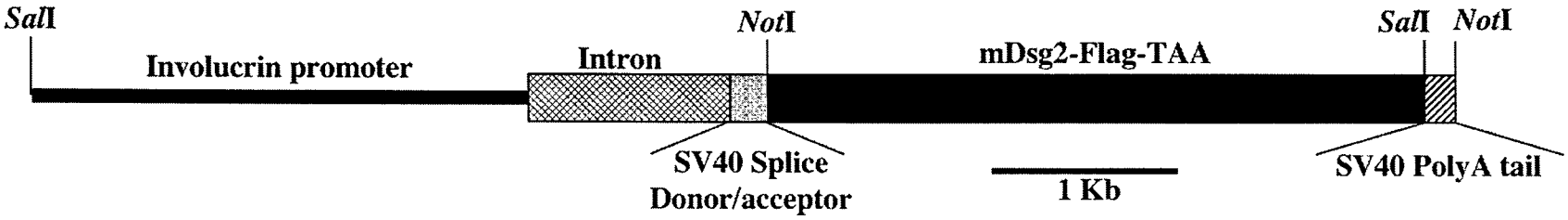

B

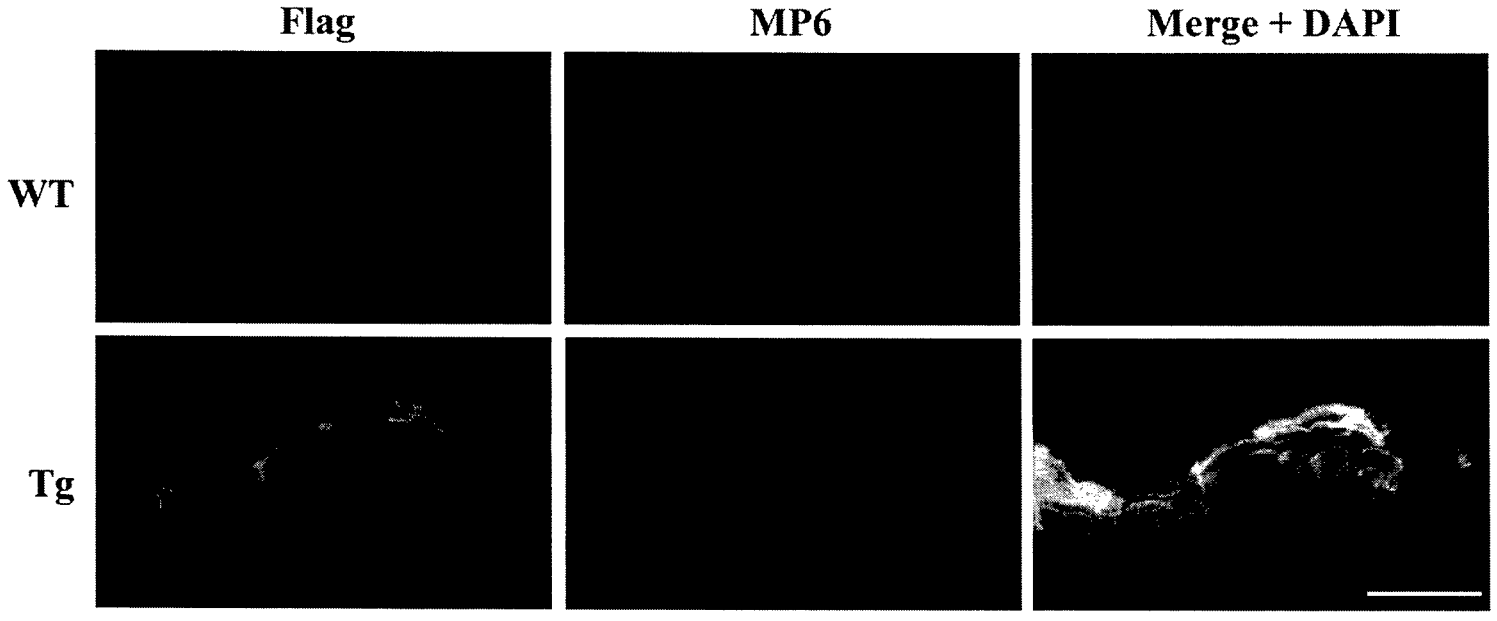

C

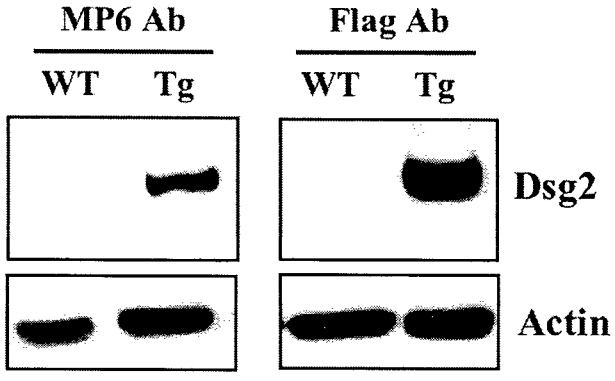

Brennan et al., 2006
Figure 1

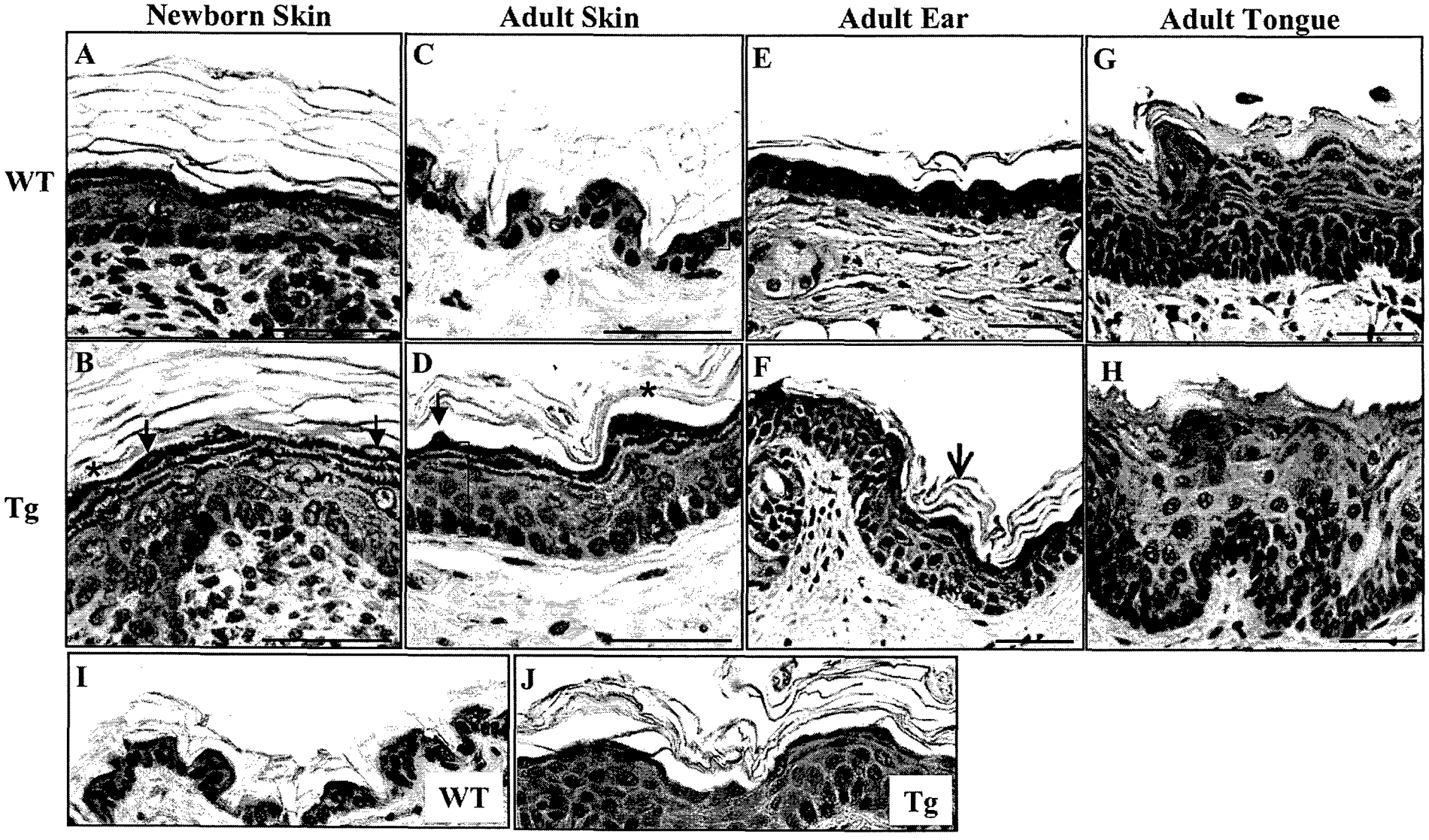

Brennan et al., 2006
Figure 2

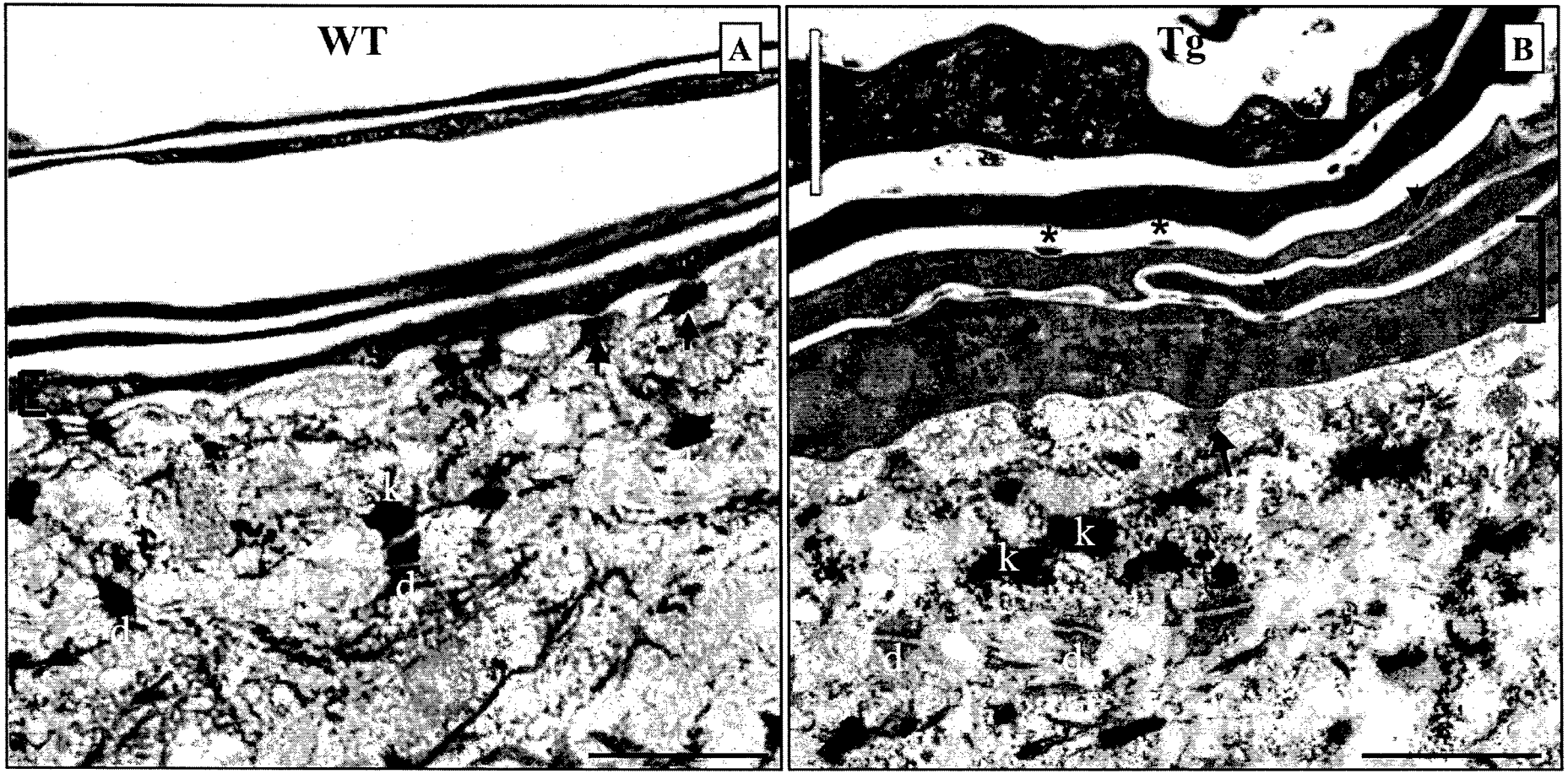

Brennan et al., 2006
Figure 3

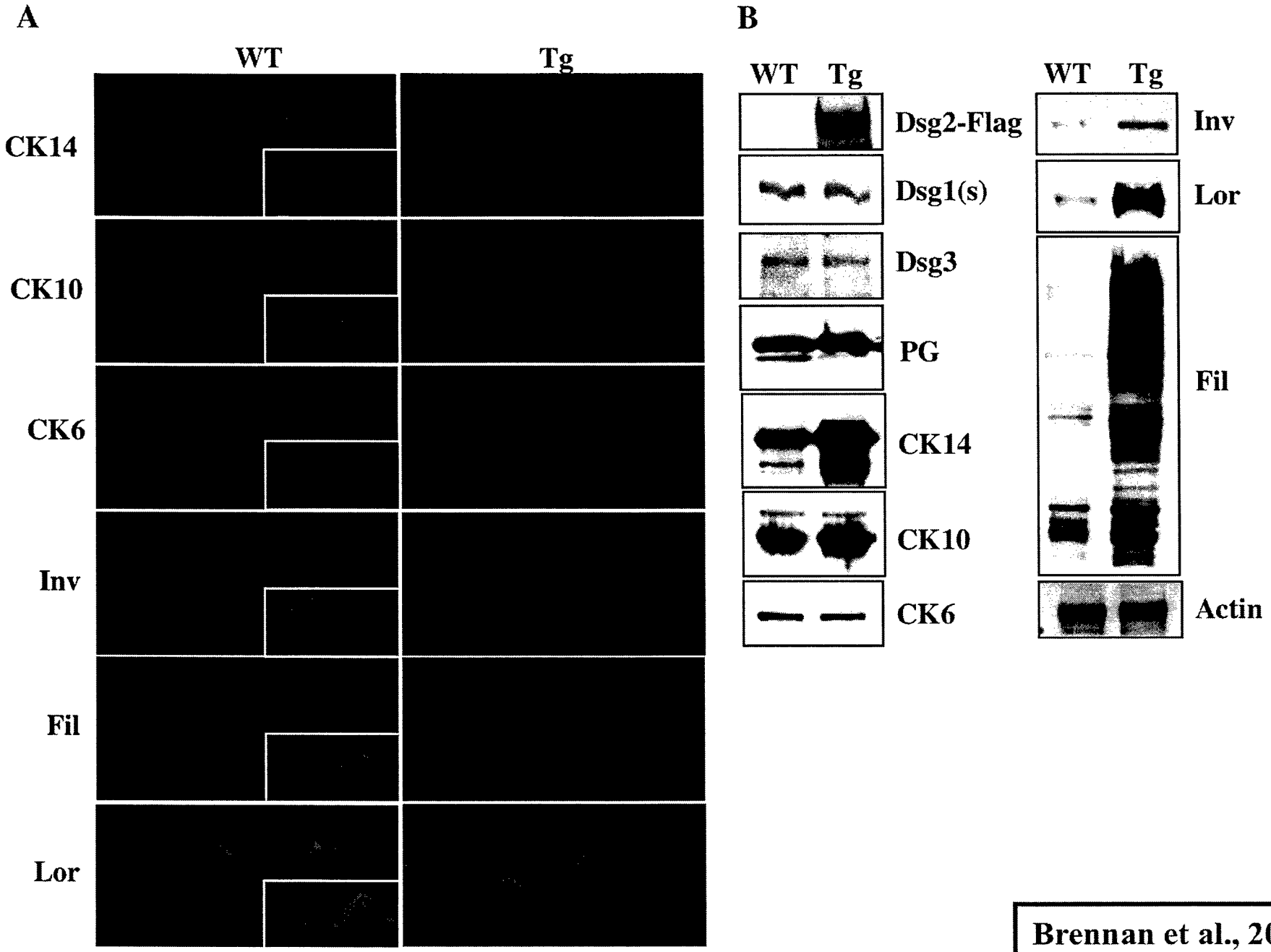

Brennan et al., 2006
Figure 4

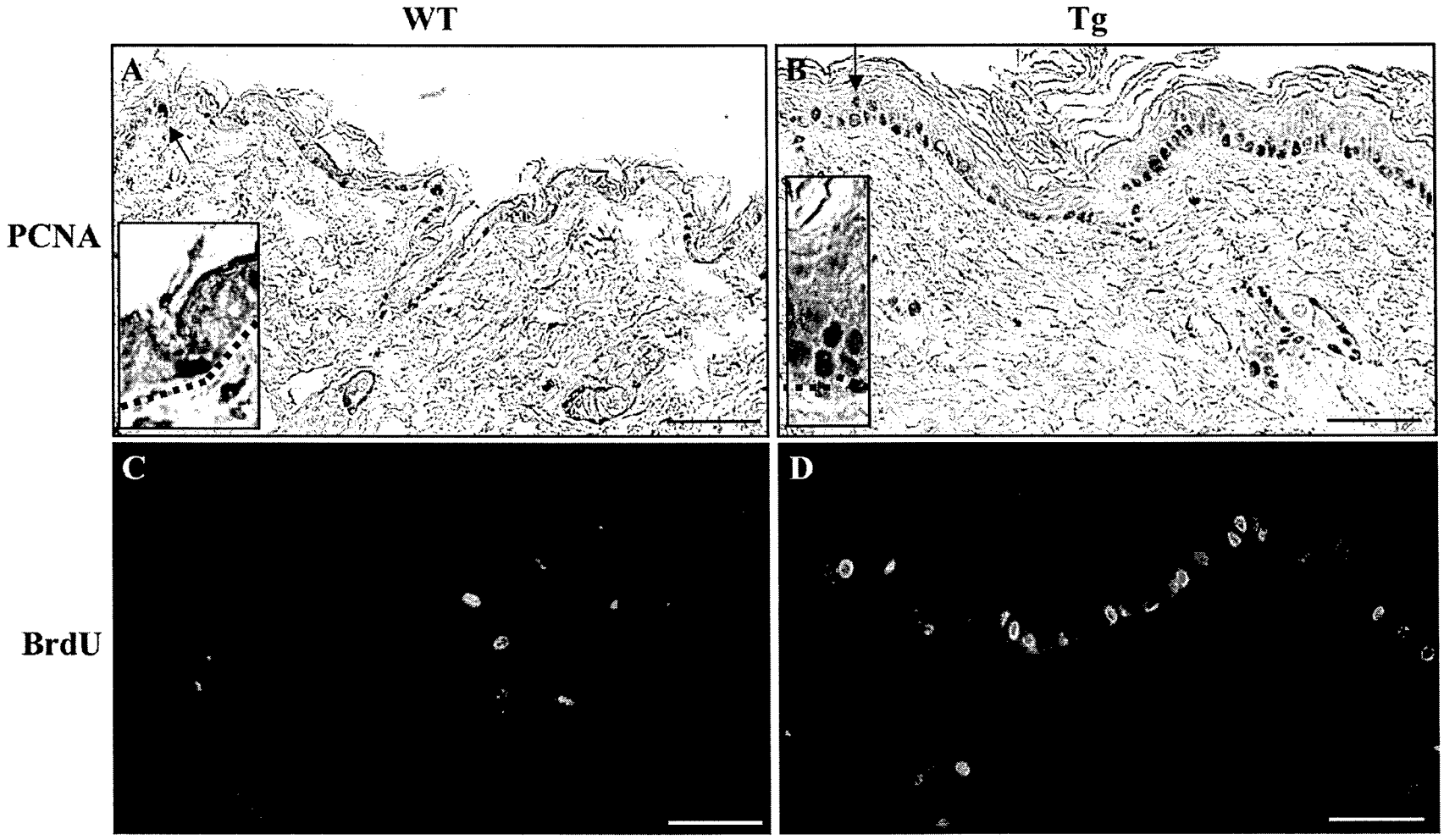

Brennan et al., 2006
Figure 5

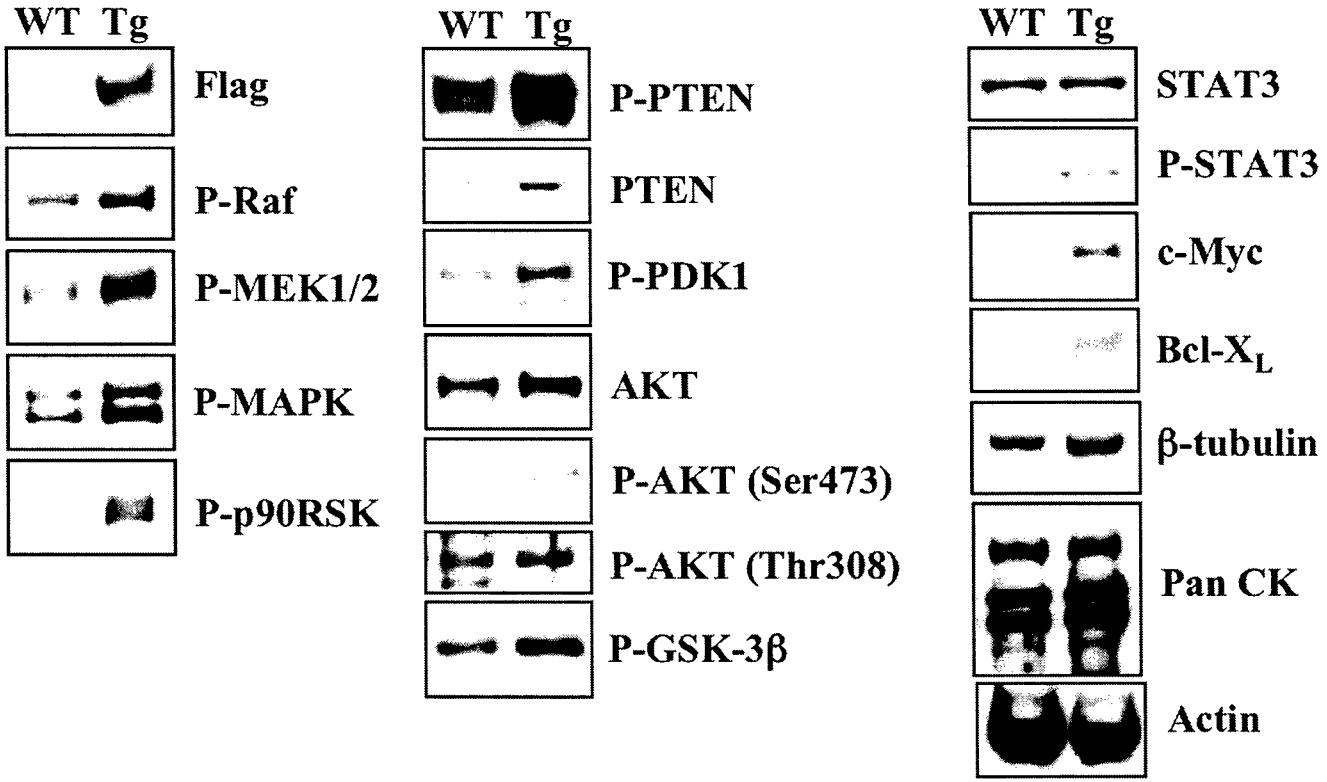

Brennan et al., 2006
Figure 6

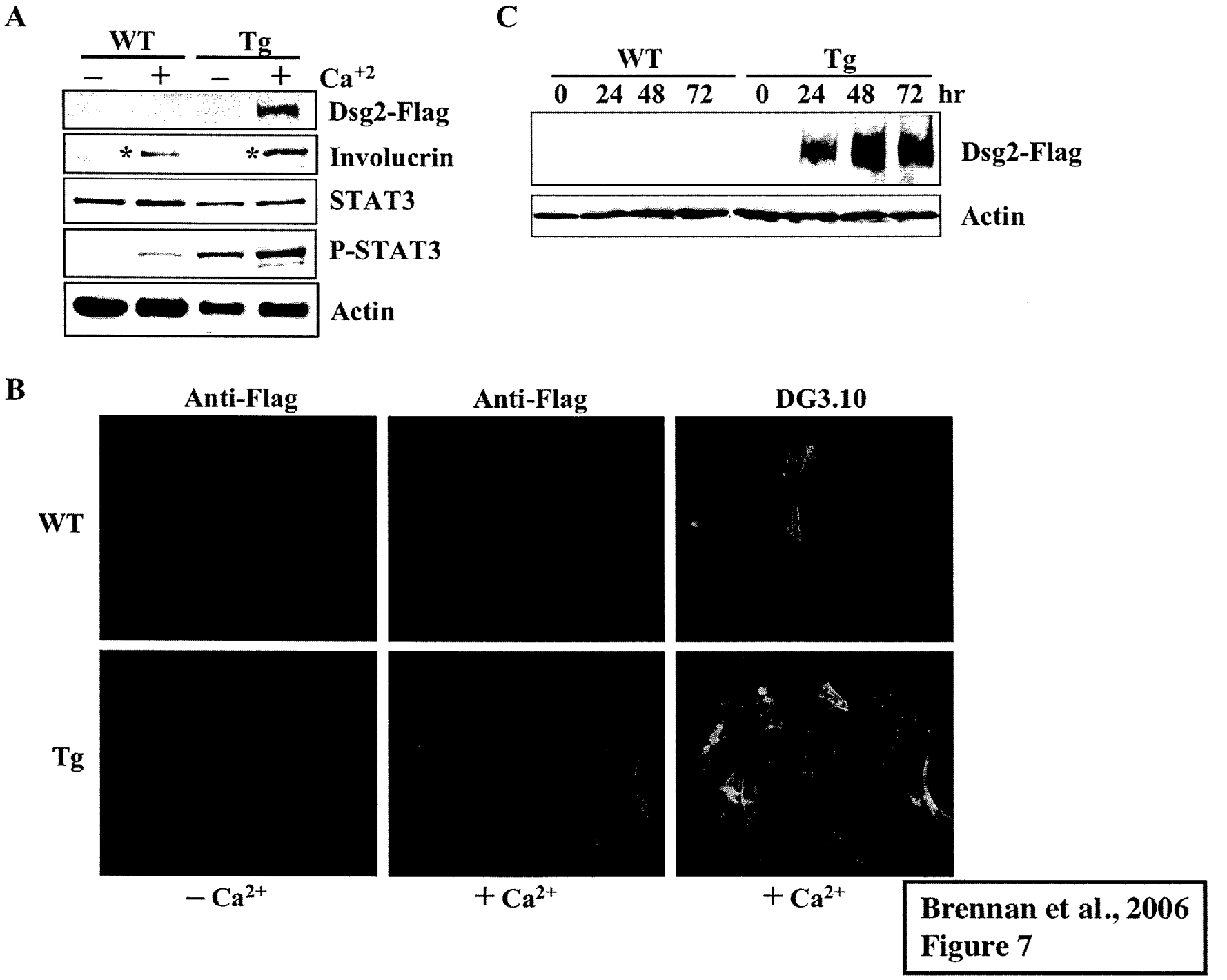

Brennan et al., 2006
Figure 7

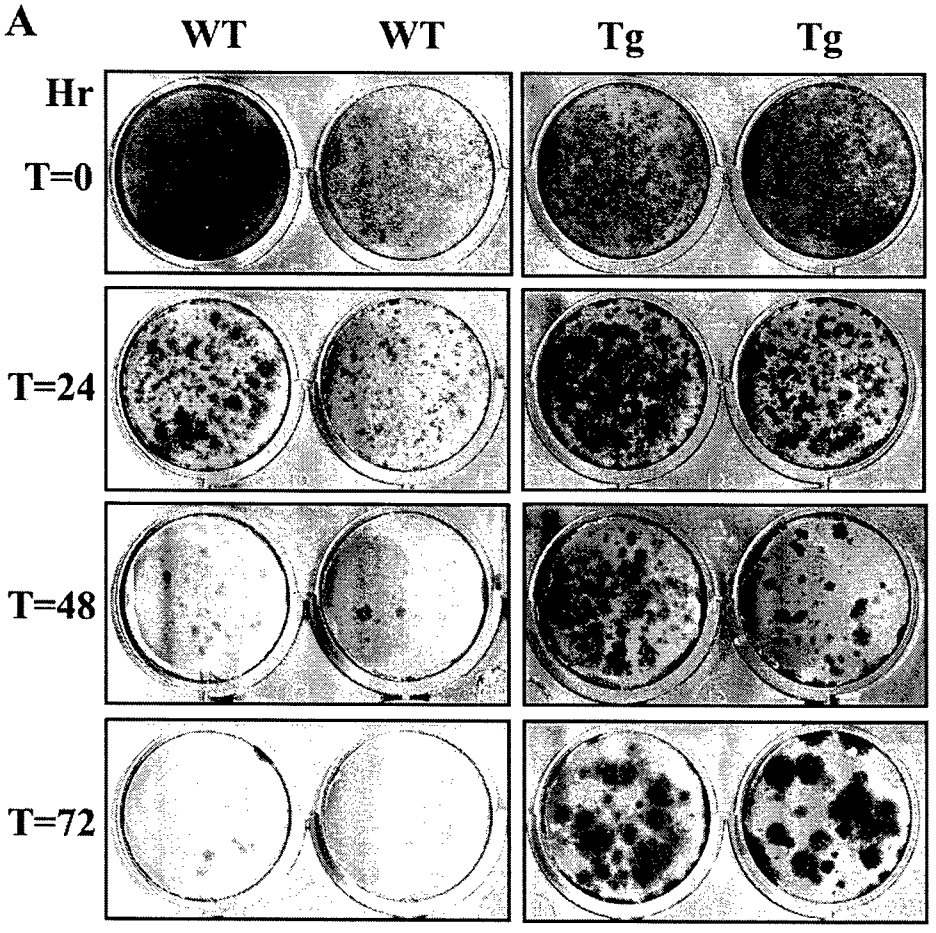

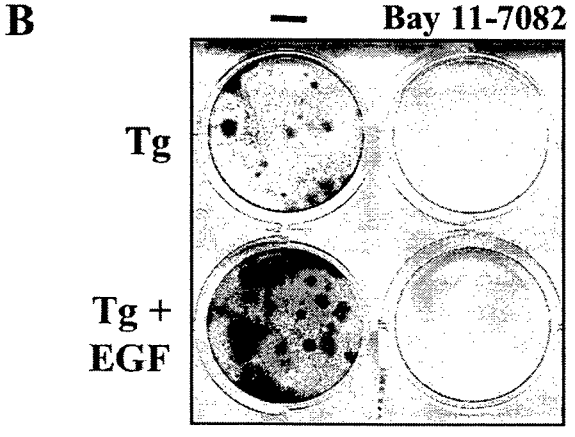

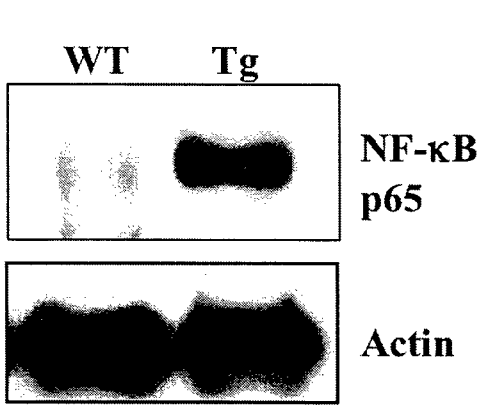

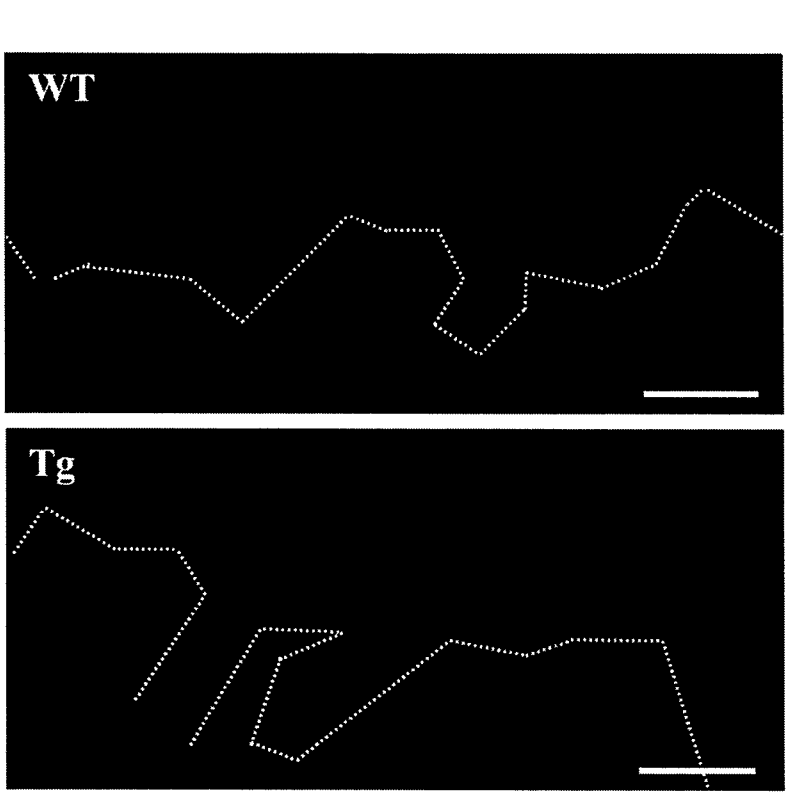

Brennan et al., 2006
Figure 8

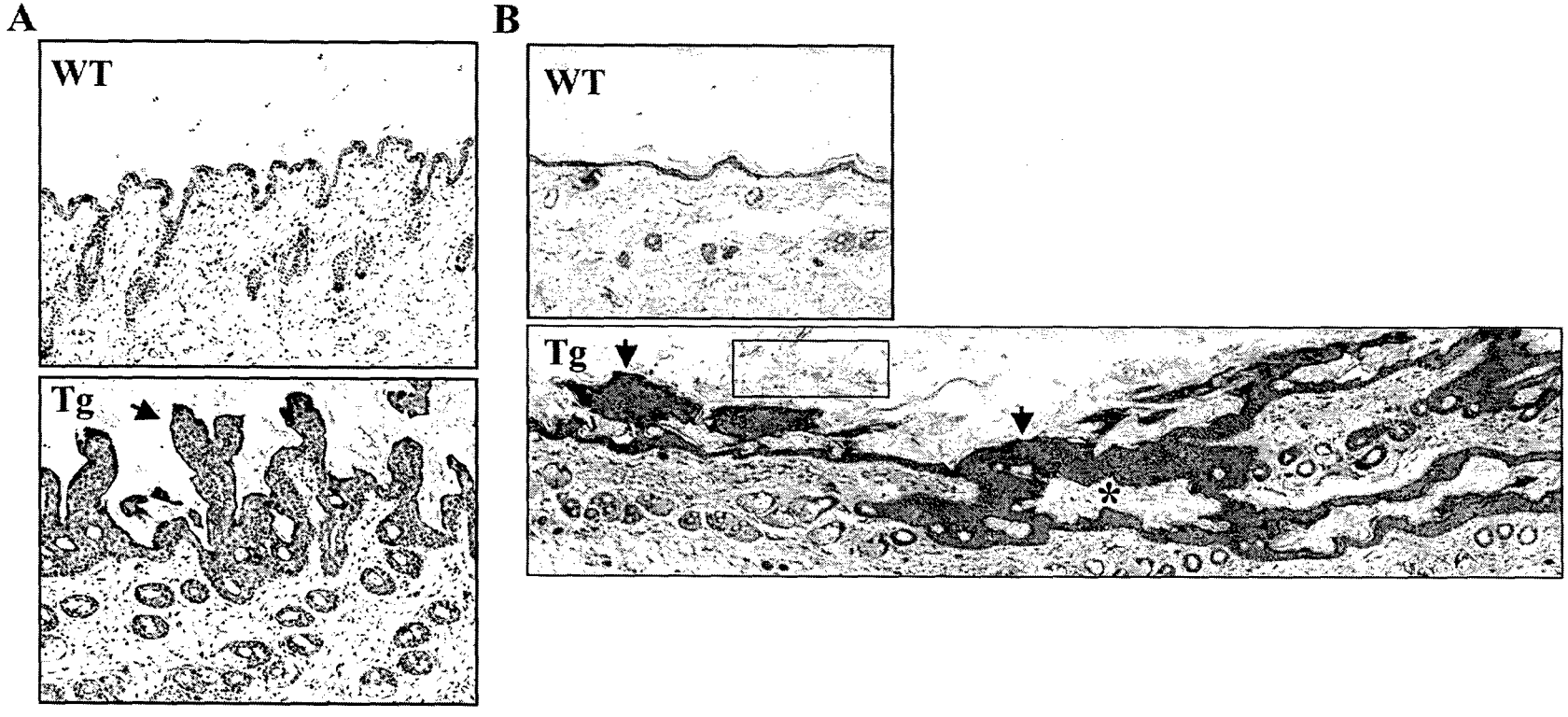

Brennan et al., 2006
Figure 9 A,B

C

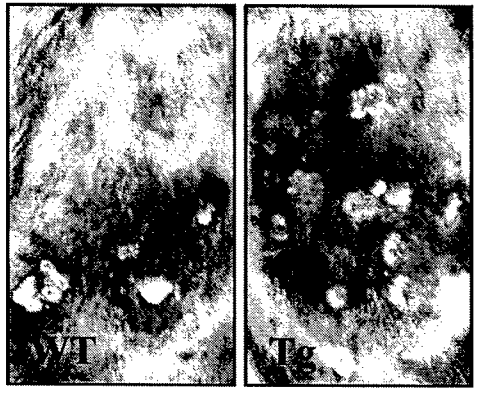

D

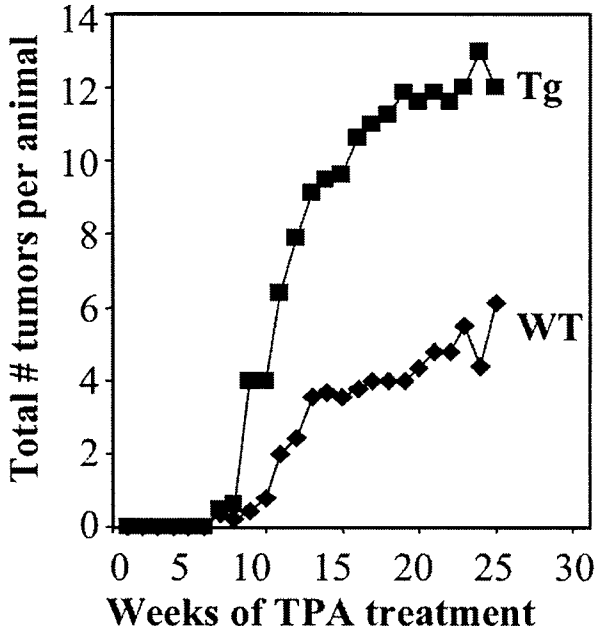

E

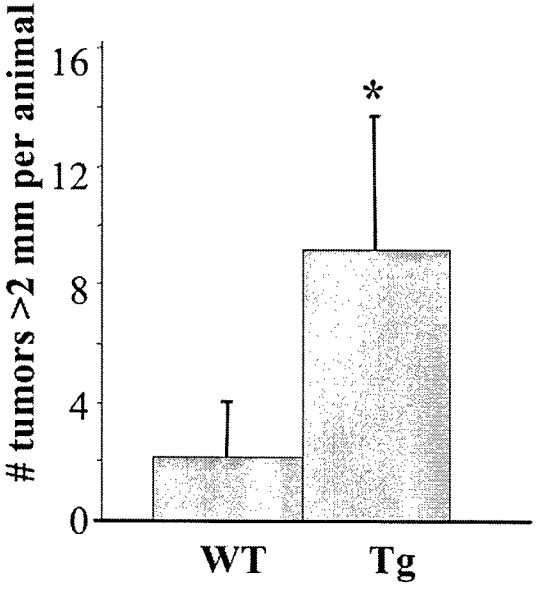

F

Brennan et al., 2006
Figure 9 C-F

A

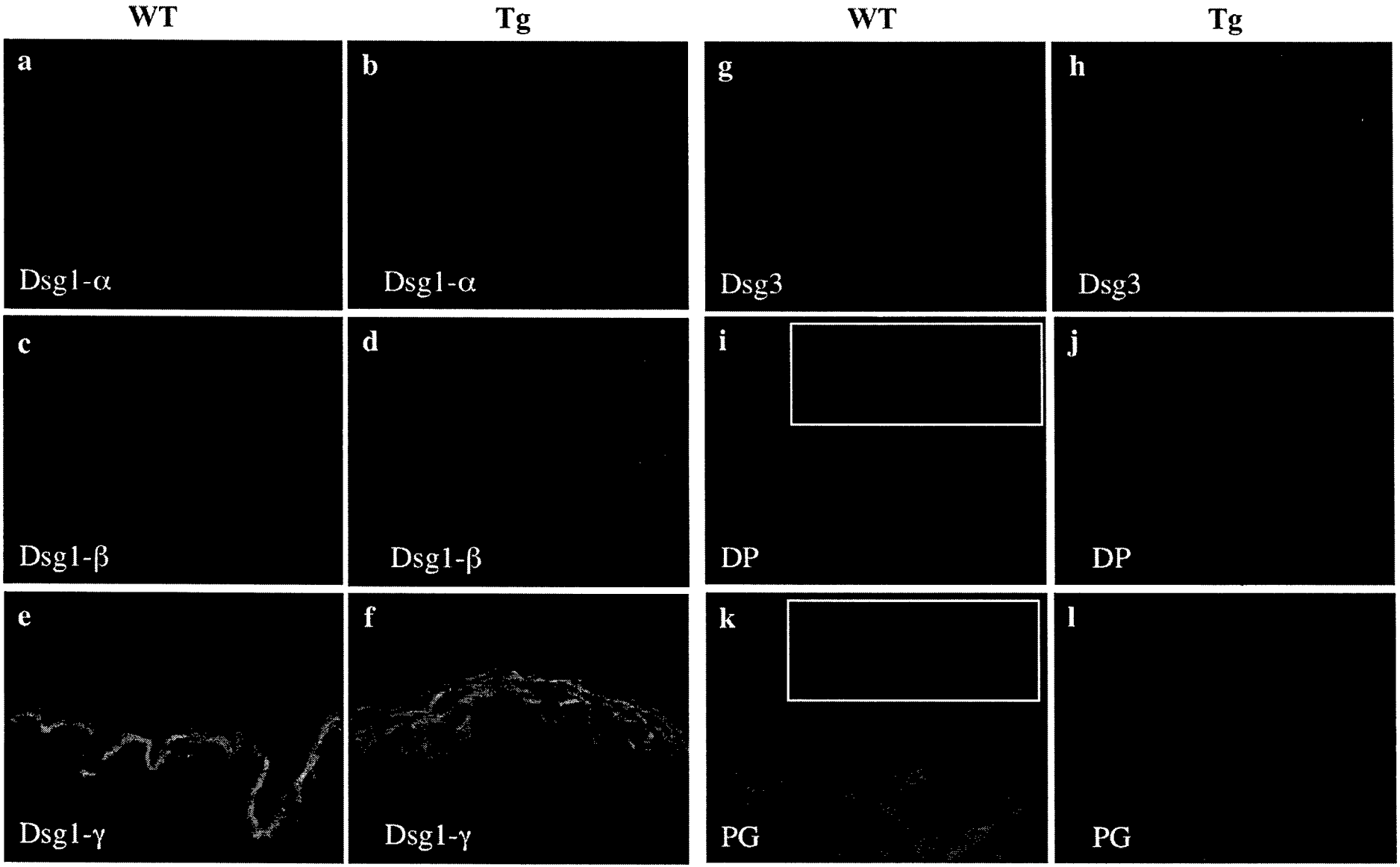

Brennan et al., 2006
Supplement Figure S1A

B

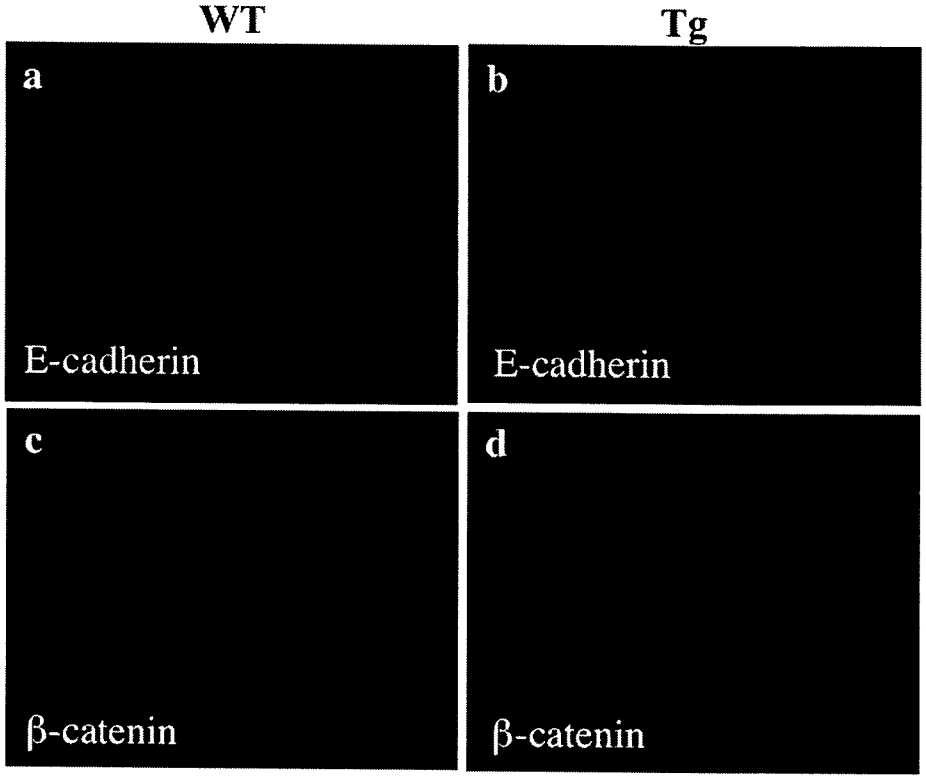

Brennan et al., 2006
Supplement Figure S1B

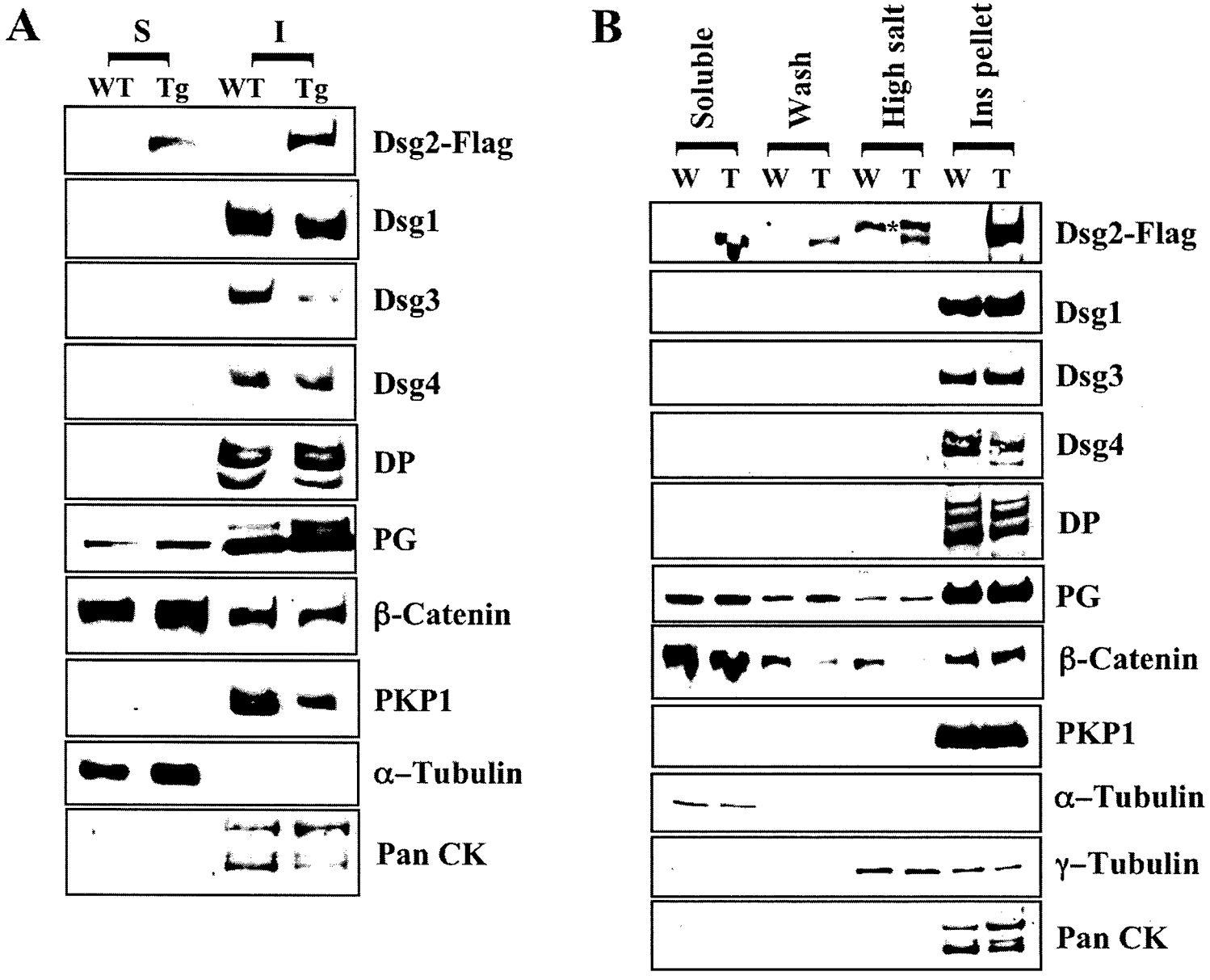

Brennan et al., 2006
Supplement Figure S2

A

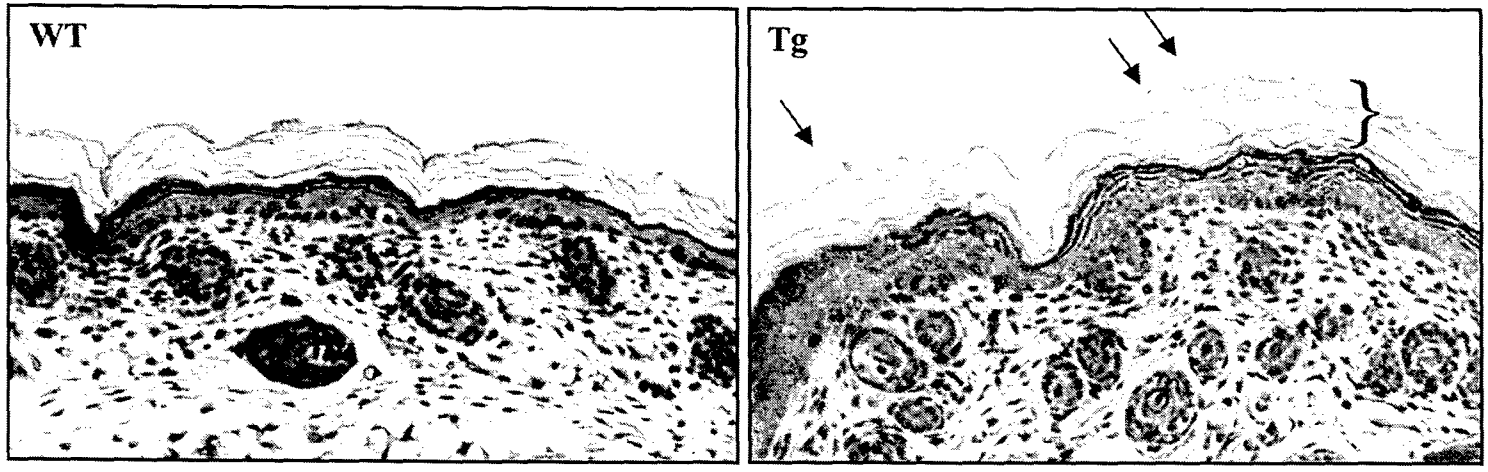

B

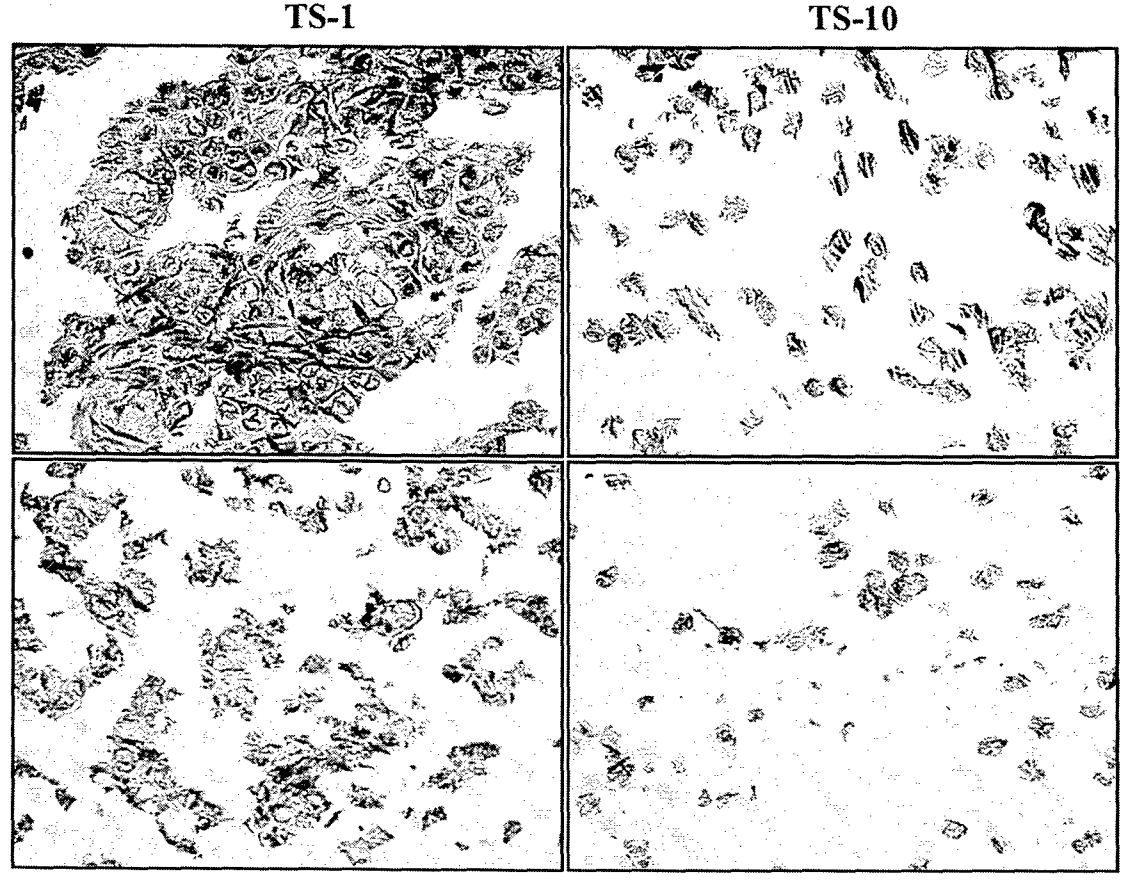

Brennan et al., 2006
Supplement Figure S3

THE JOURNAL OF BIOLOGICAL CHEMISTRY
Vol. 279, No. 31, Issue of July 30, pp. 32709–32715, 2004
Printed in U.S.A.

Upstream Determinants of Estrogen Receptor-α Regulation of Metastatic Tumor Antigen 3 Pathway*

Received for publication, March 16, 2004, and in revised form, May 28, 2004
Published, JBC Papers in Press, May 28, 2004, DOI 10.1074/jbc.M402942200

Sandip K. Mishra‡§, Amjad H. Talukder‡§, Anupama E. Gururaj‡§, Zhibo Yang‡, Rajesh R. Singh‡, My G. Mahoney¶‖, Clara Francí, Ratna K. Vadlamudi‡, and Rakesh Kumar‡ ‡‡**

*From the ‡Department of Molecular and Cellular Oncology, The University of Texas M. D. Anderson Cancer Center, Houston, Texas 77030, the ¶Department of Dermatology and Cutaneous Biology Thomas Jefferson University, Philadelphia, Pennsylvania 19107, and **Unitat de Biologia Cellular Molecular, Institute Municipal d'Investigacio Medica, Universitat Pompeu Fabra, 08003 Barcelona, Spain*

Although recent studies have shown a role of estrogen receptor-α (ER) in the regulation of epithelial-to-mesenchymal transition via MTA3, the role of upstream determinants of ER regulation of *MTA3* and the underlying molecular mechanism remains unknown. Here we show that *MTA3* gene regulation by ER is influenced by dynamic changes in levels of nuclear coregulators. *MTA3* promoter has a functional ER element half-site with which MTA1 and HDACs interact under basal conditions. Upon estrogen stimulation, these corepressors are derecruited with concomitant recruitment of ER, leading to increased *MTA3* transcription and expression. Genetic inactivation of MTA1 pathway promotes the ability of ER to up-regulate *MTA3* expression, whereas knockdown of ER enhances MTA1 association with *MTA3* gene. Modulation of ER functions, by corepressors (*i.e.* MTA1 and MTA1s) or coactivators (*i.e.* AIB1 and PELP1/MNAR), alters ER recruitment to *MTA3* chromatin, *MTA3* transcription, and expression of downstream epithelial-to-mesenchymal transition components. These studies provide novel insights into the transregulation of the *MTA3* gene and reveal novel roles of upstream determinants in modifying the outcome of MTA3 axis and cell differentiation.

The development of human breast cancer is promoted by estrogen stimulation of mammary epithelial cell growth. Estrogen receptor-α (ER)[1] is the major estrogen receptor in the human mammary epithelium. The binding of estrogen to ER triggers conformational changes that allow ER to bind to the 13-base-pair palindromic estrogen response element (ERE) in the target gene promoters and stimulates gene transcription thereby promoting the growth of breast cancer cells. The transcriptional activity of ER is affected by a number of regulatory cofactors including chromatin-remodeling complexes, coactivators, and corepressors (1–3).

Recent findings have demonstrated that the NuRD-70 polypeptide of the nucleosome-remodeling complex is identical to metastatic tumor antigen 1 (MTA1) (4, 5) and that MTA1 physically interacts with HDAC1/2 (6, 7). The *MTA1* gene is shown to correlate well with the metastatic potential of several human cell lines and cancers, including breast cancers (8–11). Using *in vitro* models, Mazumdar *et al.* (12) have shown that MTA1 interacts with ER and represses ER transcription by recruiting HDAC to the ERE-containing target gene chromatin in breast cancer cells. MTA1-overexpressing breast cancer cells exhibit aggressive phenotypes (13). MTA1s, another family member, is a naturally occurring variant of MTA1 that contains a novel sequence of 33 amino acids with one potential nuclear receptor binding motif, LRILL. MTA1s inhibits ER nuclear signaling by sequestering ER in the cytoplasm but enhances ER cytoplasmic signaling and thus promotes tumorigenesis (14).

One of the principal phenotypic changes in breast cancer metastasis is the increased tendency of the cancer cells to undergo epithelial-to-mesenchymal (EMT) transition that is characterized by reduced expression and consequently, functions of cell-adhesion components such as E-cadherin (15–17). The zinc finger transcriptional repressor, Snail, mediates the repression of E-cadherin expression and leads to the inhibition of Snail function in epithelial cells, thus, restoring the expression of E-cadherin as well as cell-to-cell junctions (18, 19). Recently, Fujita *et al.* (20) identified *MTA3* as an ER-regulated gene and showed that *MTA3* up-regulation prevents EMT by directly repressing Snail and thereby up-regulating E-cadherin. Although these observations highlight the significance of EMT in breast cancer invasiveness and suggest a complex role for MTA family members in modifying ER functions in breast cancer cells, the precise mechanism by which ER regulates MTA3 expression and the putative nature of upstream determinants of MTA3 expression remain poorly understood.

Here we show that *MTA3* contains an ER element half-site and that both ER and MTA1 are recruited to the same site in the *MTA3* promoter chromatin. Further, estrogen stimulates *MTA3* promoter activity in a corepressor-sensitive manner. In addition, modulation of ER functions by corepressors (*i.e.* MTA1 and MTA1s) or coactivators (*i.e.* AIB1 and PELP1/MNAR) results in the suppression or stimulation of ER recruitment to the *MTA3* chromatin and consequently affects the expression of EMT components. Together, these studies reveal that the dynamic changes in the levels of ER coregulators influence ER regulation of *MTA3*

* This study was supported by Grants CA90970, CA098823 (to R. K.), and in part by CA095681 (to R. V.) from the National Institutes of Health. The costs of publication of this article were defrayed in part by the payment of page charges. This article must therefore be hereby marked "*advertisement*" in accordance with 18 U.S.C. Section 1734 solely to indicate this fact.

§ These authors contributed equally to this work.

‖ Supported by Grant DAMD 17-02-1-0215 from the Department of Defense.

‡‡ To whom correspondence should be addressed. E-mail: rkumar@mdanderson.org.

[1] The abbreviations used are: ER, estrogen receptor-α; MTA, metastatic tumor antigen; mAb, monoclonal antibody; ERE, estrogen response element; EMT, epithelial-to-mesenchymal; ChIP, chromatin immunoprecipitation; siRNA, small interfering RNA; PR, progesterone receptor; HDAC, histone deacetylase.

TABLE I
Primer and siRNA sequences used in the study

MTA3 promoter cloning	
MTA3-pro1988F	tgtcagagagctcttggtgggatctctggta
MTA3-pro3066R	gagcctcgaggctctagggccaggaa
MTA3-pro2331F	ttatttgagctctttgcctcagctatgca
MTA3-pro3066R	gagcctcgaggctctagggccaggaa
MTA3 promoter deletion/mutation	
MTA3pro2073F	tgacacagagctcagaatttgacacac
MTA3pr-mut-F2	acgaggaaacagagcatagagtca
MTA3pr-mut-R2	tgactctatgctctgtttcctcgt
MTA3 reverse transcriptase-PCR F	accctcgtgttagaagtcacgtgt
MTA3 reverse transcriptase-PCR R	gcagcataattaatagcaacaaacgg
MTA3 cDNA cloning	
MTA3-start	gcgggtacccatggcggccaacatgtaccgggt
MTA3-stop	caacatctcgagttaagaatttaaaagcatct
MTA3 ChIP primers	
MTA3ChIPF1	ggaatagagagaagggacctaacgc
MTA3ChIPR1	tgagcctcaagaggggttacaa
MTA3ChIPF2	cataagcaatttctcctccttcgaa
MTAChIPR2	tcacgtccccattttatagacgag
MTAChIPR3	acacagctgtgtgctgtcgact
MTAChIPF4	tggtttctaggtggcttttg
MTAChIPR4	tggtggcttgtttggaatgt
MTA1 siRNA	
Mta1siRNA-1	aaccctgtcagtctgctataa
Mta1siRNA-2	aagaccctgctggcagataaa
Mta1siRNA-3	aagattttctcccgtggaagt
Mta1siRNA-4	aagaagcgcggctaacttatt
Control siRNA	Nonspecific pooled duplex control catalog number SD-001206–13-80

and reveal a novel role for nuclear coregulators in modifying the outcome of MTA3-mediated EMT.

EXPERIMENTAL PROCEDURES

Cell Lines and Reagents—MCF-7 human breast cancer cells and HeLa cells were maintained in Dulbecco's modified Eagle's medium-F12 (1:1) supplemented with 10% fetal calf serum. HeLa cervical cancer cells were obtained from the American Type Culture Collection (Manassas, VA). MCF-7 clones stably expressing MTA1, MTA1s, and PELP1 have been described earlier (12, 14, 21). Steroid hormone E_2, tamoxifen, and charcoal-stripped serum (*N,N′*-dicyclohexylcarbodiimide serum) was purchased from Sigma. ICI-182, 780 was purchased from Tocris, Ellisville, MO. Antibodies against MTA1 were purchased from Santa Cruz Inc. (Santa Cruz, CA) and T7 monoclonal antibodies (mAb) was procured from Novagen (Milwaukee, WI). Antibodies for E-Cadherin were obtained from Zymed Laboratories Inc., and ER antibody was purchased from UBI. The Snail antibody used here has been described before (22).

Rabbit anti-peptide against MTA3 was generated against the mouse MTA3 amino acids 420–438 (sequence SDEEKSPSPTAEDPRARSH). The MTA3-GST fusion protein was run on SDS-PAGE and transferred to nitrocellulose filter. The blot was stained with Ponceau S, and the region of the blot with the GST-MTA3 fusion protein was cut. The GST-MTA3 blots were incubated in 10 ml of 1% bovine serum albumin for 3–4 h at 4 °C to block nonspecific sites. The bovine serum albumin-treated nitrocellulose pieces were incubated with diluted rabbit antiserum in cold overnight. Subsequently, the nitrocellulose pieces were washed 4× in Tris-buffered saline with 0.01% (v/v) Tween 20 for 5 min each and transferred to Eppendor tubes, and the bound MTA3 antibody was eluted by sequential incubation with 300 μl of monoclonal antibody purification system buffer, pH 3.0, for 5 min. Immediately after elution, 200 μl of 1 M Tris, pH 9.5, was added to prevent denaturation of the antibody. The eluates were pooled and stored −20 °C.

Cloning of MTA3 Promoter and MTA3 cDNA—To clone the MTA3 promoter, we first identified the BAC clone (number RP11-314A20) containing the MTA3 genomic region using human genome sequence information. We then purchased the BAC clone from BACPAC Resources (Children's Hospital Oakland Research Institute, Oakland, CA). Two fragments (1078 and 735 bp) of the MTA3 promoter region were amplified by PCR. The amplified products were cloned into the PGL3 luciferase reporter vector (Promega Corp., Madison, WI) using SacI and XhoI sites. The sequence of the construct was verified by comparing its sequence with that in the human genome data base. PCR based cloning was used to generate the deletion construct and point mutation of the 1078 bp MTA3 promoter. PCR product of MTA3 cDNA was cloned at pcDNA3.1A using KpnI and XhoI sites (see Table I for primer sequences).

Reporter Assays—For the reporter gene transient transfections, cells were cultured for 24 h in minimal essential medium without phenol red containing 5% *N,N′*-dicyclohexylcarbodiimide serum. The MTA3-luciferase reporter constructs were transfected using FuGENE 6 according to the manufacturer's instructions (Roche Applied Science). Twenty-four hours later, the cells were treated with E_2 for 16 h. The cells were then lysed with a passive lysis buffer, and the luciferase assay was performed using a luciferase reporter assay kit (Promega). The total amount of DNA used in the transfections was kept constant by adding a parental vector. Each transfection was carried out in six-well plates in triplicate wells.

Chromatin Immunoprecipitation (ChIP) Assay—Approximately 10^6 cells were treated with 1% formaldehyde (final concentration, v/v) for 10 min at 37 °C to cross-link histones to DNA. The cells were washed twice with phosphate-buffered saline, pH 7.4, containing protease inhibitor mixture (Roche Applied Science). The ChIP assay was performed as described previously (12). An ER-α-specific antibody, MTA1 mAb, or T7 mAb were used for the immunoprecipitation of protein-bound chromatin, and precipitated DNA was amplified by PCR using primers flanking the proximal half-ERE site (see Table I for primer sequences). The amplified fragment was sequence-verified.

Gene Knockdown by Small Interfering RNA (siRNA)—ER-α-specific siRNA and control nonspecific siRNA were purchased from Dharmacon. For MTA1 knockdown, 4-for-Silencing siRNA Duplexes were designed using a Qiagen program and synthesized at Qiagen. siRNA transfections were carried out using 20 μM pooled siRNA duplexes and by using 4 μl of Oligofectamine (Invitrogen) according to the manufacturer's protocol in six-well plates. After 72 h, cells were prepared for ChIP assay or Western blotting.

Immunofluorescence and Confocal Studies—The cellular location of proteins was determined using indirect immunofluorescence, as described previously (14). In brief, MCF-7 cells were plated on glass coverslips in six-well culture plates. When the cells were 50% confluent, cells were rinsed with phosphate-buffered saline, fixed in cold methanol for 6 min, and then processed for immunofluorescence staining of endogenous MTA3, E-Cadherin, or Snail. Cells were counterstained with ToPro3 to visualize the nucleus. Slides were further processed for imaging and confocal analysis using a Zeiss LSM 510 microscope and a 40× objective.

RESULTS AND DISCUSSION

Cloning and Regulation of MTA3 Promoter by Estrogen—To delineate the mechanism of ER regulation of *MTA3* expression, we first analyzed the sequence of the putative *MTA3* promoter region (GenBank™ genomic sequence accession number NT_022184) for the presence of ER-responsive elements using

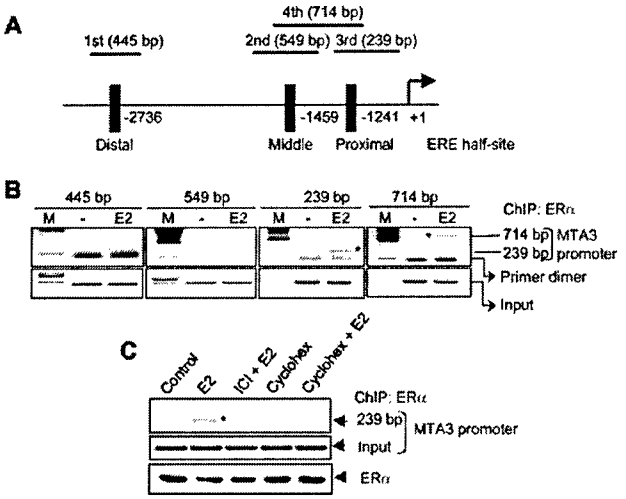

FIG. 1. **Identification of the ER interaction site on the MTA3 regulatory elements.** *A*, schematic representation of the MTA3 gene around the three possible ERE half-site-α recruitment sites. *B*, association of ER with the MTA3 chromatin. E_2 signaling promotes interaction of ER with one of the possible ERE half-sites in MTA3 chromatin. MCF-7 cells grown in a phenol red-free medium supplemented with 3% charcoal dextran-stripped fetal bovine serum were treated with or without estrogen (10^{-9} M) for 60 min. Chromatin lysates were immunoprecipitated with antibodies against ER, and samples were processed as described under "Experimental Procedures." The *lower panel* shows the PCR analysis of the input DNA of the MTA3 chromatin. The *upper panel* demonstrates the PCR analysis of the MTA3 promoter fragments for possible association with ER (n = 3). *C*, MCF-7 cells were maintained in medium supplemented with 3% charcoal dextran-stripped fetal bovine serum before treating either with estrogen (10^{-9} M), ICI-182780, both estrogen and ICI, cyclohexamide (*cyclohex*) (10 μg/ml) or cyclohexamide plus estrogen. The *top panel* demonstrates the PCR analysis of the MTA3 promoter fragments for possible association with ER. The *middle panel* shows the PCR analysis of the input DNA of the MTA3 chromatin. The *bottom panel* shows a Western blot analysis for ER under the same conditions (n = 3). *, band of interest.

Matinspector (Genomatix). This program did not reveal any consensus 13-bp ERE sites. However, we found that the *MTA3* promoter contains three potential ERE half-sites (TGACC) (Fig. 1*A*). Interestingly, all the three ERE half-sites were localized in the vicinity of AP1 binding sites. Because a number of ER-responsive genes have been shown to be regulated via ERE half-sites in conjunction with either AP1 or SP1 sites (23), we examined the potential involvement of these ERE half-sites in the regulation of *MTA3* expression by ER.

To explore the recruitment of ER to the endogenous *MTA3* promoter, MCF-7 breast cancer cells were treated with or without estrogen and subjected to ChIP assays using an anti-ER antibody. We found that ligand-activated ER is recruited to the endogenous *MTA3* promoter at the ER element half-site from positions −1256 to −1245 but not to the other two potential sites (Fig. 1*B*). To verify these results, we next designed a pair of primers that encompass proximal as well as the middle potential ERE half-sites. Results showed estrogen-induced recruitment of ER to the MTA3 promoter region of expected 714 bp (Fig. 1*B*, *right panel*). To ascertain that the detected 239-bp band indeed represents the regulatory region corresponding to the proximal ERE half-site, the PCR-amplified DNA fragment was cloned into a TOPO vector and confirmed by sequencing (data not shown). Estrogen-induced recruitment of ER to the *MTA3* promoter chromatin was effectively blocked by the inclusion of anti-estrogen ICI-182780 suggesting that estrogen-activated recruitment of ER to the *MTA3* gene was specific. Because ER recruitment to the *MTA3* promoter was also inhibited by the protein-synthesis inhibitor cycloheximide (Fig. 1*C*), it appears that this event requires new protein synthesis, and the noted effects could be mediated via an indirect mechanism. This appears to be consistent with the notion that ER action through an ERE half-site requires an associated factor and that direct interaction with DNA may not be involved (21). Given that it has been demonstrated previously that estrogen up-regulates both its own receptor, ER, as well as ER coactivators expression (21, 24), it seemed likely that sufficient quantities of ER and its coactivators were necessary for up-regulation of MTA3 expression by estrogen. To test this hypothesis, we looked at the levels of ER under the same experimental conditions and did not find changes in ER amounts in the cell for any of the conditions.

To further study the regulation of the *MTA3* promoter via the ERE half-site, a *MTA3* promoter fragment was amplified from the BAC clone and DNA fragments of desired sizes, 1078 and 735 bp, were obtained. The *MTA3* promoter fragments were cloned into a pGL3-luciferase reporter system. The functionality of MTA3-luciferase vectors was tested in MCF-7 and HeLa cells (Fig. 2, *A* and *B*). Estrogen treatment of the cells stimulated the MTA3-regulatory element-driven reporter activity from the 1078-bp fragment (−1528 to −450, contains two ERE half-sites, at −1459 and at −1241) but not from the 735-bp fragment (−1185 to −450, lacks −1241-bp ERE half-site) (Fig. 2*B*), and therefore, the MTA3 1078-bp luciferase construct was used in the subsequent studies. Estrogen-stimulated *MTA3* promoter activity was effectively blocked by tamoxifen, an estrogen antagonist, which also had a modest inhibitory effect on basal *MTA3* promoter activity (Fig. 2, *C* and *D*). To validate the proximal ERE half-site (at −1241) in the estrogen stimulation of MTA3 promoter, we created a point mutation up to −1241 and deletion at −1450 of the 1078-bp *MTA3* promoter. As shown in Fig. 2, *E* and *F*, the point mutation at the proximal ERE half-site abolished the estrogen stimulation, whereas deletion of the middle ERE half-site did not affect estrogen stimulation as compared with the 1078 bp fragment. Together, these findings confirm that the observed recruitment of ligand-activated ER to the *MTA3* promoter chromatin is accompanied by increased *MTA3* promoter activity.

Regulation of MTA3 Expression and EMT by MTA1—Because MTA1 and MTA1s are natural inhibitors of ER functions (12, 14, 25), we next tested whether the deregulation of these proteins may influence MTA3 expression and functions. Using breast cancer cells stably expressing T7-MTA1 (12) or T7-MTA1s (14), we found that the repression of ER function by MTA1 or MTA1s abolished the ability of estrogen to promote the recruitment of ER to the *MTA3* gene chromatin (Fig. 3, *A* and *B*). Because both MTA1 and MTA1s had similar effects, we used only MTA1 to repress the functions of ER in subsequent studies. Overexpression of MTA1 in breast cancer cells also resulted in the inability of estrogen to induce MTA3 mRNA (Fig. 3*C*). The observed inhibition of MTA3 expression by MTA1 was at the level of transcription, as coexpression of MTA1 inhibited both the basal and estrogen-induced stimulation of *MTA3* promoter activity (Fig. 3*D*). In MTA1 overexpressing conditions without estrogen stimulation, expression of the MTA3 protein was not inhibited, whereas *MTA3* promoter activity did show repression. Based on these results, one could speculate that there could be additional regulatory elements that may be involved in MTA3 basal expression in the physiological setting. It could also be possible that the basal repression observed in the promoter-reporter analysis is due to an inherent limitation of the assay system, because it reflects the regulation of the promoter area largely in isolation and under artificial conditions. Results from confocal scanning microscopy also demonstrated that MTA1 deregulation leads to a significant reduction in the levels of nuclear MTA3, up-regulation of

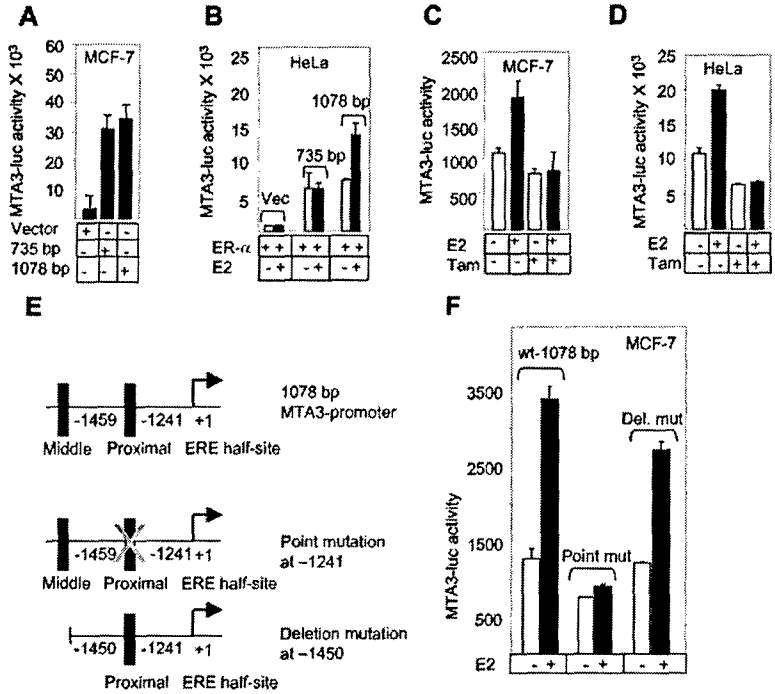

FIG. 2. **Estrogen-mediated induction of MTA3 promoter activity.** *A*, induced luciferase activity with 735- and 1078-base-pair fragments of the MTA3 promoter ($n = 3$) in MCF-7 cells. Cells were maintained in 3% *N,N'*-dicyclohexylcarbodiimide serum in phenol-red free medium for 48 h before transfection of the luciferase constructs, luciferase activity was assayed at 48 h post-transfection. Values are normalized to β-galactosidase activity ($n = 3$). *B*, induced luciferase activity with 735 and 1078 base pair of the MTA3 promoter ($n = 3$) in HeLa cells. *C* and *D*, estrogen (10^{-9} M)-mediated and 4-hydroxyl tamoxifen (10^{-8} M)-mediated regulation of MTA3 promoter activity in MCF-7 cells and in HeLa cells, respectively ($n = 3$). All treatments with ligands were for 16 h. *E*, schematic diagram of the MTA3 promoter (*top bar*) was deleted and mutated. To find out which ERE half-site is responsible for the estrogen induction, a point mutation of the proximal ERE half-site at −1241 is done (TGACC–TGCTC) (*middle bar*), and the second ERE half-site is deleted at −1450 by PCR (*bottom bar*). *F*, the 1078-base-pair wild type MTA3 promoter as well as the deletion and point mutation constructs are transfected in MCF-7 cells and treated with estrogen as before. The point mutation at the proximal ERE half-site abolishes the estrogen induction completely, whereas the deletion of the middle ERE half-site has little effect on estrogen stimulation

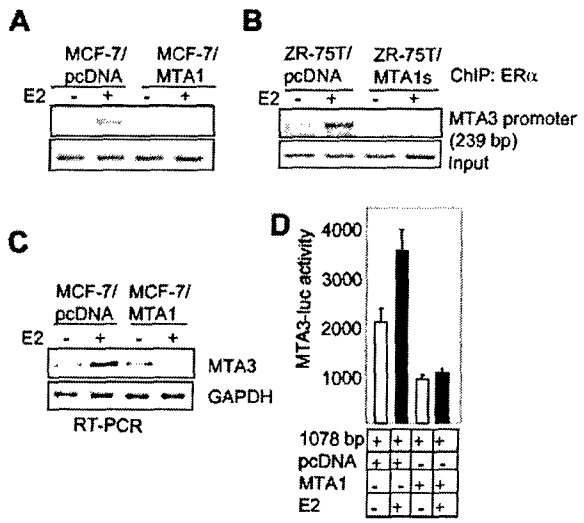

FIG. 3. **MTA1-mediated interference of association of ER with the MTA3 chromatin.** Cells were maintained in 3% charcoal dextran-stripped fetal bovine serum before treating with estrogen (10^{-9} M) in the following experiments. *A*, MTA1 inhibits ER recruitment on the MTA3 chromatin. The *lower panel* shows input DNA for the ChIP assay. MCF-7 cells overexpressing pcDNA or T7-MTA1 were taken for the above experiment. *B*, short variant of MTA1 inhibits association of ER with the MTA3 chromatin. The *lower panel* shows the input DNA for the ChIP assay. ChIP assay was performed in the ZR-75R cells overexpressing vector alone, or T7-MTA1s using the anti-ER antibody. *C*, reverse transcriptase-PCR analysis of the MTA3 mRNA level in MCF-7 cells stably expressing either control vector or T7-MTA1. *D*, MTA3 transcription activity in the presence of either control vector or T7-MTA1 with or without estrogen (10^{-9} M, 16 h).

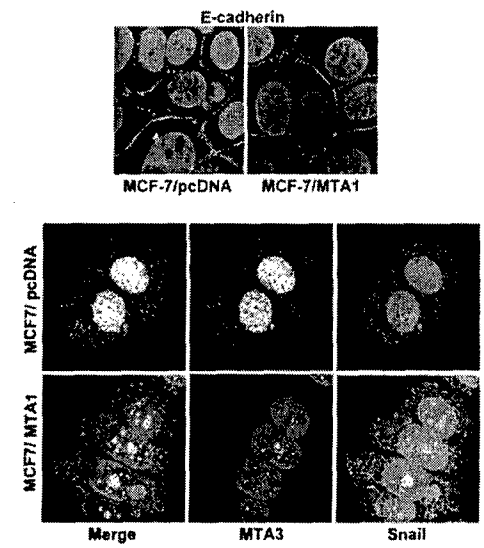

FIG. 4. **Expression of MTA3 and its downstream effectors in MTA1 overexpressing cells by confocal microscopy.** Confocal analysis of E-cadherin (*top panel*), MTA3, and Snail in MCF-7 cells expressing pcDNA (*middle panel*) and MTA1 (*bottom panel*). In the *top panel*, E-cadherin was stained *red* and in the *bottom panel*, MTA3 was stained *green*, and Snail was *red*. The nuclei were visualized using Topro3 (*blue*). The cells were all cultured in 10% serum containing medium.

Snail and consequent down-regulation of E-cadherin as compared with the levels of MTA3, Snail, and E-cadherin in control vector-transfected cells (Fig. 4). All of the above findings sug-

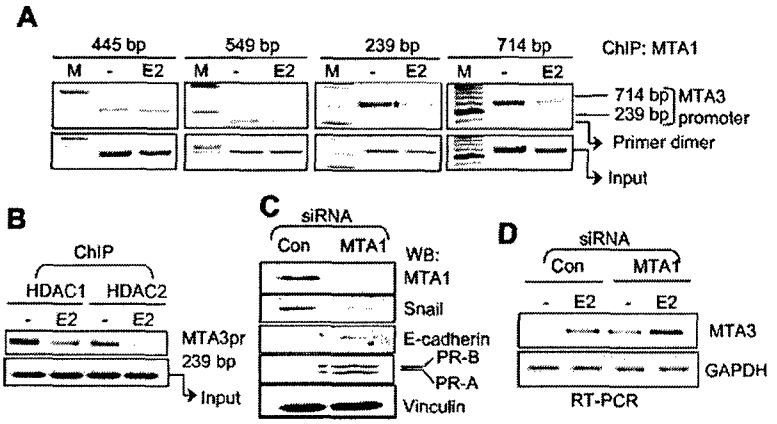

FIG. 5. **Direct association of MTA1 with the MTA3 chromatin and consequence of MTA1 and ER silencing on molecules downstream of MTA3.** *A*, ChIP analysis of direct association of MTA1 with the MTA3 chromatin in the presence or absence of estrogen. ChIP analysis was performed in MCF-7 cells. *B*, ChIP analysis of recruitment of HDAC1 and HDAC2 on the MTA3 chromatin in MCF-7 cells in the presence or absence of estrogen. *C*, Western analysis of molecules downstream of MTA3 as a result of knocking down MTA1 by siRNA in MCF-7 cells. The same blot was stripped and analyzed for expression of Snail, E-cadherin, PR-A, and PR-B as well as vinculin as a loading control. *D*, reverse transcriptase-PCR analysis of the MTA3 mRNA level in MCF-7 cells as a result of MTA1 silencing with or without estrogen. *, band of interest.

gest that the inhibition of ER transactivation functions by MTA1 could impair the ability of ER to up-regulate *MTA3* expression.

Modulation of MTA3 Chromatin by ER Coregulators—Because MTA1 prevented the recruitment of ligand-activated ER to the *MTA3* promoter, we next investigated the possibility of MTA1 recruitment to the *MTA3* promoter chromatin. MCF-7 cells were treated with or without estrogen, and chromatin lysates were immunoprecipitated with anti-MTA1 antibody. We found that MTA1 associates with the *MTA3* promoter in unstimulated MCF-7 cells but not in estrogen-stimulated cells (Fig. 5*A*). MTA1 association with the *MTA3* promoter was found to be at the proximal ERE half-site, which was also immunoprecipitated in the ER ChIP assay. These observations suggest that MTA1 associates with the basal *MTA3* promoter chromatin and upon estrogen treatment is derecruited with simultaneous recruitment of ER to the ER element half-site in the *MTA3* promoter chromatin. Because MTA1 has been shown to physically interact with HDAC1 and HDAC2 (6), we next examined whether the HDACs also interact with the basal *MTA3* promoter. Results from ChIP studies using anti-HDAC antibodies show the association of the HDACs with the *MTA3* promoter that, like MTA1, were also derecruited from the *MTA3* promoter upon estrogen treatment (Fig. 5*B*). These findings raise possibility that the basal MTA1 association with the *MTA3* promoter might influence the status of EMT components presumably because of the inhibitory effect of MTA1 on the ER transactivation functions. To test this notion, we silenced endogenous MTA1 expression using siRNA and examined the status of MTA3 target genes, as well as ER target genes in MCF-7 cells. Results indicated that inhibition of MTA1 expression leads to the down-regulation of Snail and the up-regulation of E-cadherin (Fig. 5*C*). Interestingly, there was also significant up-regulation of progesterone receptors PR-A and PR-B, well established ER target gene products, thus suggesting enhanced ER transactivation functions due to reduced levels of MTA1 and, consequently, loss of corepressor functions of MTA1. Consistent with these findings, a reduction in the levels of MTA1 by siRNA was accompanied both by an increased basal expression of MTA3 and the enhanced ability of estrogen to up-regulate MTA3 expression (Fig. 5*D*). Interestingly, there was also increased estrogen-induced stimulation in the levels of ER in MTA1 knockdown cells (data not shown) implying that in the absence of MTA1, ligand-induced up-regulation of ER might participate in the amplification of ER regulation of MTA3 expression.

Regulation of MTA3 Gene by the Endogenous MTA1—To determine whether the above changes in the levels of MTA3

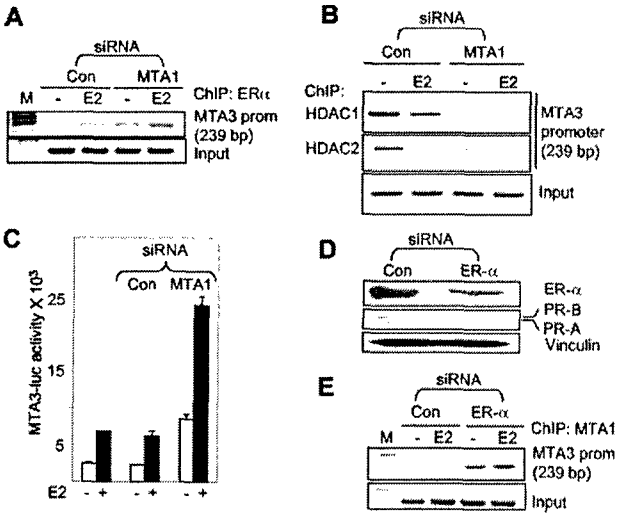

FIG. 6. **Effect of MTA1 knockdown on MTA3 gene regulation** *A*, ChIP analysis of the MTA3 chromatin for ER recruitment in MCF-7 cells with or without MTA1 silencing in the presence or absence of estrogen (10^{-9} M). *B*, ChIP analysis of the MTA3 chromatin for HDAC1 and HDAC2 recruitment in the presence or absence of estrogen in MCF-7 cells having normal or silenced MTA1 expression. *C*, effect of MTA1 silencing on MTA3 luciferase activity in MCF-7 cells in the presence or absence of estrogen (10^{-9} M). *D*, immunoblotting of samples having normal ER-α expression and silenced ER expression, which is reprobed for PR (PR-A and PR-B) and vinculin as a loading control. *E*, ER was knocked down in MCF-7 cells, and ChIP analysis was performed for T7-MTA1 recruitment on the MTA3 chromatin in the presence or absence of estrogen.

and its targets in MTA1 knockdown MCF-7 cells were because of a modification of the *MTA3* chromatin in the vicinity of the ER element half-site, we next performed ChIP analysis of ER recruitment on the *MTA3* chromatin under conditions of MTA1 knockdown (Fig. 6*A*). We found that the suppression of endogenous MTA1 expression leads to detectable basal association of ER with the *MTA3* promoter, which as expected was further enhanced upon estrogen signaling. The above result was corroborated in a luciferase assay system where the knockdown of MTA1 resulted in a significant increase in both basal and estrogen-induced *MTA3*-luciferase activity (Fig. 6*B*). Consistent with these results, silencing of the endogenous MTA1 in MCF-7 cells resulted in a substantial decrease in the recruitment of HDACs to the *MTA3* promoter segment, and estrogen stimulation led to complete dissociation of the HDACs from the *MTA3* promoter (Fig. 6*C*). To further support the notion that MTA1 and ER might be competing for the ER element half-site

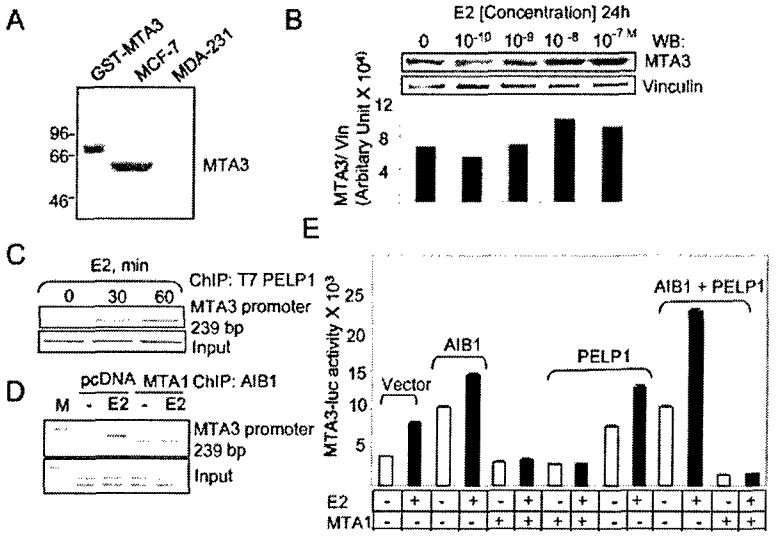

FIG. 7. **Coregulator recruitment and its effect on MTA3 promoter activity** *A*, detection of MTA3 protein in MCF-7 cell line. *B*, increased expression of MTA3 protein in MCF-7 cells in response to different concentrations of estrogen after 24 h of treatment. MTA3 protein levels were quantified using ImageQuant and normalized to vinculin levels in the cells. *C*, association of PELP1 with MTA3 promoter in a time-dependent and estrogen-sensitive manner in MCF-7 cells stably expressing T7-PELP1. For immunoprecipitation, anti-T7 antibody was used, which is targeted against the T7-PELP1. *D*, MTA1 inhibits the association of AIB1 with the MTA3 chromatin. MCF-7 cells either overexpressing the vector alone or T7-MTA1 were analyzed by ChIP assay for possible recruitment of AIB1 with or without estrogen signaling. Cross-linked cells were lysed and taken for immunoprecipitation with anti-AIB1 antibody. *E*, MTA3 luciferase activity was measured in the presence or absence of different coactivators, such as AIB1 and PELP1, and the corepressor MTA1 with or without estrogen treatment.

in the *MTA3* promoter, we next knocked down the endogenous ER in MCF-7 cells by siRNA, as assessed by the levels of ER and the ER target gene products, PR-A and PR-B (Fig. 6*D*). As before, cells were also treated with a control siRNA. Next we performed a ChIP assay to analyze the status of MTA1 recruitment on the *MTA3* promoter under the conditions of ER knockdown. We found that ER silencing indeed leads to a significantly increased association of endogenous MTA1 with the basal *MTA3* chromatin. Results also suggest that estrogen stimulation was unable to trigger derecruitment of MTA1 from the *MTA3* promoter region (Fig. 6*E*). Together, these experiments establish that the *MTA3* promoter is a target of MTA1 and that manipulation in the levels of MTA1 expression influences the recruitment pattern of ER to the *MTA3* promoter chromatin in a significant manner.

In conformity with a recent report (20), we found that estrogen signaling increases MTA3 protein levels (Fig. 7*B*) in a dose-dependent manner. Fig. 7*A* shows Western blot analysis carried out to characterize the MTA3 antibody and indicates the abundant amounts of MTA3 protein in MCF-7 cells. Because the ER-mediated activation of transcription involves recruitment of coactivators to the promoter area, we next examined the potential role of ER coactivators in the regulation of MTA3 expression. Using previously characterized MCF-7 cells stably expressing T7-PELP1 (also known as MNAR) (26), we showed that estrogen stimulation leads to enhanced recruitment of PELP1/MNAR to the *MTA3* promoter chromatin (Fig. 7*C*), implying a role of coactivators in the regulation of MTA3 expression by ER. To determine the impact of MTA1 in the recruitment of coactivators to the *MTA3* promoter chromatin, we next used MCF-7 cells expressing T7-MTA1 and examined the ability of estrogen to recruit AIB1, another ER-coactivator (27, 28), to the *MTA3* promoter chromatin. As illustrated in Fig. 7*D*, upon estrogen stimulation, we found significant recruitment of endogenous AIB1 to the *MTA3* promoter chromatin in MCF-7/vector cells. Deregulation of MTA1 completely abolished the noticed AIB1 interaction with the *MTA3* promoter chromatin. To further understand the mechanistic participation of ER coactivators in the regulation of *MTA3* expression, we next examined the ability of PELP1 and/or AIB1 to stimulate *MTA3* transcription using promoter assays (Fig. 7*E*). We observed a substantial induction of the *MTA3* promoter activity by PELP1/MNAR or AIB1 in comparison with the vector-cotransfected cells. Coexpression of both PELP1/MNAR and AIB1 further augmented transcriptional activity of the *MTA3* promoter as compared with expression of the individual coactivators by themselves. Interestingly, overexpression of MTA1 completely inhibited the ability of PELP1/MNAR and/or AIB1 to stimulate *MTA3* transcription.

In brief, these observations suggest that the *MTA3* chromatin segment, containing the *bona fide* ER recruitment site, represents a highly dynamic surface for ER as well as ER interacting coactivators and corepressors. The resulting transcriptional activity may be tightly regulated by the dynamic interplay of ER coregulators. Fujita *et al.* (20) made an interesting observation that each of the MTA family members could be essential components of distinct subsets of the Mi-2·NuRD complexes that have unique functional properties. MTA1 repression of MTA3 expression could presumably be a mechanism by which the cell type-specific transcription is controlled. We hypothesize that the levels of MTA1 in the cell would determine which subset of the Mi-2·NuRD complex would be active to carry out its specialized function. Because MTA1 has been shown to be associated with more metastasis and invasiveness in tumors, regulation of *MTA3* gene expression by MTA1, both under basal conditions as well as in the presence of estrogen, assumes importance. In this context, MTA1 overexpression, leading to the down-regulation of MTA3 and E-cadherin expression, would give the tumors survival and metastatic advantage over other cells. In our model cell lines, the overexpression of MTA1 resulted in non-responsiveness of these cells to estrogen in terms of induction of *MTA3* gene by ER. It could be speculated that this could be one of the mechanisms by which tumors eventually stop responding to estrogen and consequently, anti-estrogen therapy. Furthermore, it is also possible that MTA1 may also repress gene expression of both ER and its coactivators in these situations. If it does so, then MTA1 could be targeted for therapeutic intervention to

sensitize the tumor cells to anti-estrogen therapies, which could have tremendous clinical impact.

Acknowledgments—We thank Dr. Myles A. Brown for AIB1 antibodies, and Dr. Antonio Garcia de Herreros for helpful comments about this manuscript.

REFERENCES

1. Belandia, B., and Parker, M. G. (2003) *Cell* **114,** 277–280
2. Shao, W., and Brown, M. (2004) *Breast Cancer Res. Treat.* **6,** 39–52
3. Wagner, B. L., Valledor, A. F., Shao, G., Daige, C. L., Bischoff, E. D., Petrowski, M., Jepsen, K., Baek, S. H., Heyman, R. A., Rossenfeld, M. G., Schulman, I. G., and Glass, C. K. (2003) *Mol. Cell. Biol.* **23,** 5780–5789
4. Xue, Y., Wong, J., Moreno, G. T., Young, M. K., Cote, J., and Wang, W. (1998) *Mol. Cell.* **2,** 851–861
5. Solari, F., and Ahringer, J. (2000) *Curr. Biol.* **10,** 223–226
6. Toh, Y., Kuninaka, S., Endo, K., Oshiro, T., Ikeda, Y., Nakashima, H., Baba, H., Kohnoe, S., Okamura, T., Nicolson, G. L., and Sugimachi, K. (2000) *J. Exp. Clin. Cancer Res.* **19,** 105–111
7. Humphrey, G. W., Wang, Y., Russanova, V. R., Hirai, T., Qin, J., Nakatani, Y., and Howard, B. H. (2001) *J. Biol. Chem.* **276,** 6817–6824
8. Toh, Y., Pencil, S. D., and Nicolson, G. L. (1994) *J. Biol. Chem.* 22958–22963
9. Toh, Y., Oki, E., Oda, S., Tokunaga, E., Ohno, S., Maehara, Y., Nicolson, G.L., and Sugimachi, K. (1997) *Int. J. Cancer.* **74,** 459–463
10. Toh, Y., Kuwano, H., Mori, M., Nicolson, G.L., and Sugimachi, K. (1999) *Br. J. Cancer.* **79,** 1723–1726
11. Sasaki, H., Moriyama, S., Nakashima, Y., Kobayashi, Y., Yukiue, H., Kaji, M., Fukai, I., Kiriyama, M., Yamakawa, Y., and Fujii, Y. (2002) *Lung Cancer* **35,** 149–154
12. Mazumdar, A., Wang, R., Mishra, S. K., Adam, L., Yarmand, R. B., Mandal, M., Vadlamudi, R., and Kumar, R. (2001) *Nat. Cell Biol.* **3,** 30–37
13. Mahoney, M. G., Simpson, A., Jost, M., Noe, M., Kari, C., Pepe, D., Choi, Y. W., Uitto, J., and Rodeck, U. (2002) *Oncogene* **21,** 2161–2170
14. Kumar, R., Wang, R., Mazumdar, A., Talukder, A. H., Mandal, M., Yang, Z., Bagheri-Yarmand, R., Sahin, A., Hortobagyi, G., Adam, L., Barnes, C. J., and Vadlamudi, R. K. (2002) *Nature* **418,** 654–657
15. Imai, T., Horiuchi, A., Wang, C., Oka, K., Ohira, S., Nikaido, T., and Konishi, I. (2003) *Am. J. Pathol.* **163,** 1437–1447
16. Mercer, J.A. (2000) *Semin. Cell Dev. Biol.* **11,** 309–314
17. Conacci-Sorrell, M., Simcha, I., Ben-Yedidia, T., Blechman, J., Savagner, P., and Ben-Ze'ev, A. (2003) *J. Cell Biol,* **163,** 847–857
18. Fearon, E. R. (2003) *Cancer Cells* **3,** 307–310
19. Batlle, E., Sancho, E., Franci, C., Dominguez, D., Monfar, M., Baulida, J., and Garcia de Herreros, A. (2000) *Nat. Cell. Biol.* **2,** 84–89
20. Fujita, N., Jaye, D. L., Kajita, M., Geigerman, C., Moreno, C. S., and Wade, P. A. (2003) *Cell* **113,** 207–219
21. Balasenthil, S., and Vadlamudi, R. K. (2003) *J. Biol. Chem.* **278,** 22119–22127
22. Dominquez, D., Montserrat-Sentis, B., Virgos-Soler, A., Guaita, S., Grueso, J., Porta, M., Puig, I., Baulida, J., Franci, C., and Garcia de Herreros, A. (2003) *Mol. Cell. Biol.* **23,** 5078–5089
23. Klinge, C. M. (2001) *Nucleic Acids Res.* **29,** 2905–2919
24. Tata, J. R., Baker, B. S., Machuca, I., Rabelo, E. M., and Yamauchi, K. (1993) *J. Steroid Biochem. Mol. Biol.* **46,** 105–119
25. Kumar, R., Wang, R., and Bagheri-Yarmand, R. (2003) *Semin. Oncol.* **30,** Suppl. 16, 30–37
26. Vadlamudi, R. K., Wang, R. A., Mazumdar, A., Kim, Y., Shin, J., Sahin, A., and Kumar, R. (2001) *J. Biol. Chem.* **276,** 38272–38279
27. Shang, Y., Hu, X., DiRenzo, J., Lazar, M. A., and Brown, M., (2000) *Cell* **103,** 843–852
28. Liao, L., Kuang, S. Q., Yuan, Y., Gonzalez, S. M., O'Malley, B. W., and Xu, J. (2002) *J. Steroid Biochem. Mol. Biol.* **83,** 3–14

Oncogene (2002) 21, 2161–2170

www.nature.com/onc

Metastasis-associated protein (MTA)1 enhances migration, invasion, and anchorage-independent survival of immortalized human keratinocytes

Mỹ G Mahoney*[,1], Anisha Simpson[1], Monika Jost[1], Mariadele Noé[1], Csaba Kari[1], Deanna Pepe[1], Yoo Won Choi[1], Jouni Uitto[1,2] and Ulrich Rodeck[1]

[1]*Department of Dermatology and Cutaneous Biology, Jefferson Medical College, and Jefferson Institute of Molecular Medicine, Thomas Jefferson University, Philadelphia, Pennsylvania, PA 19107, USA;* [2]*Department of Biochemistry and Molecular Pharmacology, Jefferson Medical College, and Jefferson Institute of Molecular Medicine, Thomas Jefferson University, Philadelphia, Pennsylvania, PA 19107, USA*

The human metastasis-associated gene (MTA1), a member of the nucleosome remodeling complex with histone deacetylase activity, is frequently overexpressed in biologically aggressive epithelial neoplasms. Here, we extend this observation to squamous carcinoma cells, which express high levels of MTA1 relative to normal or immortalized keratinocytes. To address functional aspects of MTA1 expression, we established variants of human immortalized keratinocytes (HaCaT cells) by expressing *MTA1* cDNA in both the sense and antisense orientations. We demonstrate that (1) forced MTA1 expression enhances migration and invasion of immortalized keratinocytes; (2) MTA1 expression is necessary but not sufficient for cell survival in the anchorage independent state; (3) MTA1 contributes to expression of the anti-apoptotic Bcl-2 family member Bcl-x_L; (4) MTA1 expression in immortalized keratinocytes depends, in part, on activation of the epidermal growth factor receptor (EGFR). These results establish that, in keratinocytes, MTA1 expression contributes to several aspects of the metastatic phenotype including survival in the anchorage independent state, migration, and invasion. *Oncogene* (2002) **21,** 2161–2170. DOI: 10.1038/sj/onc/1205277

Keywords: anoikis; epidermal growth factor; epithelial cells

Introduction

The metastasis associated 1 (MTA1) protein (Toh *et al.*, 1994, 1995) is representative of a protein family highly conserved through evolution, which also includes the metastasis associated 1-like protein (MTA1-L1) (Futamura *et al.*, 1999), MTA2 (Zhang *et al.*, 1999) and Mta3 (Simpson *et al.*, 2001). In addition, in pancreatic acinar cells, a derivative of the rat *mta1* gene, *ZG29*, has been identified (Kleene *et al.*, 1999). MTA1 contains regions of homology with several immediate early genes (Herman *et al.*, 1999; Paterno *et al.*, 1997) encoding transcription factors involved in cell growth regulation. Recent studies demonstrate that MTA1 and MTA2 are members of the nucleosome-modeling complex with histone deacetylase activity consistent with a role of these proteins in transcriptional regulation (Toh *et al.*, 2000; Zhang *et al.*, 1999). MTA1 was originally identified based on its overexpression in metastatic rat breast cancer (Toh *et al.*, 1994, 1995). However, little is known about functional aspects of MTA1 expression as they relate to either the normal or the transformed cellular phenotype.

Recently, it was shown that, in malignant breast epithelial cells, MTA1 expression is induced by activation of the heregulin/HER2 pathway (Mazumdar *et al.*, 2001). The HER2/c-*erb*B2 receptor is an orphan receptor tyrosine kinase. When expressed at physiological levels it requires heterodimerization with and transphosphorylation by other members of the epidermal growth factor receptor (EGFR) family for activation (Pinkas-Kramarski *et al.*, 1998). Deregulated EGFR activation frequently occurs in epithelial malignancies, including squamous and breast carcinomas (Barnard *et al.*, 1994; Le Jeune *et al.*, 1993; Mukaida *et al.*, 1991; Ozawa *et al.*, 1989). Collectively, these earlier studies raised the question whether EGFR activation may contribute to MTA1 expression in epithelial cells, and, thus, may enhance their malignant potential.

In the present study we focused on functional aspects of MTA1 expression as they relate to the malignant phenotype of transformed human keratinocytes. We describe that MTA1 expression supported several cellular functions relevant to the metastatic phenotype including survival in the anchorage-independent state, migration, and invasion. In addition, we demonstrate that MTA1 expression in immortalized keratinocytes was induced by EGFR activation and was necessary for, but not sufficient to EGFR-dependent, matrix-independent survival of these cells.

*Correspondence: MG Mahoney, Department of Dermatology and Cutaneous Biology, 233 S. 10th St., Room 419 BLSB, Jefferson Medical College, Philadelphia, PA 19107, USA;
E-mail: My.Mahoney@mail.tju.edu
Received 14 September 2001; revised 14 December 2001; accepted 19 December 2001

These results highlight a previously unrecognized role of MTA1 in support of EGFR-dependent survival of epithelial cells in the anchorage-independent state.

Results

Mta1 expression in normal and immortalized epidermal keratinocytes

MTA1 was originally identified in transformed rat mammary epithelial cells (Toh *et al.*, 1994). Subsequent studies demonstrated human *MTA1* mRNA expression also in esophageal squamous cell carcinomas (Toh *et al.*, 1999). These results led us to investigate MTA1 expression patterns in a panel of normal, immortalized, and malignant keratinocyte lines. Immortalized HaCaT keratinocytes were included because they are very similar to normal keratinocytes (Boukamp *et al.*, 1988) but are amenable to stable transfection providing us with the opportunity to manipulate MTA1 expression. To assess MTA1 protein expression, we generated a polyclonal antiserum to a peptide unique to MTA1. Immunohistochemical analysis of adult human epidermis with the anti-MTA1 antiserum (Figure 1a, panel 2) but not the normal rabbit serum (Figure 1a, panel 1) demonstrated nuclear staining of normal keratinocytes *in situ* throughout the nucleated epidermis. In squamous cell carcinoma skin tissues tested, MTA1 staining was dramatically enhanced (representative example of three, Figure 1a, panels 3 and 4) compared to normal epidermis and appeared to be localized to the cytoplasm as well as the nucleus. Immunoblotting analysis of epidermal protein extracts revealed a prominent protein species of expected molecular mass ($\sim$73 kDa) reacting with the MTA1 antiserum (Figure 1b). To compare MTA1 expression in normal and malignant keratinocytes, we assessed steady-state *MTA1* mRNA and protein levels *in vitro*. As determined by RT–PCR, *MTA1* transcripts were present in both cell types, albeit at considerably lower levels in normal keratinocytes relative to a panel of squamous carcinoma cell lines (Figure 2a). *MTA1* expression levels in HaCaT keratinocytes were intermediate, i.e. slightly higher than in primary keratinocytes yet consistently lower than in squamous carcinomas. Low to moderate expression of MTA1 in normal keratinocytes and HaCaT cells as compared to A431 squamous carcinoma cells was confirmed by immunoblotting analysis using the MTA1 antiserum (Figure 2b).

MTA1 is not required for keratinocyte proliferation

To study functional aspects of MTA1 expression in keratinocytes, we established HaCaT cell variants that expressed *MTA1* cDNA in both, the sense or antisense orientation using a tetracycline-regulatable expression system. To assess transgene expression HaCaT-Mock (vector alone), HaCaT-MTA1-S (sense), and HaCaT-MTA1-AS (antisense) expressing cells were grown for 2 days in the presence or absence of tetracycline followed by Western blot analysis of MTA-1 expression. Under these conditions, HaCaT-MTA1-S cells expressed markedly higher MTA1 levels than mock-transfected cells whereas HaCaT-MTA1-AS cells expressed barely detectable MTA1 protein (Figure 3a). Densitometric quantitation of the Western blot analyses of MTA1 expression relative to β-actin signal confirmed the differences in expression levels between the different transfectants (Figure 3b). Immunostaining confirmed the results of the Western blot analysis (Figure 3c). Note that transgene expression was leaky as MTA expression was slightly diminished in MTA1-AS expressing cells and moderately elevated in MTA1-S expressing cells even in the presence of tetracycline. Thus, MTA1 expression in the MTA1-S-transfected cells in the uninduced state was consistently higher than in mock-transfected cells but reproducibly lower than that of induced MTA1-S-transfected cells.

To determine effects of MTA1 expression on cellular metabolism, HaCaT-Mock, HaCaT-MTA-S, and HaCaT-MTA-AS cells were grown for 24, 48 or 72 h in the presence or absence of FCS without tetracycline to induce transgene expression and then treated with Alamar Blue™. As determined by this assay overexpression of either sense or antisense MTA1 sequences had no significant effect on cellular metabolism (data not shown). Furthermore, cellular proliferation was unaffected as determined by counting cells at various time points after transgene induction (data not shown). Similarly, expression of sense and antisense *MTA1* sequences did not detectably affect cell cycle distribution as assessed by FACS analysis of propidium iodide stained cells (data not shown). In summary, MTA1 expression did not affect cellular metabolism, cell numbers, or cell cycle distribution within 3 days after transgene induction.

MTA1 supports keratinocyte migration and invasiveness in vitro

Next, we determined whether MTA1 expression affected keratinocyte migration using an *in vitro* wound-healing assay (Figure 4a). Migration was assessed by scratching a confluent monolayer of cells and monitoring closure of the defect over time. Relative to mock-transfected cells MTA1 overexpressing HaCaT cells demonstrated markedly enhanced migratory behavior whereas MTA1 antisense expressing cells did not migrate at all. Migration was expressed as distance from the wound edge measured 48 h after wounding (Figure 4b). MTA1 overexpression in HaCaT-MTA1-S cells was associated with a significant increase ($P \leqslant 0.05$; Student's *t*-test for unpaired samples) in migratory potential relative to mock-transfected control cells. To assess the contribution of MTA1 to invasion of HaCaT cells, we performed standard Boyden chamber assays using Biocoat® Matrigel® coated membranes and fetal bovine serum as a chemoattractant (Figure 4c).

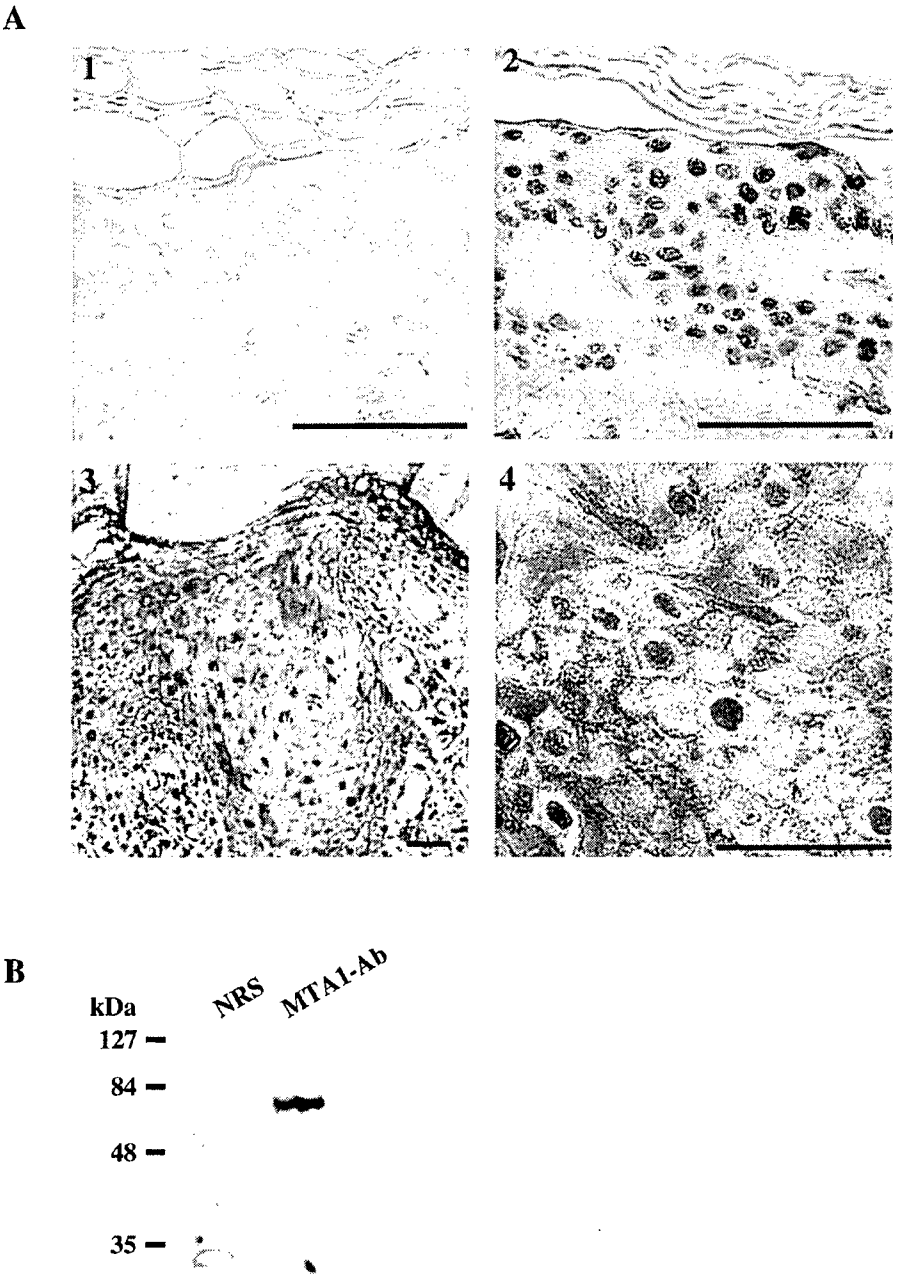

Figure 1 Expression of MTA1 in human epidermis and immortalized keratinocytes. (**a**) Immunohistochemical staining of human epidermis with normal rabbit serum (NRS, panel 1) and anti-MTA1 specific antiserum (panel 2). MTA1 staining was apparent in cell nuclei throughout the epidermis. A representative example of carcinoma malignant skin tissue (SCC) stained for MTA1 (panels 3 and 4). Bar = 50 μm. (**b**) Western blot analysis of immortalized keratinocyte (HaCaT) extracts with the MTA1 antiserum. A protein species of the expected size (approximately 73 kDa) was detected with the anti-MTA1 antiserum but not control NRS

Invasiveness was expressed as the number of cells migrating through Matrigel® relative to migration through uncoated control inserts. MTA1 overexpression in HaCaT-MTA1-S cells was associated with a significant increase ($P \leqslant 0.05$; Student's *t*-test for unpaired samples) in invasive potential as compared to mock-transfected cells. Because HaCaT cells were not normally invasive, abolishing MTA1 expression did not alter their invasive behavior.

MTA1 protects keratinocytes from anoikis

It is believed that invasion and metastatic dissemination of epithelial cells is limited by the inability of normal cells to survive in the absence of appropriate extracellular matrix. In support of this notion, immortalized (Frisch and Francis, 1994; Rodeck *et al*., 1997) and normal (Rodeck *et al*., 1997) cultured keratinocytes undergo apoptosis when denied attachment to extracellular

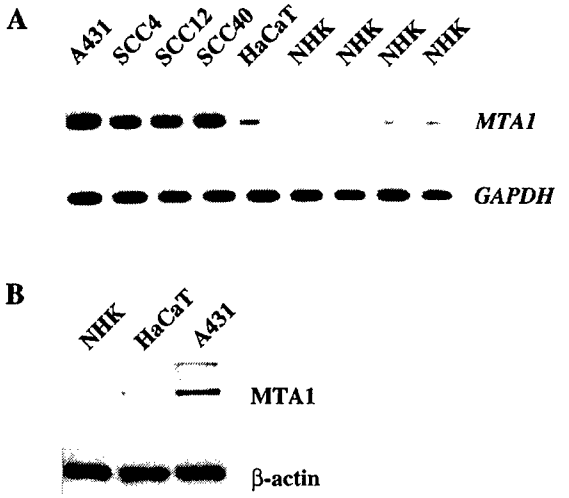

Figure 2 Expression of *MTA1* mRNA and protein in normal keratinocytes and malignant squamous carcinoma cell lines. (**a**) Semi-quantitative RT–PCR analysis of *MTA1* mRNA expression in four primary human keratinocyte (NHK) strains, immortalized keratinocytes (HaCaT), and several squamous carcinoma cell lines (SCC4,12,40 A431). To account for differences in mRNA concentrations *GAPDH* amplification products were also generated. (**b**) Expression of MTA1 protein in normal (NHK), immortalized (HaCaT), and malignant (A431) keratinocytes. A431 cells expressed higher levels of MTA1 when compared to NHK or immortalized HaCaT keratinocytes

matrix, in a process termed anoikis. Transformation of epithelial cells with either *Ras* or *Src* oncogenes provides a measure of protection from anoikis induced by forced suspension (Frisch and Francis, 1994; Rosen *et al.*, 2000). Furthermore, EGFR activation by exogenous or endogenous ligands provides partial protection against death to HaCaT cells in suspension (Jost *et al.*, 2001b). Based on these considerations we asked whether MTA1 expression affected survival of HaCaT cells in the anchorage independent state. To this end, we placed HaCaT cells expressing sense and antisense MTA1 in forced suspension culture for 24–72 h followed by transfer to tissue culture-treated plastic and assessment of clonogenic growth 7 days after reseeding. The results of a representative experiment using growth factor-free medium during suspension culture are shown in Figure 5a. In this setting, survival of mock-transfected and MTA1-sense expressing HaCaT cells was comparable. By contrast, expression of MTA antisense sequences markedly reduced the fraction of cells reattaching after 24, 48 and 72 h of suspension culture. As expected, EGFR blockade by use of the EGFR antagonistic antibody 425 (Murthy *et al.*, 1987) reduced survival of mock-transfected HaCaT cells. Importantly, survival of HaCaT-MTA1-S cells was similarly diminished by EGFR blockade suggesting that MTA1 expression alone is not sufficient to relieve the requirement for EGFR-derived signals for cell survival in the anchorage-independent state. Consistent with earlier results (Jost *et al.*, 2001a) addition of EGF to the culture medium during suspension culture markedly improved survival of HaCaT-MTA-S cells (Figure 5b). However, overexpression of MTA1 antisense sequences obviated EGF-dependent HaCaT cell survival in forced suspension culture indicating that MTA1 expression is essential to EGFR-dependent HaCaT cell survival in suspension culture. The concentrations of mAb 425 and EGF have been optimized for this assay as previously published (Jost *et al.*, 2001a). The differences in clonogenic growth after suspension culture were not due to differences in cellular proliferation in the suspended state because forced suspension of HaCaT cells induced cell cycle arrest as assessed by BrdU incorporation (DeHoratius and Rodeck, unpublished results).

Regulation of MTA1 expression through activation of the EGFR

Next, we determined whether expression of MTA1 was regulated through an EGFR-dependent pathway. To this end, we examined the effects of EGFR blockade on expression of MTA1 steady-state mRNA and protein levels in HaCaT cells. Two EGFR antagonists were used in these studies. Whereas the monoclonal EGFR antagonistic antibody 425 (mAb 425) blocks ligand binding and EGFR autophosphorylation, tyrphostin AG1478 (Levitzki and Gazit, 1995) selectively inhibits the tyrosine kinase moiety of the EGFR. Blocking the EGFR with either mAb 425 or AG1478 in attached cells for 2 days was associated with markedly down-regulated *MTA1* mRNA expression in HaCaT cells relative to expression of *GAPDH* (Figure 6a). This result was confirmed by Western blot analysis of MTA1 expression upon inhibition of EGFR signaling (Figure 6b). Treatment of HaCaT cells with either EGFR selective AG1478 or EGFR specific mAb 425 was associated with lower levels of MTA1 expression relative to untreated controls or cells treated with control tyrphostin AG1295 or control mAb BR15-6A. Down-regulation of MTA1 expression was reversible as incubation with either EGF or FCS was able to rescue the effect of mAb 425 treatment (Figure 6c).

MTA1-dependent regulation of Bcl-x_L expression

Previously, we (Rodeck *et al.*, 1997) and others (Frisch and Francis, 1994; Rosen *et al.*, 2000) described that expression of the anti-apoptotic Bcl-2 family member Bcl-x_L is important for survival of normal epithelial cells including normal keratinocytes and HaCaT cells in forced suspension culture. As MTA1 expression provided a measure of protection to HaCaT cells in suspension, we determined whether inhibiting MTA1 expression affected Bcl-x_L expression. We observed marked downregulation of Bcl-x_L protein levels in HaCaT-MTA1-AS cells as compared to HaCaT-MTA1-S cells (Figure 7). As our previous work implicated MEK/MAPK signals in regulation of Bcl-x_L expression levels in HaCaT cells (Jost *et al.*, 2001a), we asked whether inhibition of MEK activity affected MTA1 expression. Neither pharmacological inhibition of MEK activity by PD98059 nor over-

expression of a dominant negative MEK construct (Jost *et al.*, 2001a; Mansour *et al.*, 1994) in HaCaT cells affected MTA1 expression as determined by immunoblot analysis (not shown). This indicates that MEK activity was not involved in regulating MTA1 expression levels in HaCaT keratinocytes. We conclude that EGFR-dependent MTA-1 expression contributes to Bcl-x_L expression in HaCaT keratinocytes.

Discussion

The results presented here highlight a previously unrecognized role of MTA1 in support of epithelial cell survival in the anchorage-independent state. Specifically, we describe that (1) MTA1 is expressed at comparatively low levels in normal and immortalized epidermal keratinocytes; (2) forced MTA1 expression enhances migration and invasion of immortalized keratinocytes; (3) forced MTA1 expression enhances survival of immortalized keratinocytes in forced suspension culture; (4) MTA1 expression in immortalized keratinocytes is controlled, in part, by the EGFR; (5) like the EGFR, MTA1 contributes to expression of the anti-apoptotic Bcl-2 family member Bcl-x_L in keratinocytes and; (6) MTA1 acts in concert with other EGFR targets to achieve cell survival in the anchorage-independent state.

Our results confirm and significantly extend findings published during preparation of this manuscript and relating to MTA1 expression in mammary epithelial cells (Mazumdar *et al.*, 2001). Specifically, forced expression of MTA1 in MCF7 mammary carcinoma cells was associated with enhanced invasion in Boyden chamber assays and increased colony formation in soft agar. Similarly, we observed enhanced migration and invasion of HaCaT keratinocytes overexpressing MTA1. Mazumdar *et al.* (2001) reported no effect of MTA1 overexpression on [^{3}H]-thymidine uptake of MCF7 cells. Similarly, in our hands, neither overexpression nor inhibition of MTA1 expression had any detectable effect on metabolic rates, cell cycle progression, or proliferation of HaCaT keratinocytes. This is in contrast to a previous report describing growth inhibition of human MDA-MB-231 breast cancer cells upon treatment with MTA1 antisense oligonucleotides (Nawa *et al.*, 2000). The reason for this discrepancy is unknown but might relate to differences in cell type expression level of MTA1.

Here, we provide direct evidence that MTA1 expression is required for survival of immortalized keratinocytes in conditions of anchorage independence, i.e. in forced suspension culture. Taken together, the results by Mazumdar *et al.* (2001) and our findings suggest that MTA1-dependent support of epithelial cell survival enhances the capacity of epithelial cells to successfully complete metastatic dissemination to distant sites.

Mazumdar *et al.* (2001) reported upregulation of MTA1 expression in MCF7 breast cancer cells through a heregulin-mediated pathway; heregulin is a ligand for the EGFR-like receptors HER3 and HER4. Our results indicate that EGFR ligands serve a similar role in epithelial keratinocytes. Importantly, both the EGFR and HER3/HER4 activate the orphan receptor HER2. As HER2 is expressed in HaCaT keratinocytes (Ahmed *et al.*, 1997) it is possible that EGFR activation upregulates MTA1 expression through a mechanism involving HER2 transphosphorylation. This possibility is presently under investigation.

Interestingly we observed that HaCaT cells transfected with MTA1-antisense sequences expressed markedly lower levels of Bcl-x_L. We described previously that EGFR-dependent Bcl-x_L expression is required for matrix-independent HaCaT cell survival (Jost *et al.*, 2001b; Rodeck *et al.*, 1997). Furthermore, Bcl-x_L expression in these cells is controlled, in part, by MEK/MAPK signaling (Jost *et al.*, 2001a). Consistent with a role of MTA1 in EGFR-dependent Bcl-x_L regulation we observed that inhibition of EGFR activation was associated with reduced MTA1 expression in HaCaT keratinocytes. However, MTA1 expression in these cells did not depend on MAPK phosphorylation as neither the MEK inhibitor PD98059 nor a dominant negative MEK construct downregulated MTA1 expression. These results suggest that EGFR-dependent MTA1 expression and MEK/MAPK signaling cooperatively support Bcl-x_L expression in keratinocytes. It remains to be investigated whether regulation of Bcl-x_L expression by MTA1 is due to its histone deacetylase activity (Zhang *et al.*, 1999).

A recent study demonstrated that, in melanoma cells selected for survival in suspension culture, resistance to anoikis cosegregates with the ability of these cells to invade across Matrigel barriers (Zhu *et al.*, 2001). It is possible that forced MTA1 expression similarly enhances both, resistance to anoikis and invasive capacity of HaCaT cells. However, we observed that overexpression of MTA1 in HaCaT cells did not provide an unequivocal survival advantage relative to mock-transfected cells when these cells were placed in forced suspension culture. Yet, MTA1 overexpression markedly increased invasion across Matrigel-coated membranes. Thus, it remains to be investigated whether MTA1-dependent increased invasiveness is linked to enhanced survival of HaCaT cells in transit or whether MTA1 enhances the invasive phenotype independently of its role in support of cell survival.

In summary, MTA1 expression appears to be an important component of EGFR-dependent keratinocyte survival in the anchorage-independent state.

Materials and methods

Chemicals and reagents

Purified mouse EGF was from Collaborative Research (Bedford, MA, USA). Monoclonal anti-EGFR antibody (mAb425) binds specifically to EGFR and blocks the binding of both EGF and TGF-α to EGFR (Murthy *et al.*, 1987, 1990; Rodeck *et al.*, 1987). Control mAb BR15-6A (363-15-6A) binds to but does not inhibit the EGFR expressed on epithelial cells (Basu *et al.*, 1987). Tyrphostin AG1478 (Levitzki and Gazit, 1995;

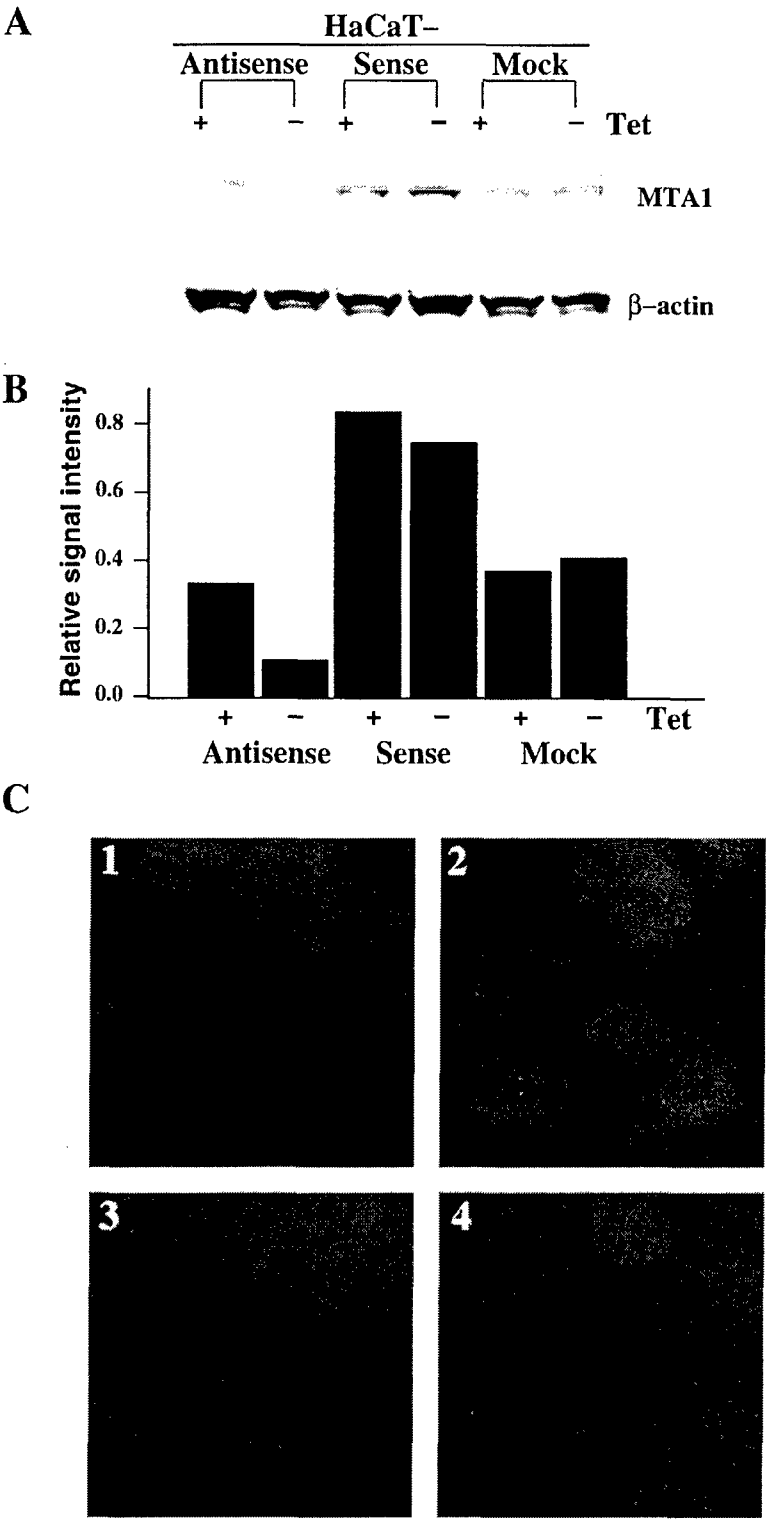

Figure 3 Establishment of HaCaT cells with regulated expression of MTA1 by transfection of sense and antisense *MTA1* sequences using an tetracycline-regulated expression system. (**a**) Western blot analysis of MTA1 expression. Upon transgene expression in the absence of tetracycline, HaCaT-MTA1-S (sense) transfected cells expressed higher MTA1 levels, whereas HaCaT-MTA1-AS (antisense) cells expressed low to undetectable MTA1 levels. Tetracycline removal had no effect on MTA1 expression of HaCaT-Mock cells. (**b**) Densitometric analysis of MTA1 relative to β-actin signal from the Western blotting results above. (**c**) Immunohistochemical detection of MTA1 in mock-transfected HaCaT cells (panel 2) compared to staining with the normal rabbit serum (panel 1). In the absence of tetracycline, MTA1 was overexpressed in the nuclei of HaCaT-MTA1-S cells (panel 3) and barely detectable in HaCaT-MTA1-AS cells (panel 4)

Yoneda *et al.*, 1991) and control AG1295 were purchased from Calbiochem (San Diego, CA, USA). DAPI and antibodies to β-actin were from Sigma (St. Louis, MO, USA).

Total RNA preparation, reverse transcription, and semi-quantitative PCR

Total cellular RNA was extracted from cultured cells using the Qiagen RNeasy kit (Qiagen, Valencia, CA, USA) or Tri Reagent (Sigma) according to the manufacturer's protocols. RT–PCR analyses were performed using the Titan kit (Roche Molecular Biochemical, Indianapolis, IN, USA) according to the manufacturer's protocol. Alternatively, cDNA was generated from total RNA using oligo(dT) primers and MMLV reverse transcriptase (Gibco-BRL) in a final volume of 20 μl consisting of 1 μg total RNA, 2.5 μM oligo(dT) primers, 10 mM DTT, 0.5 mM dNTP, and 10 units of MMLV reverse transcriptase. Primers specific to human MTA1 were: forward; 5′-AGC TAC GAG CAG CAC AAC GGG GT-3′; and reverse, 5′-CAC GCT TGG TTT CCG AGG AT-3′. The PCR conditions were 94°C (3 min) and 20–30 cycles of 94°C (1 min), 58°C (1 min), and 72°C (2 min). PCR products were electrophoresed on a 2% SeaKem agarose gel (FMC) and semiquantitative evaluation of *MTA1* RNA expression levels was performed relative to expression of the house keeping genes glyceraldehyde-3-phosphate dehydrogenase (*GAPDH*) or *β-actin*. The primers for *GAPDH* were: forward, 5′-ACA GTC CAT GCC ATC ACT GCC-3′; and reverse, 5′-GCC TGC TTC ACC ACC TTC TTG-3′. The primers for *β-actin* were: forward, 5′-GTG GGG CGC CCC AGG CAC CA-3′; and reverse, 5′-CTC CTT AAT GTC ACG CAC GAT TTC-3′. The expected PCR products were 290 bp for *MTA1*, 268 bp for *GAPDH* and 540 bp for *β-actin*.

Preparation of anti-MTA1 antiserum

Based on the rat (GenBank accession number U02522) and mouse (Simpson *et al.*, 2001) cDNA sequences, we designed and synthesized the following peptide 'N'-RLDGERPGPNR-NNMSPH-'C' (Genemed Synthesis, San Francisco, CA, USA). This peptide shares sequence homology with the

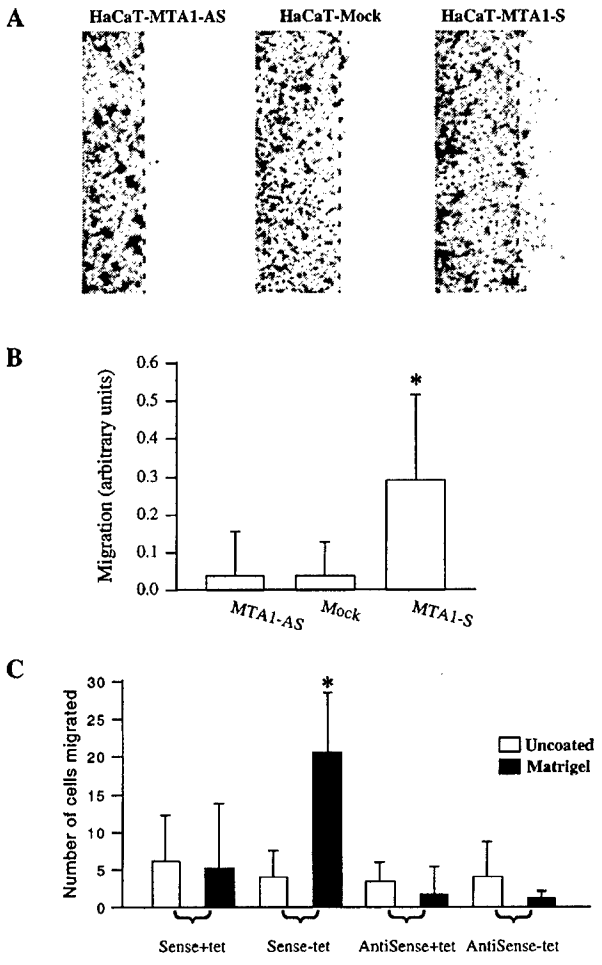

Figure 4 Effects of MTA1 expression on migration and invasion of HaCaT keratinocytes. (**a**) In an *in vitro* cell wounding assay MTA1 sense expressing cells migrated at a faster rate than either mock-transfected or antisense-transfected cells. Migration was evaluated 48 h after wounding by staining cells with crystal violet. Dashed lines demarcate wound edges at the beginning of the experiment. (**b**) Graph shown represents the mean distance of migration ± s.d. of three experiments per condition. (**c**) Boyden chamber assays reveal increased invasiveness in HaCaT-MTA1-S cells when compared to HaCaT-MTA1-AS cells. Invasiveness is expressed as the number of cells that migrated across either uncoated or Matrigel-coated inserts. Results shown represent the mean ± s.d. of 30 fields counted per condition. Asterisks indicate statistically significant differences relative to mock-transfected cells ($P<0.05$; Student's *t*-tests for unpaired samples)

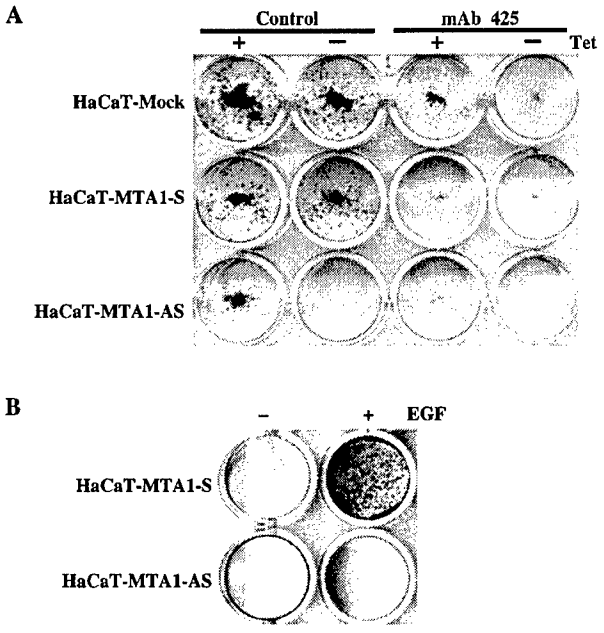

Figure 5 Effects of MTA1 expression on EGFR-dependent survival of keratinocytes in the anchorage-independent state. Clonal growth of cells after 48 h in forced suspension culture was assessed by replating cells on tissue culture-treated plastic and allowing cell proliferation for 7 days after replating. (**a**) HaCaT cells overexpressing MTA1 (HaCaT-MTA1-S) and mock-transfected cells showed comparable survival and regrowth in this setting. By contrast, expression of MTA1 antisense sequences in HaCaT-MTA1-AS cells dramatically reduced the fraction of surviving cells in suspension culture. Addition of the EGFR antagonistic mAb 425 during suspension culture reduced survival of all three cell-lines tested. (**b**) EGFR activation enhanced survival of MTA1-sense expressing HaCaT cells but not of MTA1 antisense-expressing cells

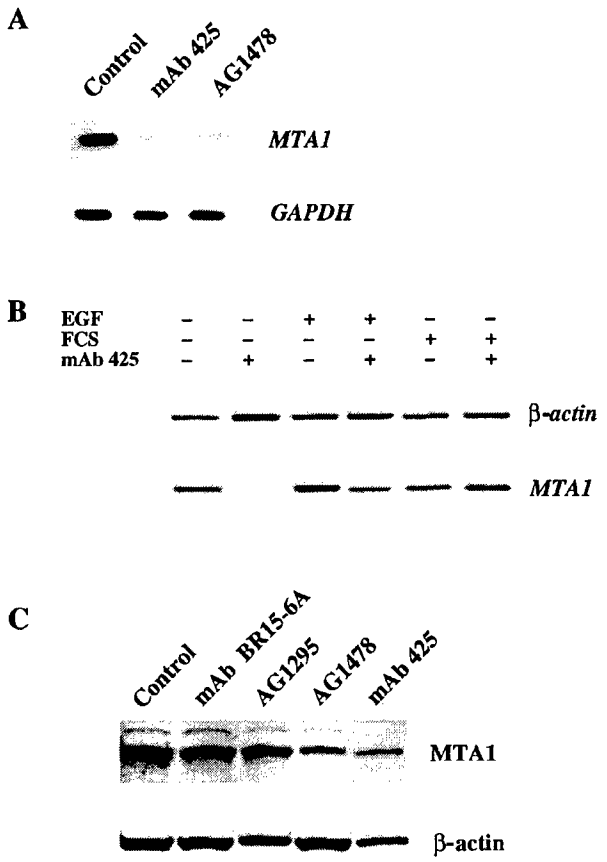

Figure 6 EGFR-dependent MTA1 expression in HaCaT keratinocytes. (**a**) *MTA1* mRNA expression in HaCaT cells as determined by semi-quantitative RT–PCR. HaCaT cells were grown in the absence of exogenous growth factors (Control) or in the presence of mAb 425 or tyrphostin AG1478 as indicated. *GAPDH* expression was determined to account for differences in RNA concentrations. (**b**) Down regulation of MTA1 expression by mAb 425 is reversible. Cells grown in defined medium were treated with FCS (2%) or EGF (50 ng/ml) in the presence or absence of mAb 425 (10 μg/ml). Total RNA was prepared and *MTA1* and *β-actin* levels were determined by RT–PCR. The significant reduction in *MTA1* by mAb 425 was rescued by treatments with either EGF or FCS. (**c**) MTA1 expression in the presence and absence of EGFR antagonists, mAb 425 and AG1478, as determined by Western blot analysis. Reduced levels of MTA1 protein were apparent in extracts of cultures treated with either mAb 425 or AG1478 whereas treatment with control mAb BR15-6A and control tyrphostin had no effect on MTA1 expression. All samples were normalized to β-actin RNA for equal loading

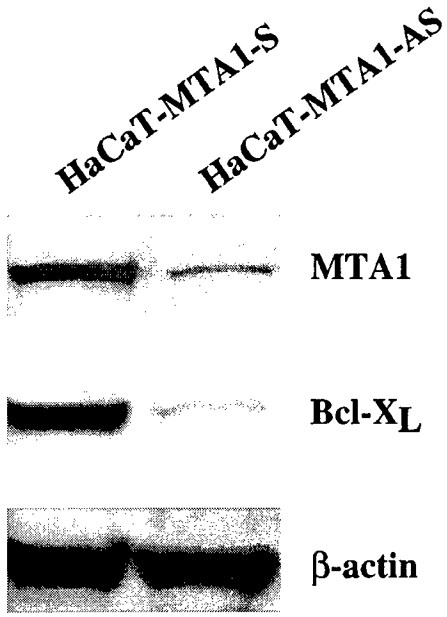

Figure 7 MTA1 expression contributes to Bcl-x_L expression in HaCaT keratinocytes. HaCaT-MTA1-S and HaCaT-MTA1-AS cells were grown for 48 h in the absence of tetracycline. Cell lysates were subjected to Western blot analysis using anti-MTA1 (top), anti-Bcl-x_L (middle), and anti-β-actin (bottom) antibodies. Results of one representative experiment of three are shown

human MTA1 'N'-RLDGERPGPNRSNMSPH-'C' with the exception of the serine residue. This peptide does not share homology with other human MTA proteins, MTA1-L1 or MTA2. The peptide was conjugated to keyhole limpet hemocyanin and used to immunize male New Zealand rabbits and antisera were prepared by CoCalico Biologicals (Reamstown, PA, USA).

Cell lines and tissues

Freshly isolated primary keratinocytes and HaCaT cells were obtained from Dr PJ Jensen (University of Pennsylvania, Philadelphia, PA, USA) and Dr N Fusenig (DKFZ, Heidelberg, Germany), respectively. A431 and SCC lines (SCC4, SCC9, SCC12, and SCC40) were either obtained from the American Type Culture Collection (ATCC, Bethesda, MD, USA) or kindly provided by Dr J Rheinwald (Harvard Institutes of Medicine, Boston, MA, USA). Human neonatal foreskin keratinocyte cultures were initiated and propagated in an MCDB base medium (MCDB153, Sigma) containing 30 μM Ca^{2+} supplemented with ethanolamine, phosphorylethanolamine, hydrocortisone, insulin, purified EGF, and bovine pituitary extract, as previously described in detail (McNeill and Jensen, 1990). HaCaT, A431, and SCC cells were grown in W489 medium consisting of four parts of MCDB153 and one part L15 media supplemented with 2% fetal bovine serum (Rodeck *et al.*, 1991). To inhibit EGFR activation, cells were treated for 2–4 days with mAb 425 (10 μg/ml), control mAb BR15-6A (10 μg/ml), AG1478 (10 μM), or control AG1295 (10 μM) as previously described (Jost *et al.*, 1999).

Expression of MTA1 sense and antisense sequences in HaCaT keratinocytes

Expression of *MTA1* full-length sense and antisense sequences was achieved using an episomally maintained tetracycline (Tc)-regulatable eukaryotic expression vector system based on the *Escherichia coli* Tn10 tetracycline operon (Gossen and Bujard, 1992; Jost *et al.*, 1997). The following primers, forward 5′ -ATG GCC GCC AAC ATG TAC AGG-3′ and reverse 5′-CTA GTC CTC GAT GAC GAT GG-3′, were used to amplify, from human placenta cDNA (Clontech), a 2.2 kb fragment encoding for human MTA1. The PCR conditions were as follows: 94°C for 2 min, followed by 35 cycles of 94°C for 30 s, 58°C for 1 min, and 72°C for 2 min. The MTA1 cDNA was

inserted in the sense or antisense orientations into an EBNA-based plasmid vector (pCEPTeTp) that contained the Tc responsive promoter-operator. This construct was transfected into HaCaT cells carrying the plasmid vector tTA encoding the transactivator (HaCaT-tTA, (Jost *et al.*, 1999)). Cells were selected in medium containing neomycin (G418; 400 μg/ml), hygromycin (0.2 μg/ml), and tetracycline (2 μg/ml) for 3 weeks. Expression of MTA1 cDNA in the sense (HaCaT-MTA1-S) or antisense (Ha-MTA1-AS) orientation was induced by removal of tetracycline from the culture medium. Mock-transfected HaCaT cells (HaCaT-Mock) expressed an empty pCEPTetP vector (Jost *et al.*, 1997).

Immunocytochemistry and Western blot analysis

To determine MTA1 expression, cells were washed in ice cold PBS and fixed for 10 min with 50% acetone in methanol at −20°C. After nonspecific sites were blocked for 30 min with 1% BSA in PBS, cells were then incubated with anti-MTA1 (1 : 100) or anti-α-tubulin (1 : 1000; Sigma) antibodies for 1 h at room temperature or 4°C overnight. After a 15 min wash with PBS, cells were incubated with Texas-Red-conjugated goat anti-rabbit (1 : 200) or FITC-conjugated goat anti-mouse (1 : 200) antibodies for 1 h at room temperature. Samples were washed with PBS and, where indicated, treated with 100 ng/ml DAPI (Sigma) for DNA counterstaining.

To determine MTA1 expression *in situ*, skin sections (5 μm) from formalin-fixed and paraffin-embedded tissues were used. Sections were deparaffinized in 100% xylene (5 min; two times), 100% ethanol (5 min; two times), 95% ethanol (5 min; two times), 75% ethanol (2 min), 50% ethanol (2 min) and H_2O (2 min). Antigen retrieval was performed by incubating sections in 0.3% H_2O_2 for 30 min at room temperature followed by treatment with an antigen retrieval solution (TUF, Signet Labs, Dedham, MA, USA) for 20 min at 95°C. Nonspecific binding sites were blocked with Biotin/Avidin Blocking Kit (Vector Labs, Burlingame, CA, USA) and with BSA (1%). Sections were then incubated with primary antibodies for 2 h at room temperature or overnight at 4°C followed by incubation with biotinylated-goat anti rabbit antibodies (1 : 200; Vector Labs) for 1 h at room temperature. After washing in PBS for 10 min, sections were incubated in VectaStain ABC (Vector Labs) for 30 min at room temperature, washed in PBS for 10 min and then stained with stable DAB (approximately 1–5 min; Vector Labs). Finally, sections were washed with H_2O, counterstained for 1 min with Gill's #3 Hematoxylin (diluted 1 : 10 in H_2O; Fisher Scientific, Pittsburgh, PA, USA), washed again with H_2O, mounted in elvanol and examined by light microscopy.

For Western blot analysis, cultured cells were washed in ice cold PBS and scraped into lysis buffer (62.5 mM Tris-HCl (pH 6.8), 2% SDS, 10% glycerol, and protease inhibitor cocktail; Boehringer Mannheim). Cell lysates were vortexed for 30 s, incubated on ice for 30 min, and centrifuged at 12 000 *g* for 10 min at 4°C. Supernatants were boiled for 10 min in Laemmli buffer and resolved by 10% SDS–PAGE. Western blot analysis was performed as described previously (Mahoney *et al.*, 1998). Antibodies were used at the following dilutions: rabbit anti-MTA1 antibody (1 : 200); goat anti-rabbit IgG-horse radish peroxidase (HRP) (1 : 2000; BioRad Labs, Hercules, CA, USA); monoclonal anti-β-actin antibodies (1 : 1000; Calbiochem), and goat anti-mouse IgM-HRP (1 : 1000; Calbiochem).

Cell invasion assay

Biocoat® Matrigel® Invasion chambers (Becton Dickinson Labware, Bedford, MA, USA) were used following a protocol established previously for SCC cells (Kawahara *et al.*, 1995). The assay was carried out using 8 μm tissue culture inserts (Falcon-Fisher Scientific) coated with 90 μg of Matrigel (Becton Dickinson Labware) suspension in PBS per cm^2. Control samples were plated onto uncoated inserts. Briefly, HaCaT-MTA1-S and HaCaT-MTA1-AS cells were grown to 50% confluency in the presence of tetracycline which was then removed from the medium for 2 days to induce transgene expression. The cells were then plated in the upper chambers using serum free medium at 5×10^4 cells/chamber while 10% FBS containing medium was added to the medium in the lower chambers. After incubation for 24 h at 37°C in 95% air/5% CO_2, the non-invading cells in the top chamber were removed. The membranes were fixed with Diff-Quick kit (Dade Behring, Deerfield, IL, USA), and cells which had traversed the side facing the lower chamber were counted using an inverted light microscope (30 optical fields; 2.5 × 2.5 mm grid). Each experimental condition was done in triplicate.

Cell proliferation and viability assays

To assess cell viability and cell proliferation, cells (5×10^4) were grown in 96-well flat-bottom culture dishes in the presence or absence of FCS for 24, 48 or 72 h. Cells were then incubated with 10% Alamar Blue™ (BioSource) in medium for 2 h. The Alamar Blue™ assay provides a measure of the oxidative metabolism of cells. Specifically, the active metabolism of proliferating cells favors a more reduced state as compared to non-proliferating cells. Thus, upon internalization into metabolically active cells the Alamar-Blue™ dye shifts in color from the oxidized indigo blue, non-fluorescing state to the reduced fluorescent pink state. The redox state of Alamar Blue™ was measured spectrophotometrically by monitoring the absorption of Alamar Blue™ at two wavelengths, 530 and 590 nm, in a microtiter plate reader.

In addition, we used FACS analysis to assess cell viability and cell cycle distribution. Cells were trypsinized, washed once with PBS, and fixed with 70% ethanol (−20°C) for 2 h. After a brief wash with PBS, cells were treated with RNAse (1 mg/ml in PBS; Roche Molecular Biochemicals) for 5 min at 37°C and stained with propidium iodide (5 μg/ml in PBS; Molecular Probes) for 20 min at 4°C. Propidium iodide content of cells was analysed with a FACSort cytofluorograph (Becton Dickinson, San José, CA, USA) and Lysis II Software (Becton Dickinson). A minimum of 10^5 cells was accrued for each experimental condition. Furthermore, cellular proliferation was also assessed by determining cell numbers using a hemocytometer.

Forced suspension culture

Forced suspension cultures were performed as described previously (Jost *et al.*, 2001a). Cells were suspended in growth factor-free MCDB base medium containing 0.2% fatty-acid-free bovine serum albumin (Boehringer Mannheim) and seeded at 4×10^5 cells/well in 6-well culture dishes coated with 0.9% agarose gels prepared in the same medium. In select experiments, the base medium was supplemented with EGF (10 ng/ml; Sigma). After 48–72 h, cell aliquots (4×10^5 cells) were reseeded into 12-well culture dishes in W489 medium supplemented with 2% FCS and containing

neomycin, hygromycin, and tetracycline. To assess survival and clonogenic capacity, reattached cells were fixed with 70% ethanol 7 days after reseeding and stained with crystal violet.

Abbreviations

EGFR, epidermal growth factor receptor; MTA1, metastasis-associated protein 1.

Acknowledgments

We thank Dr PJ Jensen (University of Pennsylvania, Philadelphia, PA, USA) for primary keratinocytes, Dr N Fusenig for HaCaT keratinocytes, and Dr J Rheinwald for squamous carcinoma cells. This work was supported by grants from the National Institutes of Health and the Dermatology Foundation to U Rodeck and MG Mahoney, respectively. MG Mahoney is a recipient of a Career Development Award from the Dermatology Foundation.

References

Ahmed NU, Ueda M and Ichihashi M. (1997). *Br. J. Derm.*, **136,** 908–912.

Barnard JA, Graves-Deal R, Pittelkow MR, Du Bois R, Cook P, Ramsey GW, Bishop PR, Damstrup L and Coffey RJ. (1994). *J. Biol. Chem.*, **269,** 22817–22822.

Basu A, Murthy U, Rodeck U, Herlyn M, Mattes L and Das M. (1987). *Cancer Res.*, **47,** 2531–2536.

Boukamp P, Petrussevska RT, Breitkreutz D, Hornung J, Markham A and Fusenig NE. (1988). *J. Cell Biol.*, **106,** 761–771.

Frisch SM and Francis H. (1994). *J. Cell Biol.*, **124,** 619–626.

Futamura M, Nishimori H, Shiratsuchi T, Saji S, Nakamura Y and Tokino T. (1999). *J. Hum. Genet.*, **44,** 52–66.

Gossen M and Bujard H. (1992). *Proc. Natl. Acad. Sci. USA*, **89,** 5547–5551.

Herman MA, Ch'ng Q, Hettenbach SM, Ratliff TM, Kenyon C and Herman RK. (1999). *Development*, **126,** 1055–1064.

Jost M, Class R, Kari C, Jensen PJ and Rodeck U. (1999). *J. Invest. Dermatol.*, **112,** 443–449.

Jost M, Huggett TM, Kari C and Rodeck U. (2001a). *Mol. Biol. Cell*, **12,** 1519–1527.

Jost M, Huggett TM, Kari C, Boise LH and Rodeck U. (2001b). *J. Biol. Chem.*, **276,** 6320–6326.

Jost M, Kari C and Rodeck U. (1997). *Nucleic Acids Res.*, **25,** 3131–3134.

Kawahara E, Imai K, Kumagai S, Yamamoto E and Nakanishi I. (1995). *J. Cancer Res. Clin. Oncol.*, **121,** 133–140.

Kleene R, Zdzieblo J, Wege K and Kern H. (1999). *J. Cell Sci.*, **112,** 2539–2548.

Le Jeune S, Leek R, Horak E, Plowman G, Greenall M and Harris AL. (1993). *Cancer Res.*, **53,** 3597–3602.

Levitzki A and Gazit A. (1995). *Science*, **267,** 1782–1788.

Mahoney MG, Aho S, Uitto J and Stanley JR. (1998). *J. Invest. Dermatol.*, **111,** 308–313.

Mansour SJ, Matten WT, Hermann AS, Candia JM, Rong S, Fukasawa K, Vande Woude GF and Ahn NG. (1994). *Science*, **265,** 966–970.

Mazumdar A, Wang RA, Mishra SK, Adam L, Bagheri-Yarmand R, Mandal M, Vadlamudi RK and Kumar R. (2001). *Nature Cell Biol.*, **3,** 30–37.

McNeill H and Jensen PJ. (1990). *Cell Regul.*, **1,** 843–852.

Mukaida H, Toi M, Hirai T, Yamashita Y and Toge T. (1991). *Cancer*, **68,** 142–148.

Murthy U, Basu A, Rodeck U, Herlyn M, Ross AH and Das M. (1987). *Arch. Biochem. Biophys.*, **252,** 549–560.

Murthy U, Rieman DJ and Rodeck U. (1990). *Biochem. Biophys. Res. Commun.*, **172,** 471–476.

Nawa A, Nishimori K, Lin P, Maki Y, Moue K, Sawada H, Toh Y, Fumitaka K and Nicolson GL. (2000). *J. Cell Biochem.*, **79,** 202–212.

Ozawa S, Ueda M, Ando N, Shimizu N and Ab O. (1989). *Cancer*, **63,** 2169–2173.

Paterno GD, Li Y, Luchman HA, Ryan PJ and Gillespie LL. (1997). *J. Biol. Chem.*, **272,** 25592–25595.

Pinkas-Kramarski R, Lenferink AE, Bacus SS, Lyass L, van de Poll ML, Klapper LN, Tzahar E, Sela M, van Zoelen EJ and Yarden Y. (1998). *Oncogene*, **16,** 1249–1258.

Rodeck U, Herlyn M, Herlyn D, Motlhoff C, Atkinson B, Varello M, Steplewski Z and Koprowski H. (1987). *Cancer Res.*, **47,** 3692–3696.

Rodeck U, Jost M, DuHadaway J, Kari C, Jensen P, Risse B and Ewert D. (1997). *Proc. Natl. Acad. Sci. USA*, **94,** 5067–5072.

Rodeck U, Melber K, Kath R, Menssen HD, Varello M, Atkinson B and Herlyn M. (1991). *J. Invest. Dermatol.*, **97,** 20–26.

Rosen K, Rak J, Leung R, Dean NM, Kerbel RS and Filmus J. (2000). *J. Cell Biol.*, **149,** 447–455.

Simpson S, Uitto J, Rodeck U and Mahoney MG. (2001). *Gene*, **273,** 29–39.

Toh Y, Kuninaka S, Endo K, Oshiro T, Ikeda Y, Nakashima H, Baba H, Kohnoe S, Okamura T, Nicolson GL and Sugimachi K. (2000). *J. Exp. Clin. Cancer Res.*, **19,** 105–111.

Toh Y, Kuwano H, Mori M, Nicolson GL and Sugimachi K. (1999). *Br. J. Cancer*, **79,** 1723–1726.

Toh Y, Pencil SD and Nicolson GL. (1995). *Gene*, **159,** 97–104.

Toh Y, Pencil SD and Nicolson GL. (1994). *J. Biol. Chem.*, **37,** 22958–22963.

Yoneda T, Lyall RM, Alsina MM, Persons PE, Spada AP, Levitzki A, Zilberstein A and Mundy GR. (1991). *Cancer Res.*, **51,** 4430–4435.

Zhang Y, Ng HH, Erdjument-Bromage H, Tempst P, Bird A and Reinberg D. (1999). *Genes Dev.*, **13,** 1924–1935.

Zhu Z, Sanchez-Sweatman O, Huang X, Wiltrout R, Khokha R, Zhao Q and Gorelik E. (2001). *Cancer Res.*, **61,** 1707–1716.

ELSEVIER

Gene 273 (2001) 29–39

GENE
AN INTERNATIONAL JOURNAL ON GENES AND GENOMES

www.elsevier.com/locate/gene

Differential expression and subcellular distribution of the mouse metastasis-associated proteins Mta1 and Mta3☆

Anisha Simpson[a], Jouni Uitto[a,b], Ulrich Rodeck[a], Mỹ G. Mahoney[a,*]

[a]*Department of Dermatology and Cutaneous Biology, Jefferson Medical College, Philadelphia, PA 19107, USA*
[b]*Department of Biochemistry and Molecular Pharmacology, Jefferson Institute of Molecular Medicine, Thomas Jefferson University, Philadelphia, PA 19107, USA*

Received 20 November 2000; received in revised form 25 February 2001; accepted 6 June 2001
Received by J. Widom

Abstract

The human metastasis-associated gene (*MTA1*) is overexpressed in cell lines and tissues representing metastatic tumors. Here we report cloning of the mouse *Mta1* as well as a novel structurally related mouse gene, *Mta3*. The mouse Mta1 protein shares 94 and 59% homology to the human MTA1 and mouse Mta3 proteins, respectively. Northern blotting analysis using an *Mta1* cDNA probe revealed a prevalent 3 kb hybridization signal in all mouse tissues except the skeletal muscle while a smaller ~1.0 kb mRNA product was also detected in the heart. Mta3 transcripts (~2 kb) were detected in most tissues with an additional ~6.2 kb signal detected in the brain. In vitro transcription/translation of the full-length Mta1 and Mta3 cDNAs generated products of the expected molecular masses, i.e. 80 and 60 kDa, respectively. To assess subcellular localization, green fluorescence protein (GFP)-tagged expression constructs of *Mta1* and *Mta3* and various deletion constructs of GFP-Mta1 were transiently expressed in Balb/MK keratinocytes. GFP-Mta1 was found exclusively in the nucleus while GFP-Mta3 was present in both the nucleus and cytoplasm. Compared to Mta3, the carboxy terminal end of Mta1 contains an additional nuclear localization signal (NLS) and a proline-rich Src homology 3 (SH3) ligand. The results of transient expression experiments of various Mta1 fragments containing these domains in different combinations indicated that nuclear localization of Mta1 depended on the presence of at least one NLS and one SH3 binding site. These SH3 ligands appeared to be functional as they facilitated interaction with the adaptor protein, Grb2, and the Src-family tyrosine kinase, Fyn.

Keywords: Fyn; Grb2; Nucleosome-remodeling histone-deacetylase complex; Src homology 3 binding domain

1. Introduction

The metastasis associated gene 1 (*mta1*) was originally identified by differential cDNA screening using rat adenocarcinoma cell lines with high and low metastatic potential (Pencil et al., 1993; Toh et al., 1994, 1995). Rat *mta1* is overexpressed four-fold in highly metastatic (MTLn3) as compared to non-metastatic (MTC.4) cells (Toh et al., 1994). Similarly, human *MTA1* is expressed at high levels in highly metastatic breast, esophageal, colorectal and gastric carcinomas as compared to less aggressive lesions or normal tissues (Toh et al., 1994, 1997, 1999). In culture, highly proliferative breast adenocarcinoma cells overexpress MTA1 compared to normal human breast epithelial cells and growth is inhibited by treatment with *MTA1* antisense phosphorothioate oligonucleotides (Nawa et al., 2000). It is unclear whether and how MTA1 contributes to the metastatic phenotype of tumor cells. However, recent evidence has implicated MTA1 in the regulation of gene expression by covalent modification of histone proteins. In support of this notion, MTA1 and its homolog, MTA2, are components of and functionally contribute to the nucleosome-remodeling histone-deacetylase (NuRD) complex (Toh et al., 2000; Xue et al., 1998; Zhang et al., 1998, 1999). The NuRD complex has both histone deacetylase and nucleosome remodeling activities (Tong et al., 1998; Xue et al., 1998; Zhang et al., 1998). The core complex is composed of histone deacetylases (HDAC1 and HDAC2) and the histone binding proteins RbAp48 and RbAp46.

Abbreviations: Grb2, growth-factor receptor binding protein-2; MTA, metastasis-associated; MTA1-L1, metastasis associated 1-like; SH3 Src homology 3 binding domain; ZG29, zymogen granule 29 kDa protein

☆ GenBank Accession numbers: Mta1, AF288137; Mta3, AF288138.

* Corresponding author. Department of Dermatology and Cutaneous Biology, 233 S. 10th St., Room 419 BLSB, Jefferson Medical College, Philadelphia, PA 19107, USA. Tel.: +1-215-503-3240; fax: +1-215-503-5788.

E-mail address: my.mahoney@mail.tju.edu (M.G. Mahoney).

0378-1119/01/$ - see front matter
PII: S0378-1119(01)00563-7

MTA2 is recruited to the core complex by the methyl-CpG-binding-domain-containing protein (MDB3) and serves to enhance the complex's histone deacetylase activity (Zhang et al., 1999). Histone deacetylation by the NuRD complex (Herman et al., 1999; Paterno et al., 1997) has been linked to transcriptional repression, cellular proliferation and cancer (Kadosh and Struhl, 1998; Kuo and Allis, 1998; Archer and Hodin, 1999). However, the contributory role of members of the MTA family and NuRD complex to the metastatic potential of tumor cells remains to be defined.

MTA1 is representative of a family of genes which is highly conserved through evolution and includes the metastasis associated 1-like protein (*MTA1-L1*) (Futamura et al., 1999; Zhang et al., 1999), and *MTA2* (Zhang et al., 1999). *MTA1-L1* has been cloned from human (Futamura et al., 1999), mouse (Zhang et al., 1999), *Drosophila melanogaster* (GenBank Accession number: AF170345), and *Xenopus laevis* (GenBank Accession number: AF170344). In addition, in pancreatic acinar cells a derivative of the rat *mta1* gene, *ZG29*, has been identified (Kleene et al., 1999). *ZG29* encodes an N-terminally truncated form of *mta1* due to alternative transcription initiation of the rat *mta1* gene and is highly expressed in hormonally stimulated acinar cells.

Here we describe cloning and initial characterization of mouse Mta1 and a novel Mta family member, *Mta3*. We compared tissue expression patterns and subcellular localizations of *Mta1* and *Mta3* transcripts and proteins, respectively. We provide evidence for the presence of both Mta1 and Mta3 in cell nuclei consistent with roles in histone modification or transcriptional regulation. Furthermore, we show enhanced nuclear retention of Mta1, compared to Mta3, possibly imparted by the carboxy terminal sequences of Mta1 containing an additional nuclear localization signal (NLS) and a proline-rich SH3 binding site. Finally, we demonstrate that the putative SH3 ligand sites on Mta1 and Mta3 enable binding to SH3 domain-containing proteins such as Fyn and Grb2.

2. Materials and methods

2.1. Cloning of mouse Mta1 and Mta3

The following primers, forward 5′-ACA TGG CCG CCA ACA TGT AC-3′ (position −2–18) and reverse 5′-CTG CCA GCA GGG TCT TCT GC-3′ (position 468–487), were used to PCR amplify a 489 bp fragment of human cDNA (Clontech, Palo Alto, CA) encoding for human MTA1. The PCR conditions were as follows: 94°C for 2 min, followed by 35 cycles of 94°C for 30 s, 58°C for 1 min, and 72°C for 1 min. This DNA product was used to probe a mouse keratinocyte cDNA Uni-Zap XR library (Stratagene, La Jolla, CA) according to the manufacturer's protocol. We isolated one clone containing the complete cDNA (2.8 kb) for *Mta1* and four partial clones encoding for mouse *Mta3*. In order to compare the intron sequences of mouse *Mta1* to rat *mta1*, we screened a phage library to clone mouse *Mta1* genomic DNA. The mouse *Mta1* cDNA was used as a probe to screen a lambda Fix II phage library of mouse Sv129 genomic DNA (Stratagene). All plasmid inserts were sequenced using specific primers and the Prism Ready Reaction DyeDeoxy Terminator cycle sequencing systems.

To map the *Mta1* gene, we used the mouse/hamster radiation hybrid panel which was subjected to PCR using primers corresponding to two intronic sequences, forward 5′-GCC TAG CAG GAG CCA CAC-3′ and reverse 5′-CAG GAC GAG CAC AGC TCT C-3′ of *Mta1*. The resulting 320 bp PCR product was analyzed by the RHMapper program from the Whitehead Institute for Biomedical Research, Massachusetts Institute of Technology (Whitehead Institute, 1997).

To complete the sequence of mouse *Mta3*, we performed 5′ rapid amplification of cDNA ends (RACE) (Eyal et al., 1999). Skin from newborn C57Bl/6J mice was used to obtain total RNA using the RNeasy protocol according to the manufacturer (Qiagen, Valencia, CA). The reverse primer 5′-TTG CCT CAC GGA GCT CTG C-3′ (position 632–650) was phosphorylated using T4 polykinase (Promega, Madison, WI) with ATP. The phosphorylated primer was used with total mouse skin RNA to generate single-strand cDNA using Super-Script II reverse transcriptase (Promega). The reaction was hydrolyzed with 0.4 N NaOH and neutralized with 0.4 N glacial acetic acid. The single-stranded cDNA was purified using the QiaQUICK PCR DNA purification kit (Qiagen) and self-ligated using T4 RNA ligase (Promega). The ligated product was used in a PCR reaction using primers forward 5′-AGC TGA CAT TCC AGA CAT GC-3′ (position 471–490) and reverse 5′-GTC AAG GTA TGA CAA CAC GGA-3′ (position 632–650) to generate double-stranded cDNA. The PCR conditions were as follows: 94°C for 3 min, followed by 35 cycles of 94°C for 30 s, 58°C for 1 min, and 72°C for 2 min. The DNA product was purified and sequenced.

2.2. RNA expression and in vitro transcription/translation studies

Northern blots containing poly(A)$^+$ RNA (50 μg/lane) from adult C57Bl/6 mouse tissues were obtained from Clontech. The blots were hybridized with the random primed ^{32}P-labeled *Mta1* or *Mta3* DNA probes (Stratagene) according to the manufacturer's recommendation. The blots were then washed with 0.1× standard saline citrate (SSC), 0.1% sodium dodecylsulfate (SDS) at 65°C. Filters were exposed for autoradiography at −80°C. Hybridization with the β-actin probe (Clontech) was performed to confirm equal loading.

Additionally, a Mouse Multiple Tissue cDNA Panel was obtained from Clontech. The cDNAs were used as templates for PCR analysis according to the manufacturer's protocols. PCR primers were mouse *Mta1*, forward 5′-GTA CCA

GGC TGA CAT CAC TG-3′ (position 465–484) and reverse 5′-TTC GGG CAG CCG TGC TGT G-3′ (position 1485–1503), and mouse *Mta3*, forward 5′-CAA CGA CAT TCG TCA GGA CT-3′ (position 867–886) and reverse 5′-TTC GGC ATG TCT GTC TGC-3′ (position 1519–1536). Mouse *GAPDH* primers were provided by Clontech. PCR conditions were as follows: 94°C for 2 min, followed by 30 cycles of 94°C for 30 s, 58°C for 1 min, and 72°C for 1 min.

To determine the size of mouse Mta1 and Mta3 proteins, the complete *Mta1* and *Mta3* cDNAs were subcloned into pGEM T-easy followed by in vitro transcription/translation using the rabbit reticulocyte lysate system (Promega). Briefly, 1 μg of plasmid DNA and 1 μl of [^{35}S]methionine were added to 40 μl of reticulocyte lysate. The mixture (50 μl final volume) was incubated at 30°C for 90 min and 10 μl of sample was boiled in Laemmli buffer for 10 min. Proteins were separated over 10% SDS-PAGE and gel was dried and autoradiographed. The human *MTA1* cDNA was obtained by PCR amplification using human skin cDNA (Clontech) and the primers forward 5′-ATG GCC GCC AAC ATG TAC AGG-3′ (position 1–18) and reverse 5′-CTA GTC CTC GAT GAC GAT GG-3′ (position 2129–2148).

2.3. Protein expression and transient transfection studies

For expression studies, we used a mammalian expression vector, pEGFP-C1, to fuse Mta proteins to the C-terminus of GFP (Clontech). The fusion proteins were then expressed under the control of the immediate early promoter of human cytomegalovirus (CMV). The *Mta* PCR products were generated using primers listed in Table 1 and purified using the QiaQuick PCR purification system according to the manufacturer's protocol (Qiagen). The PCR products were digested with *Eco*RI and *Sal*I or with *Xho*I and *Bam*HI and ligated into pEGFP-C1. All constructs were sequenced.

Balb/MK (from Dr S.A. Aaronson, Derald H. Ruttenberg Cancer Center, Mount Sinai School of Medicine, New York, NY) cells were maintained in medium containing L15:MCDB (1:4) from Sigma (St. Louis, MO) in the presence of 2% fetal bovine serum (Gibco BRL, Grand Island, NY) and penicillin/streptomycin (Gibco BRL). The cells were plated at 50% confluency onto two-well slide chambers (Fisher Scientific, Pittsburgh, PA). Eight hours after plating, the cells were transfected by Fugene6 according to the manufacturer's protocol (Boehringer Mannheim, Indianapolis, IN) using 6 μl of Fugene6 and 2 μg plasmid DNA. Twelve to 14 h after transfection, the cells were washed with PBS and fixed for 10 min in methanol (−20°C). For immunostaining, the cells were washed in PBS, non-specific sites blocked with PBS + 1% BSA, and incubated with mouse anti-GFP antibodies (1:100) for 2 h at room temperature. After a 15 min wash, the cells were incubated with Texas-Red conjugated goat anti-mouse antibodies (1:200; Molecular probe, Eugene, OR) for 1 h at room temperature. Cells were again washed and mounted for viewing.

2.4. GST pull-down assay

GST fusion proteins were produced and affinity-purified on glutathione Sepharose beads according to the manufacturer (Pharmacia Biotech Inc., Piscataway, NJ) and as previously described (Mahoney et al., 1998). For binding assay, 10 μg of GST, GST-Nck, GST-Grb2, GST-Fyn 1-255, GST-Fyn 1-144 (SH3 domain) and GST-Fyn 1-27 were incubated with 50 μl glutathione Sepharose beads for 1 h at 4°C. The Nck and Grb2 GST fusion proteins were from Dr Jeffrey Benovic (Thomas Jefferson University, Philadelphia, PA). The GST-Fyn constructs were from Drs Paul Stein and John Seykora (University of Pennsylvania, Philadelphia, PA) and were previously described (Anderson et al., 1997; Pleiman et al., 1993). The beads were washed with

Table 1
PCR primers for human *MTA1* and mouse *Mta1* and *Mta3*

Name	Nucleotide sequence[a]	Nucleotide position
Human *MTA1*, forward	5′-GCG AAT TCA TGG CCG CCA ACA TGT AC-3′	1–18
Human *MTA1*, reverse	5′-GCG TCG ACC TAG TCC TCG ATG ACG ATG GGC TC-3′	2129–2148
Mouse *Mta1*, forward	5′-GCG AAT TCA TGG CCG CCA ACA TGT AC-3′	1–18
Mouse *Mta1*, reverse	5′-GCG TCG ACC TAG TCC TCA ATA ACG ATG GGC TC-3′	2074–2097
Mouse *Mta3*, forward	5′-GCC TCG AGC ATG GCG GCC AAC ATG TAC-3′	1–18
Mouse *Mta3*, reverse	5′-GCG GAT CCT TAC CTG CTT AGC CAT CG-3′	1759–1776
Mouse *Mta1-A*, forward	5′-GCG AAT TCA TGG CCG CCA ACA TGT AC-3′	1–18
Mouse *Mta1-A*, reverse	5′-GCG TCG ACC ACA GAG CGG GAC CAC-3′	592–602
Mouse *Mta1-B*, forward	5′-GCG AAT TCG TGG TGG CCC GCT CTG TG-3′	592–609
Mouse *Mta1-B*, reverse	5′-GCG TCG ACG GAG GCT TCG GGC AGC CG-3′	1492–1509
Mouse *Mta1-C*, forward	5′-GCG AAT TCC CCG AAG CCT CCC AGA GCC-3′	1498–1516
Mouse *Mta1-C*, reverse	5′-GCG TCG ACC CTA CTG GGC ATC AAG AG-3′	1744–1761
Mouse *Mta1-D*, forward	5′-GCG AAT TCA TGG CCG CCA ACA TGT AC-3′	1–18
Mouse *Mta1-D*, reverse	5′-GCG TCG ACC CTA CTG GGC ATC AAG AG-3′	1744–1761
Mouse *Mta1-E*, forward	5′-GCG AAT TCG GTC TGG CAA ACC ATG G-3′	1762–1778
Mouse *Mta1-E*, reverse	5′-GCG TCG ACC TAG TCC TCA ATA ACG ATG GGC TC-3′	2074–2097

[a] Primer protection groups and cloning restriction sites are underlined.

PBS, non-specific sites blocked with PBS + 1% Triton X-100 + 1% BSA for 1 h at 4°C, and incubated for 2 h at 4°C with ^{35}S-labeled Mta1 or Mta3 produced by in vitro transcription/translation using the rabbit reticulocyte lysate system (Promega, Madison, WI). The beads were washed five times with PBS + 1% Triton X-100, boiled in Laemmli buffer, proteins separated by SDS-PAGE, and subjected to autoradiography.

Additionally, 50 μg of GST, GST-Mta1-B and GST-Mta1-C was incubated with 100 μl glutathione Sepharose beads for 1 h at 4°C. The beads were washed with PBS and non-specific sites blocked with PBS + 1% BSA for 1 h at 4°C. Balb/MK cells grown in 100 mm dishes to 70% confluency were scraped into RIPA lysis buffer containing 50 mM Tris (pH 8.0), 150 mM NaCl, 1% NP40, 0.5% DOC, 0.1% SDS, and protease inhibitor cocktail (Boehringer Mannheim). The cell lysate was vortexed, incubated on ice for 30 min and centrifuged at 14,000 rev./min for 10 min. The supernatant was incubated with the prepared glutathione beads at 4°C for 2 h. The beads were washed five times with RIPA buffer, boiled in Laemmli buffer, proteins separated by SDS-PAGE and subjected to immunoblotting with anti-Fyn antibodies (Santa Cruz Biotechnology, Santa Cruz, CA).

3. Results

3.1. Identification and cloning of mouse Mta1 and Mta3

A 489 bp fragment of human cDNA encoding for human *MTA1* was generated by RT-PCR and used to screen a mouse keratinocyte cDNA Uni-Zap XR library. We obtained one clone containing the complete cDNA for *Mta1* of 2.8 kb. The cDNA includes a 2.1 kb open reading frame encoding a protein of 698 amino acids (Fig. 1A). The putative translation initiation codon (ATG) lies downstream of a GC-rich region (96% within 102 bp). The open reading frame is followed by a translation termination codon (TAG) and a 517 bp 3′ UTR containing a polyadenylation signal (ATTAAA).

Using the human *MTA1* probe we obtained four additional clones containing open reading frames for partial cDNA sequences of a novel gene sharing sequence homology with *Mta1* (Fig. 1A) and *Mta2*. In the following this new gene is referred to as *Mta3*. To obtain the complete *Mta3* cDNA sequence, we performed 5′ RACE using total RNA from newborn C57Bl/6J mouse skin. In addition, we identified four mouse ESTs (GenBank) that share perfect homology to *Mta3* cDNA (Fig. 1B). Clones A and B contained open reading frames followed by a translation termination codon (TAA) and two different 3′ UTR sequences with a polyadenylation signal (ATTAAA).

The deduced amino acid sequence and several structural motifs of mouse Mta1, Mta2 and Mta3 are shown in Fig. 1C. Overall, mouse Mta1 protein shares 94 and 95% homology

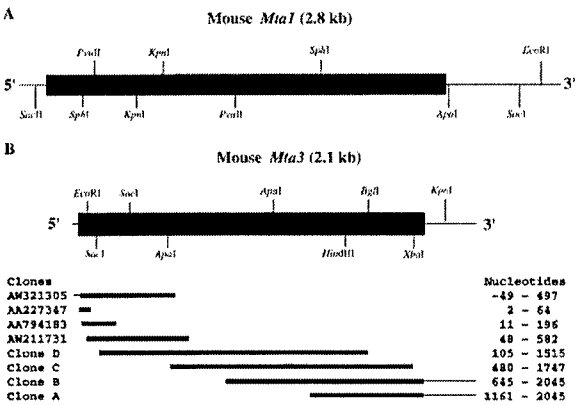

C

Fig. 1. Cloning of mouse *Mta1* and *Mta3*. (A) Partial restriction map of the mouse *Mta1* cDNA. The 2.8 kb full-length mouse *Mta1* cDNA sequence encodes for an open reading frame (shown as a horizontal block) of 698 amino acids. (B) Partial restriction map of the putative *Mta3* cDNA deduced from the four partial cDNA clones (Clones A–D), three published GenBank mouse ESTs, and a 5′ RACE product (data not shown). (C) Deduced amino acid sequence analysis of mouse Mta1, Mta2, and Mta3. Putative leucine zipper (underlined), zinc finger DNA binding site (white on black), and bipartite nuclear localization signals (bold) are indicated. The proline-rich putative SH3 binding sites are shown (shaded). Amino acid alignment was determined by MacVector. Identical amino acids are marked with an asterisk and conserved amino acids are marked with a period.

to human MTA1 and rat mta1, respectively. Within the same species, mouse Mtas share significantly lower levels of homology (Mta1 vs. Mta2, 60%; and Mta1 vs. Mta3, 59%). However, the degree of sequence homology varied among the different domains. All three Mta proteins contain a putative leucine zipper and a zinc finger DNA binding site. Both Mta1 and Mta2 proteins contain two potential bipartite nuclear localization signals (NLS), while the Mta3 protein contains only one bipartite NLS. The Mta1 sequence encodes two putative SH3 binding sites characterized by high proline content. By contrast, Mta2 and Mta3 contain one imperfect SH3 binding recognition site each. These results demonstrate that there is significant sequence conservation between the different Mtas within the same species, as well as in the different species.

3.2. Chromosomal mapping of mouse Mta1

By use of the *Mta1* genomic sequence, we mapped the *Mta1* gene using the mouse/hamster radiation hybrid panel, which was subjected to PCR using primers corresponding to two different *Mta1* introns. An amplimer of expected size (320 bp) was recovered from a single hybrid and mapped to chromosome 12p (5.23 cR from D12Mit280, LOD > 3.0).

3.3. Expression patterns of Mta1 and Mta3 in development and post-partum

To determine expression patterns of Mta1 and Mta3, Northern blot analyses were employed using an mRNA blot containing poly(A)$^+$ RNA derived from adult C57Bl/6 mice. An *Mta1* cDNA probe identified an RNA transcript of approximately 3.0 kb (Fig. 2A) consistent with the size of the 2.8 kb cDNA described above (Fig. 1A). Thus, the 2.8 kb *Mta1* clone is likely to encompass the full-length *Mta1* cDNA. *Mta1* transcripts were observed in all tissues examined except skeletal muscle (Fig. 2A). In addition to the prevalent 3 kb transcript, we observed a smaller ~1.0 kb RNA transcript expressed only in the heart and a larger RNA species that cross-hybridized with the *Mta1* probe. The identity of these products is unknown.

The *Mta3* cDNA probe identified two smaller transcripts (~2.0–2.4 kb) expressed in the heart, brain, spleen, lung, liver and kidney (Fig. 2B). Interestingly, a variant ~6.2 kb transcript was detected exclusively in the brain (Fig. 2B). Next, we examined the expression pattern of *Mta1* and *Mta3* during mouse embryonic development between days 7 and 17. A multiple tissue cDNA panel was used as a template for PCR with primers specific for mouse *Mta1* and *Mta3* cDNAs. Both *Mta1* and *Mta3* were detected in embryos at days 7, 11, 15 and 17 (Fig. 2C). Taken together, these results demonstrate widespread expression of *Mta1* and *Mta3* during embryonic development and after birth and expression of differently sized mRNA species in select tissues.

Next, we focused on expression of the 1.0 kb *Mta1* transcript expressed in the mouse heart (Fig. 2A). Recently the zymogen granule protein (ZG29) expressed in rat pancreatic acinar cells was found to represent an N-terminally truncated form of *mta1* generated by alternative transcription initiation (Kleene et al., 1999). Transcription from this alternative site appears to be controlled by a TATA box in conjunction with several binding sites for pancreas-specific enhancers and gives rise to a transcript with a predicted size of ~1.3 kb (Kleene et al., 1999). Because the mouse *Mta1* and rat *mta1* genes share high sequence homology, we speculated that the RNA product expressed in the mouse heart (Fig. 2A) is generated by a mechanism similar to that described for rat ZG29.

In order to determine whether the mouse *Mta1* sequence

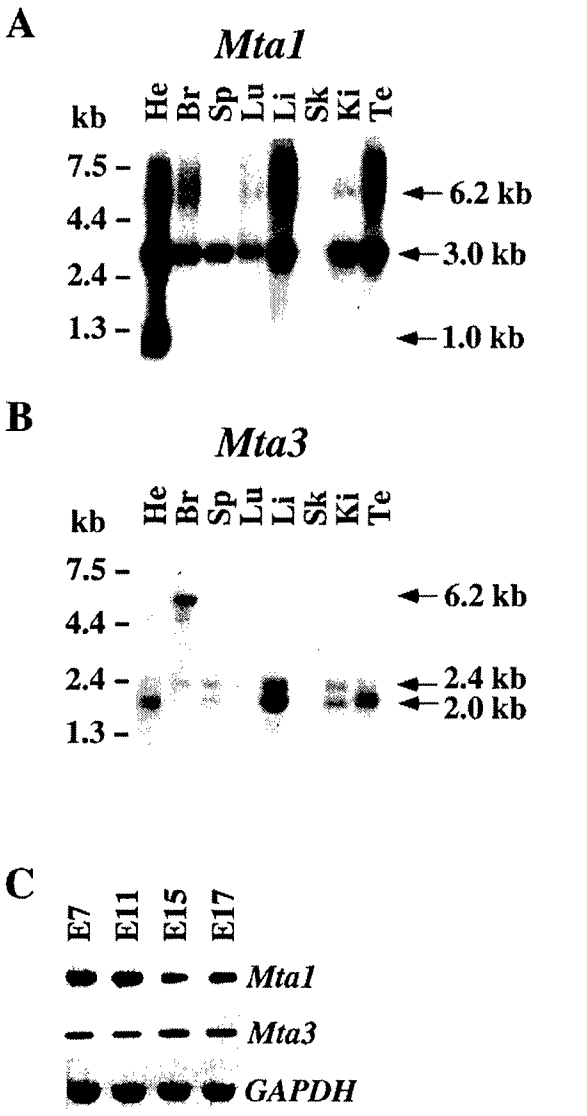

Fig. 2. Tissue-specific expression of *Mta1* and *Mta3* transcripts. Multitissue Northern blot of *Mta1* (A) and *Mta3* transcripts (B). All samples were normalized to β-actin RNA for equal loading by Clontech. He, heart; Br, brain; Sp, spleen; Lu, lung; Li, liver; Sk, skeletal muscle; Ki, kidney; Te, testis. Molecular weight markers are on the left. (C) A Multiple Tissue cDNA Panel (Clontech) was used as templates for PCR with specific primers for mouse *Mta1*, *Mta3*, and *GAPDH*. E7, embryo day 7; E11, embryo day 11; E15, embryo day 15; E17, embryo day 17.

permitted alternative transcription initiation analogous to that described for *ZG29*, we cloned the terminal end of mouse *Mta1* genomic DNA including the relevant sequences. The mouse *Mta1* cDNA was used as a probe to screen a lambda Fix II phage library of mouse Sv129 genomic DNA. Of 5000 clones screened, six independent positive clones were isolated. Initial sequencing of the ends of these clones confirmed the presence of *Mta1* exonic sequences. The structure of the last nine exons of the mouse *Mta1* gene was deduced and is shown in Fig. 3A. Sequencing revealed consensus intron/exon borders, AG-exon-GT. Based on the published rat *ZG29* sequence, the corresponding alternative transcription start site (highlighted) in the mouse *Mta1* gene was predicted to be in the exon in Fig. 3B. The genomic sequence of this region is shown in Fig. 3B. Similar to the rat *mta1* gene, the mouse *Mta1* intron contains a putative TATA box (TATAT; position −33 to −37), a muscle-specific consensus sequence (E-box; CACCTG; position −79 to −84), and a pancreatic-specific enhancer element (A-box; TGGGA; position −103 to −107). The downstream ATG start codon is in-frame with the full-length *Mta1* cDNA encoding for a protein of 251 amino acids (Fig. 3B).

3.4. In vitro transcription/translation of Mta1 and Mta3

Based on the nucleotide sequence of the coding region,

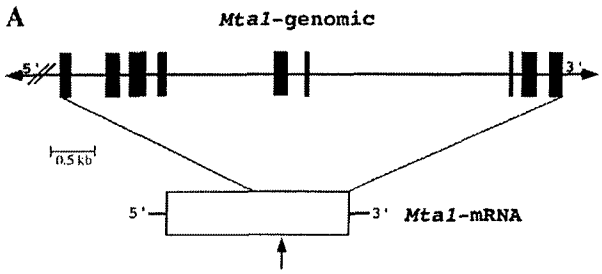

B

CACACAGTCTTACCAGTGGTATTCTTGGGGTCCCCCTAACATGCAGTGTC
GCCTCTGCGCATCTTGGTGGACATATTGGAAGAAATATGGTGGCTTGAAA
ATGCCAACCCGGTTAGATGGAGAGAGGCCGGGACCAAACCGCAATAACAT
GGTAAGTGGGACACACCATACTGATCTGCCACCTGCTGCATGTCAGCCTC
GGGTCCTTGGCTTCCAGTCACAGTGCTATATTGGGGCACCGTGCCCCATT
CCACAGAGTCCCCATGGCATTCCAGCTCGGAGCAGTGGAAGCCCCAAGTT
TGCCATGAAGACAAGGCAGGCCTTCTACCTGCATACTACCAAGTTGACAC
GCATTGCCCGGCGCTTGTGCCGTGAGATCCTACGCCCATGGCATGCTGCC
CGCCACCCCTACATGCCCATCAACAGCGCAGCAATCAAGGCTGAATGTGA
GTCTTCCCCTGTTCTCTTTCTTGGGCCTAGCAGGAGCCACACTCAGGCAG
AGTGTCCAGGTTGGGGTACAGGTTCTTGGGGAACATGGTTCTTCACCGTA
CCTTGTCCTGTCCTTGTACAGGCACAGCACGGCTGCCCGAAGCCTCCCAG
AGCCCACTGGTGCTGAAGCAGGTAGTACGGAAGCCCCTGGAGGCCGTGCT
CCGGTATCTTG

Fig. 3. Putative alternative transcriptional start site in mouse *Mta1*. (A) Schematic diagram of the *Mta1*-mRNA and the last nine exons of mouse *Mta1* genomic DNA. The region within the *Mta1* genomic sequence that contains a potential alternative transcriptional start site similar to the rat ZG29 gene is indicated with an arrow. (B) Nucleotide sequence of the exons (bold) and introns (normal) within this region are shown. The TATA box (TATAT), the pancreas-specific enhancer (A-box, TGGGA) and the muscle-specific enhancer (E-box, CACCTG) are underlined. The first ATG start codon is hightlighted.

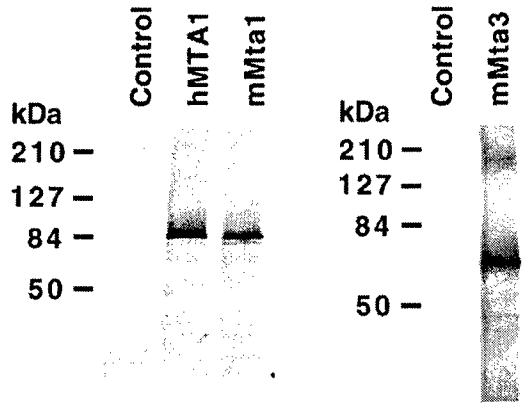

Fig. 4. In vitro expression of *Mta1* and *Mta3* cDNA. By in vitro transcription/translation using the rabbit reticulocyte system (TnT system, Promega), the 2.1 kb human *MTA1* open reading frame generated a product of approximately 80 kDa and similar results were observed with the mouse *Mta1* cDNA (left panel). The 1.8 kb *Mta3* open reading frame produced a protein of approximately 60 kDa (right panel). The control vector did not produce a labeled protein product.

the calculated molecular weights of Mta proteins were 79.2 kDa (pI = 9.9) for Mta1 and 67.0 kDa (pI = 9.1) for Mta3. To confirm these values, the complete *Mta1* and *Mta3* cDNAs were subcloned into pGEM T-easy followed by in vitro transcription and translation. Protein products for *Mta1* and *Mta3* of approximately 80 and 60 kDa, respectively, were derived consistent with the predicted molecular masses (Fig. 4). The human *MTA1* cDNA was obtained by PCR amplification using human skin cDNA and primers based on the published human *MTA1* cDNA sequence. In vitro transcription/translation of this *MTA1* cDNA cloned into pGEM T-easy produced a protein product of the expected mass (~80 kDa) while a control vector without insert did not generate a labeled protein product (Fig. 4).

3.5. Transient expression of Mta1 and Mta3 reporter constructs

To determine the subcellular localization of Mta family members, we first subcloned full-length human *MTA1* and mouse *Mta1* and *Mta3* cDNAs into GFP vectors as shown schematically in Fig. 5A. These constructs were transiently expressed in mouse Balb/MK keratinocytes followed by analysis of subcellular distribution patterns. When a control vector encoding GFP alone was used, diffuse autofluorescence throughout the cytoplasm and, to a lesser extent, the nuclei of transfected cells was observed (Fig. 5B, GFP). By contrast human GFP-MTA1 and mouse GFP-Mta1 proteins were detected exclusively in cell nuclei but not in the cytoplasm (Fig. 5B). To determine which domains in Mta1 contribute to nuclear retention, we generated deletion constructs of Mta1 encoding proteins containing the NLS and SH3 binding domains in different combinations as outlined in Fig. 5A. The results of transient expression experiments of these Mta1 fragments are

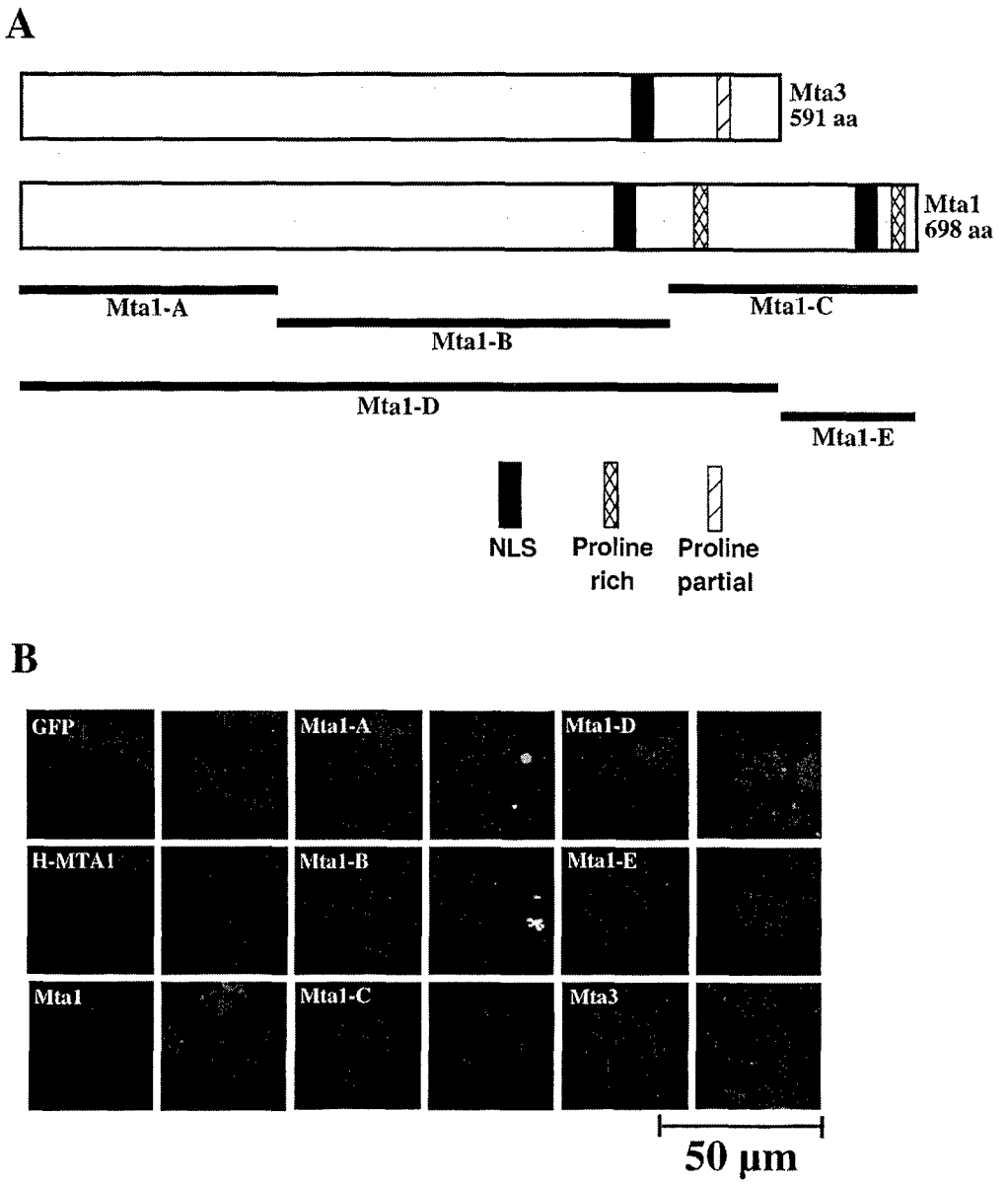

Fig. 5. SH3 binding sites on Mta1 promote nuclear localization. (A) Schematic diagram of various GFP fusion constructs generated with *Mta1* and *Mta3*. (B) These constructs were used in transient expression studies in mouse keratinocyte Balb/MK cells. The GFP fusion construct alone and constructs generated with human MTA1, mouse Mta1, mouse Mta3, Mta1-A, Mta1-B, Mta1-C, Mta1-D, and Mta1-E are shown. The GFP signal was detected using anti-GFP antibodies and Texas-Red conjugated goat anti-mouse antibodies (red). All cultures were counter-stained with DAPI nuclear dye (blue; shown to the right). Similar results were observed in human HaCaT cells.

shown in Fig. 5B and can be summarized as follows: (1) nuclear localization of Mta1 requires the presence of at least one NLS because construct Mta1-A which lacks both NLS is expressed predominantly in the cytoplasm; (2) the Mta1 fragment containing an NLS but none of the SH3 binding domains assumes mainly nuclear but also cytoplasmic localizations; this was observed for Mta1-B; (3) coexpression of at least one NLS and one SH3 binding domain is associated with predominantly nuclear localization as observed for Mta1-C, Mta1-D and Mta1-E. Interestingly, mouse Mta3-GFP was observed in both the cytoplasmic and nuclear locations (Fig. 5B, Mta3). When compared to Mta1, Mta3 contains one bipartite NLS and a partial proline-rich region. These results (summarized in Table 2) demonstrate that while both Mta1 and Mta3 are localized to the nucleus, Mta3 can also be found in the cytoplasm.

3.6. Association of Mta1 and Mta3 with Grb2 and Fyn

To determine whether the proline-containing regions in Mta1 and Mta3 can bind to SH3 domain-containing

Table 2
Differential cellular localization of GFP fusion proteins

GFP fusion protein	Cellular localization
GFP alone	Cytoplasm and nucleus
GFP-Human MTA1	Nucleus
GFP-Mouse Mta1	Nucleus
GFP-Mouse Mta3	Cytoplasm and nucleus
GFP-Mouse Mta1-A	Cytoplasm
GFP-Mouse Mta1-B	Cytoplasm and nucleus
GFP-Mouse Mta1-C	Nucleus
GFP-Mouse Mta1-D	Nucleus
GFP-Mouse Mta1	Nucleus

proteins, we performed pull-down assays using Sepharose-bound Nck-, Grb2- and Fyn-GST fusion proteins and Mta1 or Mta3. [^{35}S]Methionine-labeled full-length Mta1 and Mta3 were generated using the rabbit reticulocyte in vitro transcription/translation assay as described in Section 2. Mta1 bound strongly to Fyn, moderately to Grb2 and weakly to Nck but not to GST alone (Fig. 6A, top row). Mta3 also bound strongly to Fyn but weakly to Grb2 and Nck (Fig. 6A, bottom row). Mta3 did not bind to GST alone (Fig. 6A, bottom row). To determine whether the binding of Mtas to Fyn was mediated through the SH3 domain, we performed the pull-down assay with GST fusion proteins of various Fyn constructs, Fyn 1-255, Fyn 1-144, and Fyn 1-27 (Anderson et al., 1997; Pleiman et al., 1993). Fyn 1-255 encompassed the non-catalytic amino terminal region including the SH3 and SH2 domains. Fyn 1-144 contained only the SH3 but not the SH2 domains while Fyn 1-27 only encompassed the first 27 amino acids lacking both SH3 and SH2 domains. Both Mta1 and Mta3 bound to Fyn 1-255 (Fig. 6B). An essentially identical binding result was observed with Fyn 1-144 suggesting that the SH2 domain was not required for Mta1 or Mta3 binding. Mta1 and Mta3 did not bind to the first 27 amino acids of Fyn or to the GST protein alone (Fig. 6B).

To verify that the binding of the SH3 ligand site on Mta1 mediated the interaction with Fyn (59 kDa), we generated GST fusion proteins containing two SH3 binding domains (Mta1-C) or, as a control, none (Mta1-B). The GST fusion proteins were non-covalently immobilized using glutathione Sepharose beads and incubated with Balb/MK total cell lysate. After washing, the bound proteins were eluted, separated by SDS-PAGE, and immunoblotting was performed with anti-Fyn. The anti-Fyn antibodies recognized a protein of approximately 59 kDa from Balb/MK total cell lysate (Fig. 6C). As expected, GST-Mta1-B did not bind to and pull down Fyn, whereas GST-Mta1-C which contained two SH3 binding sites did bind to and pull down Fyn (Fig. 6C). Thus, Mta1 and Mta3 interacted and bound to Grb2 and Fyn, most likely through the SH3 ligand sites on Mta1 and Mta3 and the SH3 domains on the Grb2 and Fyn.

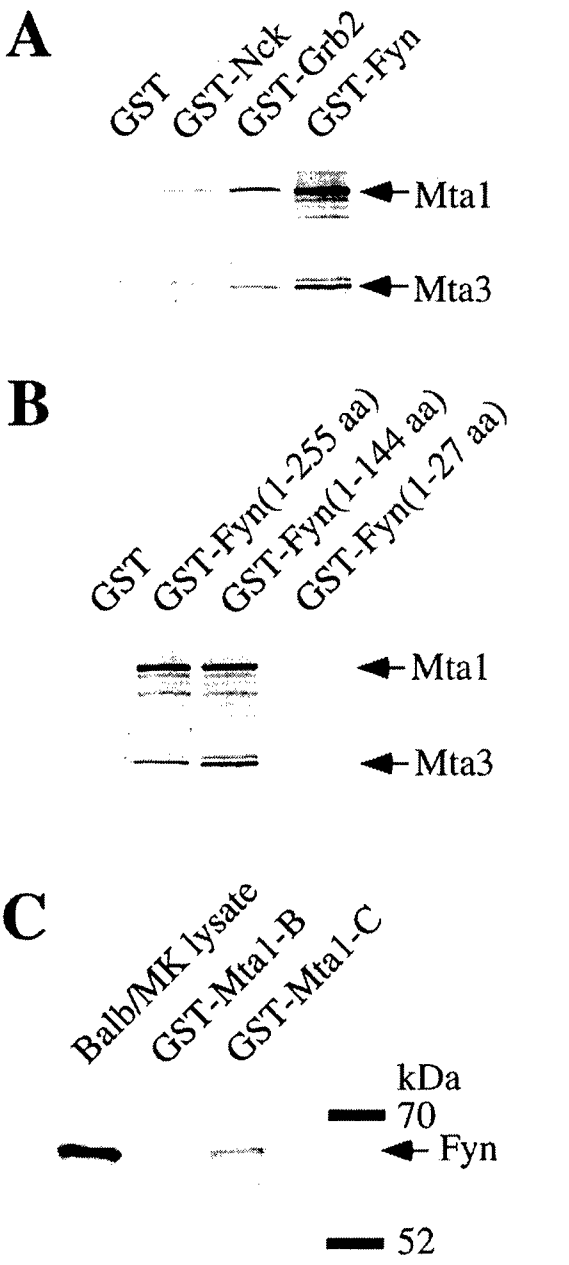

Fig. 6. Association of Mta1 and Mta3 with Grb2 and Fyn. (A) [^{35}S]Methionine-labeled Mta1 and Mta3 proteins were allowed to bind to Nck-, Grb2- and Fyn-GST fusion proteins which were non-covalently bound to glutathione Sepharose beads. Mta1 and Mta3 did not bind to GST proteins alone but did bind to Grb2 and Fyn and weakly to Nck. (B) Both Mta1 and Mta3 bound to Fyn 1-255 (amino terminal 255 amino acids containing the SH2 and SH3 domains) and to Fyn 1-144 (amino terminal 144 amino acids containing only the SH3 but not the SH2 domain) but not to Fyn 1-27 (first 27 amino acids) or GST alone. (C) In the total Balb/MK cell lysate, anti-Fyn antibodies detected a band at approximately 59 kDa. Fyn interacted with GST-Mta1-C containing two putative SH3 ligand sites but not with GST-Mta1-B which lacked the proline-rich sequence.

4. Discussion

Here we report two new members of the mouse *Mta* family, *Mta1* and *Mta3*. They share sequence homology with rat *mta1* and the human *MTA1* and *MTA1-L1*, genes that are expressed at high levels in cell lines and tissues representing highly metastatic tumors. Mouse Mta1 and Mta3 contain different functional domains associated with distinct subcellular expression patterns.

Mta3 was expressed in all tissues examined except skeletal muscle. A similar expression pattern has been reported previously for human MTA1-L1 (Futamura et al., 1999). The *Mta3* cDNA probe revealed two RNA products of approximately ~2.0–2.4 kb in size possibly due to 3′ UTRs of different lengths. Additionally, a larger ~6.2 kb transcript was detected in the brain but not in any other tissue. The identity of this transcript is currently being investigated. Similar to the rat and human *MTAs* (Futamura et al., 1999; Toh et al., 1995) and to mouse *Mta3* (see above), mouse *Mta1* was expressed in all major organs examined, including the heart, brain, spleen, lung, liver, kidney and testis but not in skeletal muscle. Interestingly, in addition to a 3 kb *Mta1* transcript prevalent in most tissues, a smaller 1.0 kb *Mta1* RNA product was detected in the mouse heart tissue (Fig. 2A). This product may be the result of an alternative transcription initiation site of *Mta1* (Fig. 3). This conclusion is based on the size of this transcript which corresponds to an alternative transcript of rat *mta1* encoding the rat ZG29 protein (Kleene et al., 1999); ZG29 is homologous to the carboxyl terminus of rat mta1. As shown here, both rat *mta1* and mouse *Mta1* contain an alternative in-frame ATG preceded by a putative TATA box and binding sites of tissue-specific enhancers including pancreas and muscle enhancers. In pancreatic acinar cells, ZG29 is primarily found in the zymogen granules associated with amylase-containing protein complexes. It was speculated that ZG29 might play a role in granule formation. The function of a similar protein in the mouse heart needs to be further elucidated.

When transiently expressed in mouse Balb/MK keratinocytes, Mta1 was detected exclusively in cell nuclei, whereas Mta3 was present in both nuclei and cytoplasm. Nuclear transport of either protein is likely to be enabled by bipartite NLS (Robbins et al., 1991) of which Mta1 contains two and Mta3 has one. Interestingly, the Mta1-D deletion construct that contains only one NLS and one proline-rich putative SH3 binding domain (Parsons and Weber, 1989) was retained in cell nuclei similar to the full-length Mta1 construct. Furthermore, Mta1-C containing one NLS and two SH3 binding domains and Mta1-E containing one NLS and one SH3 domain were both retained in the nucleus. However, Mta1-B containing one NLS but no SH3 binding domain was found at both nuclear and cytoplasmic locations. Collectively, these results indicate that the presence of one NLS was sufficient for nuclear import of either Mta1 or Mta3 notwithstanding the fact that multiple NLSs can increase nuclear localization (Goldfarb et al., 1986; Lanford et al., 1986). More importantly, our results suggest that the SH3 binding domains or flanking sequence thereof in Mta1 contribute to nuclear localization.

The cellular functions of Mta1 and Mta3 are unknown. A putative function of Mtas is regulating gene transcription. Human *MTA1* and rat *mta1* share homology with two early immediate genes encoding transcription factors involved in cell growth regulation (Herman et al., 1999; Paterno et al., 1997; Solari et al., 1999). These are the early response gene (*ER1*) expressed in *X. laevis* embryos (Paterno et al., 1997) and the *Caenorhabditis elegans* early immediate gene (*EGL-27*) (Herman et al., 1999; Solari et al., 1999). *ER1* is differentially expressed during embryonic development and is regulated through the fibroblast growth factor receptor pathway. *EGL-27* is involved in embryonic cell polarity, migration, and patterning. Recent data demonstrate that human MTA1 and MTA2 are also members of the nucleosome remodeling complex (Zhang et al., 1999; Toh et al., 2000). The methyl-CpG-binding-domain-containing protein (MDB3) recruits human MTA2 to the NuRD core complex composed of histone deacetylases (HDAC1 and HDAC2) and histone binding proteins (RbAp48 and RbAp46). Recently, MTA1 has been shown to also interact with HDAC1 (Toh et al., 2000). It was demonstrated that human MTA2 enhances the NuRD complex's histone deacetylase activity (Zhang et al., 1999). The NuRD complex binds and deacetylates histones and then binds methylated DNA, which may lead to transcriptional repression and gene silencing (Kadosh and Struhl, 1998; Kuo and Allis, 1998). There is mounting evidence suggesting a causal relationship between regulation of gene repression by DNA acetylation, cellular proliferation, and cancer. However, the role of the MTA1/NuRD complex in regulating the metastatic potential of tumor cells remains to be elucidated.

In this report, we demonstrated that the proline-rich putative SH3 binding domains in Mta1 and Mta3 are functional in mediating protein–protein interaction. We showed that Mta1 and Mta3 physically interact with Fyn, most likely via the SH3 domain of Fyn and SH3 ligand sites on Mtas. Fyn is a src family tyrosine kinase that is responsible for the calcium-induced tyrosine phosphorylation of several proteins and is crucial for epithelial cell differentiation (Calautti et al., 1995). Thus, the association with Fyn provides a potential link between the function of Mta1 and Mta3 and signal transduction during epithelial cell differentiation. In addition, Mta1 and Mta3 interacted with the adaptor proteins Grb2 and Nck, which contain two and three SH3 domains, respectively. Grb2 and Nck function as linker molecules between activated receptor tyrosine kinases and intracellular signaling proteins (Chardin et al., 1995; Lehmann et al., 1990). Both Nck (Lawe et al., 1997; Matuoka et al., 1997) and Grb2 (Romero et al., 1998; Verbeek et al., 1997) have been detected in the nucleus as well as the cytoplasm. This provides a second mechanism

for Mta1 and Mta3 to be translocated into the nuclei by associating with Nck, Grb2, or their associated proteins. Interestingly, MTA1 and Grb2 are both overexpressed in human breast cancer cells (Verbeek et al., 1997). Thus, differential subcellular localization of Mta1 and Mta3 may provide the means for these proteins to perform multiple functions by associating with different cellular signaling molecules. The lack of available antibodies specific for Mta1 and Mta3 has precluded us from demonstrating their subcellular distribution and interactions with Fyn and Grb2 in vivo.

These data suggest that in mammalian cells, the MTA family of proteins may serve to regulate normal cell growth and/or motility either through the modulation of histone acetylation or as bona fide transcription factors. Nuclear import of Mta1 and Mta3 proteins as shown in this study is required for both histone modification and transcriptional regulation. Future studies will focus on the effects of Mta proteins on gene expression patterns as they relate to the invasive/metastatic phenotype.

Acknowledgements

We would like to thank Dayna Levin, Sonul Mehta and Rachel Altman for their excellent technical help. We thank Drs Gabriele Richard and Joy Mulholland for critically reading this manuscript. We also thank Drs Paul Stein and John Seykora (Department of Dermatology, University of Pennsylvania, Philadelphia, PA) for the Fyn-GST proteins and Dr Jeffrey Benovic (Kimmel Cancer Institute, Thomas Jefferson University, Philadelphia, PA) for the Nck- and Grb2-GST fusion proteins. This work was supported by grants from the National Institutes of Health and the Dermatology Foundation. M.G.M. is a recipient of a Career Development Award from the Dermatology Foundation.

References

Anderson, S.M., Burton, E.A., Koch, B.L., 1997. Phosphorylation of Cbl following stimulation with interleukin-3 and its association with Grb2, Fyn, and phosphatidylinositol 3-kinase. J. Biol. Chem. 272, 739–745.

Archer, S.Y., Hodin, R.A., 1999. Histone acetylation and cancer. Curr. Opin. Genet. Dev. 9, 171–174.

Calautti, E., Missero, C., Stein, P.L., Ezzell, R.M., Dotto, G.P., 1995. Fyn tyrosine kinase is involved in keratinocyte differentiation control. Genes Dev. 9, 2279–2291.

Chardin, P., Cussac, D., Maignan, S., Ducruix, A., 1995. The Grb2 adaptor. FEBS Lett. 369, 47–51.

Eyal, Y., Neumann, H., Or, E., Frydman, A., 1999. Inverse single-strand RACE: an adapter-independent method of 5′ RACE. BioTechniques 27, 656–658.

Futamura, M., Nishimori, H., Shiratsuchi, T., Saji, S., Nakamura, Y., Tokino, T., 1999. Molecular cloning, mapping, and characterization of a novel human gene, MTA1-L1, showing homology to a metastasis-associated gene, MTA1. J. Hum. Genet. 44, 52–56.

Goldfarb, D.S., Gariepy, J., Schoolnik, G., Kornberg, R.D., 1986. Synthetic peptides as nuclear localization signals. Nature 322, 641–644.

Herman, M.A., Ch'ng, Q., Hettenbach, S.M., Ratliff, T.M., Kenyon, C., Herman, R.K., 1999. EGL-27 is similar to a metastasis-associated factor and controls cell polarity and cell migration in C. elegans. Development 126, 1055–1064.

Kadosh, D., Struhl, K., 1998. Histone deacetylase activity of Rpd3 is important for transcriptional repression in vivo. Genes Dev. 12, 797–805.

Kleene, R., Zdzieblo, J., Wege, K., Kern, H., 1999. A novel zymogen granule protein (ZG29p) and the nuclear protein MTA1p are differentially expressed by alternative transcription initiation in pancreatic acinar cells of the rat. J. Cell Sci. 112, 2539–2548.

Kuo, M.H., Allis, C.D., 1998. Role of histones acetyltransferases and deacetylases in gene regulation. Bioessays 20, 615–626.

Lanford, R.E., Kanda, P., Kennedy, R.C., 1986. Induction of nuclear transport with a synthetic peptide homologous to the SV40 T antigen transport signal. Cell 46, 575–582.

Lawe, D.C., Hahn, C., Wong, A.J., 1997. The Nck SH2/SH3 adaptor protein is present in the nucleus and associates with the nuclear protein SAM68. Oncogene 14, 223–231.

Lehmann, J.M., Riethmuller, G., Johnson, J.P., 1990. Nck, a melanoma cDNA encoding a cytoplasmic protein consisting of the src homology units SH2 and SH3. Nucleic Acids Res. 18, 1048.

Mahoney, M.G., Aho, S., Uitto, J., Stanley, J.R., 1998. The members of the plakin family of proteins recognized by paraneoplastic pemphigus antibodies include periplakin. J. Invest. Dermatol. 111, 308–313.

Matuoka, K., Miki, H., Takahashi, K., Takenaw, T., 1997. A novel ligand for an SH3 domain of the adaptor protein Nck bears an SH2 domain and nuclear signaling motifs. Biochem. Biophys. Res. Commun. 239, 488–492.

Nawa, A., Nishimori, K., Lin, P., Maki, Y., Moue, K., Sawada, H., Toh, Y., Fumitaka, K., Nicolson, G.L., 2000. Tumor metastasis-associated human MTA1 gene: its deduced protein sequence, localization, and association with breast cancer cell proliferation using antisense phosphorothioate oligonucleotides. J. Cell. Biochem. 79, 202–212.

Parsons, J.T., Weber, M.J., 1989. Genetics of src: structure and functional organization of a protein tyrosine kinase. Curr. Top. Microbiol. Immunol. 147, 79–127.

Paterno, G.D., Li, Y., Luchman, H.A., Ryan, P.J., Gillespie, L.L., 1997. cDNA cloning of a novel, developmentally regulated immediate early gene activated by fibroblast growth factor and encoding a nuclear protein. J. Biol. Chem. 272, 25592–25595.

Pencil, S.D., Toh, Y., Nicolson, G.L., 1993. Candidate metastasis-associated genes of the rat 13762NF mammary adenocarcinoma. Breast Cancer Res. Treat. 25, 165–174.

Pleiman, C.M., Clark, M.R., Gauen, L.K., Winitz, S., Coggeshall, K.M., Johnson, G.L., Shaw, A.S., Cambier, J.C., 1993. Mapping of sites on the Src family protein tyrosine kinases p55blk, p59fyn, and p56lyn which interact with the effector molecules phospholipase C-gamma 2, microtubule-associated protein kinase, GTPase-activating protein, and phosphatidylinositol 3-kinase. Mol. Cell. Biol. 13, 5877–5887.

Robbins, J., Dilworth, S.M., Laskey, R.A., Dingwall, C., 1991. Two interdependent basic domains in nucleoplasmin nuclear targeting sequence: identification of a class of bipartite nuclear targeting sequence. Cell 64, 615–623.

Romero, F., Ramos-Morales, F., Domínguez, A., Rios, R.M., Schweighoffer, F., Tocqué, B., Pintor-Toro, J.A., Fischer, S., Tortolero, M., 1998. Grb2 and its apoptotic isoform Grb3-3 associate with heterogeneous nuclear ribonucleoprotein C, and these interactions are modulated by poly (U) RNA. J. Biol. Chem. 273, 7776–7781.

Solari, F., Bateman, A., Ahringer, J., 1999. The Caenorhabditis elegans genes egl-27 and egr-1 are similar to MTA1, a member of a chromatin regulatory complex, and are redundantly required for embryonic patterning. Development 126, 2483–2494.

Toh, Y., Pencil, S.D., Nicolson, G.L., 1994. A novel candidate metastasis-associated gene, mta1, differentially expressed in highly metastatic mammary adenocarcinoma cell lines. J. Biol. Chem. 37, 22958–22963.

Toh, Y., Pencil, S.D., Nicolson, G.L., 1995. Analysis of the complete sequence of the novel metastasis-associated candidate gene, mta1,

differentially expressed in mammary adenocarcinoma and breast cancer cell lines. Gene 159, 97–104.

Toh, Y., Oki, E., Oda, S., Tokunaga, E., Ohno, S., Maehara, Y., Nicolson, G.L., 1997. Overexpression of the MTA1 gene in gastrointestinal carcinomas: correlation with invasion and metastasis. Int. J. Cancer 74, 459–463.

Toh, Y., Kuwano, H., Mori, M., Nicolson, G.L., Sugimachi, K., 1999. Overexpression of metastasis-associated MTA1 mRNA in invasive oesophageal carcinomas. Br. J. Cancer 79, 1723–1726.

Toh, Y., Kuninaka, S., Endo, K., Oshiro, T., Ikeda, Y., Nakashima, H., Baba, H., Kohnoe, S., Okamura, T., Nicolson, G.L., Sugimachi, K., 2000. Molecular analysis of a candidate metastasis-associated gene, MTA1: possible interaction with histone deacetylase 1. J. Exp. Clin. Cancer Res. 19, 105–111.

Tong, J.K., Hassig, C.A., Schnitzler, G.R., Kinsgton, R.E., Schreiber, S.L., 1998. Chromatin deacetylation by an ATP-dependent nucleosome remodelling complex. Nature 395, 917–921.

Verbeek, B.S., Adriaansen-Slot, S.S., Rijksen, G., Vroom, T.M., 1997. Grb2 overexpression in nuclei and cytoplasm of human breast cells: a histochemical and biochemical study of normal and neoplastic mammary tissue specimens. J. Pathol. 183, 195–203.

Xue, Y., Wong, J., Moreno, G.T., Young, M.K., Côté, J., Wang, W., 1998. NURD, a novel complex with both ATP-dependent chromatin-remodeling and histone deacetylase activities. Mol. Cell 2, 851–861.

Zhang, Y., LeRoy, G., Seelig, H.P., Lane, W.S., Reinberg, D., 1998. The dermatomyositis-specific autoantigen Mi2 is a component of a complex containing histone deacetylase and nucleosome remodeling activities. Cell 95, 279–289.

Zhang, Y., Ng, H.-H., Erdjument-Bromage, H., Tempst, P., Bird, A., Reinberg, D., 1999. Analysis of the NuRD subunits reveals a histone deacetylase core complex and a connection with DNA methylation. Genes Dev. 13, 1924–1935.